

PREPARATION AND STABILIZATION OF SACCHARIDE FIBER PRODUCED BY CENTRIFUGAL
SPINNING



A Thesis Submitted in Partial Fulfillment of the Requirements
for the Degree of Master of Science in Pharmacy in Industrial Pharmacy
Department of Pharmaceutics and Industrial Pharmacy
Faculty of Pharmaceutical Sciences
Chulalongkorn University
Academic Year 2018
Copyright of Chulalongkorn University

การเตรียมและการเพิ่มความคงตัวของเส้นใยแซ็ทคาไรด์ที่ผลิตโดยวิธีปั่นเหวี่ยงหนีศูนย์กลาง



วิทยานิพนธ์นี้เป็นส่วนหนึ่งของการศึกษาตามหลักสูตรปริญญาเภสัชศาสตรมหาบัณฑิต
สาขาวิชาเภสัชอุตสาหกรรม ภาควิชาวิทยาการเภสัชกรรมและเภสัชอุตสาหกรรม
คณะเภสัชศาสตร์ จุฬาลงกรณ์มหาวิทยาลัย
ปีการศึกษา 2561
ลิขสิทธิ์ของจุฬาลงกรณ์มหาวิทยาลัย

Thesis Title	PREPARATION AND STABILIZATION OF SACCHARIDE FIBER PRODUCED BY CENTRIFUGAL SPINNING
By	Miss Pattama Donghuntong
Field of Study	Industrial Pharmacy
Thesis Advisor	Wanchai Chongcharoen, Ph.D.
Thesis Co Advisor	Narueporn Sutanthavibul, Ph.D.

Accepted by the Faculty of Pharmaceutical Sciences, Chulalongkorn University in Partial Fulfillment of the Requirement for the Master of Science in Pharmacy

..... Dean of the Faculty of
Pharmaceutical Sciences
(Assistant Professor Rungpetch Sakulbumrungsil, Ph.D.)

THESIS COMMITTEE

..... Chairman
(Associate Professor PARKPOOM TENGAMNUAY, Ph.D.)

..... Thesis Advisor
(Wanchai Chongcharoen, Ph.D.)

..... Thesis Co-Advisor
(Narueporn Sutanthavibul, Ph.D.)

..... Examiner
(Assistant Professor Dusadee Charnvanich, Ph.D.)

..... External Examiner
(Associate Professor Waree Limwibrant, Ph.D.)

ปฐมา ดอนจันทร์ทอง : การเตรียมและการเพิ่มความคงตัวของเส้นใยแซ็กคาไรด์ที่ผลิตโดยวิธีปั่นเหวี่ยงหนีศูนย์กลาง. (PREPARATION AND STABILIZATION OF SACCHARIDE FIBER PRODUCED BY CENTRIFUGAL SPINNING) อ.ที่ปรึกษาหลัก : อ. ภก. ดร.วันชัย จงเจริญ, อ.ที่ปรึกษาร่วม : อ. ภญ. ดร.นฤพร สุดฉันทวิบูลย์

วัตถุประสงค์การศึกษานี้เพื่อเตรียมเส้นใยแซ็กคาไรด์โดยผ่านการปั่นเหวี่ยงหนีศูนย์กลางและติดตามความคงสภาพภายใต้สภาวะแรง แซ็กคาไรด์ต่างชนิดถูกเลือกนำมาปั่นเหวี่ยงด้วยแรงหนีศูนย์กลางเพื่อก่อรูปในแบบคล้ายเส้นด้าย ผลการศึกษาชี้ให้เห็นว่าซูโครส (SC) และทรีฮาโลส (TH) สามารถเตรียมในรูปแบบเส้นใยได้ในขณะที่แซ็กคาไรด์ชนิดอื่นไม่สามารถเตรียมได้ การก่อรูปของเส้นใยส่วนใหญ่เกี่ยวข้องกับอุณหภูมิสถานะแก้ว ความสามารถในการหลอมตัวรวมถึงความคงสภาพภายหลังหลอมละลายของแซ็กคาไรด์ แซ็กคาไรด์ชนิดที่มีอุณหภูมิของสถานะแก้วสูงเป็นตัวเลือกที่ดีในการเตรียมเส้นใย การหลอมที่เป็นเนื้อเดียวกันโดยมีความคงสภาพเป็นที่น่าสนใจเป็นอีกหนึ่งปัจจัยที่ส่งผลกระทบต่อเตรียมเส้นใย การเสื่อมสภาพหลังหลอมละลายของแซ็กคาไรด์บางชนิดนำไปสู่ความไม่สำเร็จในการเตรียมเส้นใย ปัจจัยหลักสามประการที่เกี่ยวข้องกับความคงสภาพของเส้นใย ได้แก่ อุณหภูมิสถานะแก้ว ปริมาณอสัณฐาน และความบกพร่องของพื้นผิวเส้นใย อุณหภูมิสถานะแก้วของเส้นใย SC และ TH เท่ากับ 58.13 และ 60.10 องศาเซลเซียสซึ่งสูงกว่าอุณหภูมิห้องจึงควรทำให้เส้นใยทั้งสองมีความคงสภาพ เนื่องจากอุณหภูมิสถานะแก้วที่สูงหรือการเกิดสถานะแก้ว แต่อย่างไรก็ตามโครงสร้างของเส้นใยทั้งสองเกิดการล้มตัวลงในระยะเวลาระดับชั่วโมงซึ่งเป็นเหตุจากรวมชาติของอสัณฐานและความบกพร่องของพื้นผิวในเส้นใย เส้นใย SC เป็นอสัณฐานที่มีพื้นผิวขรุขระมากกว่าเส้นใย TH ดังนั้นเส้นใย TH จึงมีความคงสภาพมากกว่าเส้นใย SC

เพื่อปรับปรุงความคงสภาพของเส้นใย การผสมแซ็กคาไรด์ต่างชนิดเข้าด้วยกันถูกนำเสนอเนื่องจากความสามารถในการเปลี่ยนแปลงของอุณหภูมิสถานะแก้ว ในการศึกษานี้ SC ถูกเลือกเป็นแซ็กคาไรด์ชนิดหลัก หลังจากนั้น TH จะถูกเติมลงไปก่อนเตรียมเป็นเส้นใย จากการตรวจติดตามอุณหภูมิสถานะแก้วของของผสมแสดงความสัมพันธ์แบบไม่เป็นเชิงเส้นตรงระหว่างอุณหภูมิสถานะแก้วของของผสมกับปริมาณ TH ที่เติมเข้าไป ที่สัดส่วนโดยน้ำหนักต่ำของ TH ให้ผลของพลาสติกไซเซชันในขณะที่สัดส่วนโดยน้ำหนักสูงของ TH (มากกว่า 0.5) ให้ผลของแอนติพลาสติกไซเซชัน อุณหภูมิสถานะแก้วของของผสมทั้งหมดที่ตรวจพบมีค่าต่ำกว่าหรือใกล้เคียงอุณหภูมิห้องซึ่งส่งผลกระทบต่อากลุ่มตัวของโครงสร้างเส้นใย มากกว่าไปกว่านั้นเส้นใยเหล่านี้เป็นอสัณฐานที่มีพื้นผิวเรียบ ดังนั้นอุณหภูมิสถานะแก้วและอสัณฐานจึงเป็นปัจจัยที่มีนัยสำคัญต่อความคงสภาพของเส้นใยที่เตรียมจากของผสมของ SC และ TH แต่อย่างไรก็ตามไม่เพียงแต่การตรวจพื้นผิวของเส้นใยด้วยกล้องจุลทรรศน์แบบส่องกราดหากความเรียบของพื้นผิวยังคงถูกประเมินจากรูปแบบการดูดซับความชื้น ผลการศึกษาแสดงให้เห็นว่าเส้นใยผสมระหว่าง SC และ TH ใช้เวลาในการดูดซับความชื้นหรือที่เรียกว่าเวลาทรานซิชันรวมถึงเวลาในการตกผลึกกลับที่ยาวนานขึ้นเมื่อเพิ่มอัตราส่วนโดยน้ำหนักของ TH สรุปได้ว่าเวลาทรานซิชันและเวลาในการตกผลึกกลับที่ยาวนานขึ้นหมายถึงพื้นผิวเส้นใยที่เรียบมากขึ้นหรือมีจุดบกพร่องน้อย ดังนั้น TH สามารถใช้ปรับปรุงความคงสภาพของเส้นใย SC ได้โดยการก่อรูปของเส้นใยที่มีจุดบกพร่องของพื้นผิวที่น้อยลงมากกว่าการปรับเปลี่ยนอุณหภูมิสถานะแก้วหรือการเพิ่มขึ้นของความเป็นผลึก

โดยสรุปเส้นใย SC คงสภาพมากขึ้นโดยการเติม TH อย่างไรก็ตามความคงสภาพทางกายภาพของเส้นใยปั่นเหวี่ยง TH น่าจะมากกว่าเมื่อเปรียบเทียบกับเส้นใยผสมระหว่าง SC และ TH ดังนั้น TH ควรถูกเลือกใช้เป็นแซ็กคาไรด์พื้นฐานในการเตรียมเส้นใยโดยการปั่นเหวี่ยงหนีศูนย์กลาง จึงแนะนำให้ทำการศึกษาเพิ่มเติมถึงผลของตัวเหนียวหรือตัวเปลี่ยนแปลงการตกผลึกที่มีต่อการก่อรูปของเส้นใย TH

จุฬาลงกรณ์มหาวิทยาลัย
CHULALONGKORN UNIVERSITY

สาขาวิชา เกษษุศาสตร์
ปีการศึกษา 2561

ลายมือชื่อนิสิต
ลายมือชื่อ อ.ที่ปรึกษาหลัก
ลายมือชื่อ อ.ที่ปรึกษาร่วม

5876113033 : MAJOR INDUSTRIAL PHARMACY

KEYWORD: SACCHARIDE FIBER, SUCROSE, TREHALOSE, SACCHARIDE-SUCROSE INTERACTION, CENTRIFUGAL SPINNING,
GLASS TRANSITION TEMPERATURE

Pattama Donghunting :
PREPARATION AND STABILIZATION OF SACCHARIDE FIBER PRODUCED BY CENTRIFUGAL SPINNING. Advisor: Wanchai
Chongcharoen, Ph.D. Co-advisor: Narueporn Sutanthavibul, Ph.D.

The objectives of this study were to prepare saccharide fiber via centrifugal spinning and further investigate its stability under stress condition. Different saccharides were chosen and spun via centrifugal force to form thread like matter. The results indicated that sucrose (SC) and trehalose (TH) could be fabricated as fiber whereas other saccharides were not able to form. The formation of fiber mainly involved with glass transition temperature (T_g), molten ability including stability of saccharide after melting. High T_g saccharides were a good candidate on fiber preparation. Homogeneous melting with appreciable stability was another factor affecting on fiber preparation. Decomposing after melting of some saccharides was prone to unsuccessful fiber formation. Three main factors regarding to the stability of fiber produced were T_g , amorphous content and defect on the surface. T_g of both SC and TH fiber were found to be 58.13 and 60.10 °C that were higher than room temperature. They should be thus stable due to high T_g or glassy state. However, their fiber structure collapsed within hour time of scale. It was due to amorphous nature with surface defect. SC fiber was amorphous with rougher surface compared to TH fiber. Thus, TH fiber was more stable than SC fiber.

In order to improve the stability of fiber, blending of different saccharides was proposed due to the ability for changing T_g . In this study, SC was selected as the main saccharide. TH was then incorporated before fiber fabricating. Monitoring of the T_g of mixture ($T_{g(mix)}$) showed the non-linear relationship between $T_{g(mix)}$ and the amount of TH added. Low weight fraction of TH showed plasticization while higher weight fraction (>0.5) TH provided antiplasticization. All $T_{g(mix)}$ observed were lower or close to ambient temperature that impacted on the collapsible of fiber structure. In addition, they existed as amorphous with smoother surface. Therefore, T_g and amorphous were the significance factors on the stability of fiber produced from the mixture of SC&TH. Nevertheless, not only the scanning of fiber morphology with scanning microscope but the smoothness of surface was also assessed with moisture sorption profile. The result showed that the SC&TH fiber took longer time of moisture sorption or known as "transition time" including longer recrystallization time when increasing the weight ratio of TH. It could be concluded that longer of transition and recrystallization time meant to the smoother surface or less defect of fiber. Therefore, TH could improve the stability of SC fiber via the formation of less surface defect fiber more than the adjustment of T_g or the increasing of crystallinity.

In conclusion, SC fiber was more stable by the incorporation of TH. However, the physical stability of TH spinning fiber sound to be better compared to SC&TH fibers. Thus, TH should be selected as saccharide base for centrifugal spinning fiber. The further study of the effect of crystallization enhancer or modifier on TH fiber formation was recommended.

Field of Study: Industrial Pharmacy

Academic Year: 2018

Student's Signature

Advisor's Signature

Co-advisor's Signature

ACKNOWLEDGEMENTS

I would like to express my deep gratitude to Dr. Wanchai Chongcharoen, my research advisor for invaluable advice, enthusiastic encouragement and useful critiques of this research work. I would also like to thank my thesis co-advisor Dr. Narueporn Sutanthavibul who supported me by keeping my progress on schedule. This research was contributed by the Chulalongkorn University Drugs and Health Product Innovation Production Promotion Center. I am also thank the Scientific and Technological Research Equipment Centre. I am thankful to Nagase (Thailand) Co.,LTD. for supporting the TREHA® (trehalose dihydrate).I am so grateful to Pharmaceutical division, Health department, Bangkok Metropolitan Authority. I am also deeply thankful Mrs. Sriwimol Chuengsatiansup, my director of Pharmaceutical division, Health department and Mr. Teerapol Chieuroongroj, my supervisor of production pharmaceutical for giving me the opportunity to earn an up to date knowledge for improving my role and responsibility.

Finally, I would like to thank my colleagues, scientists and staff in the Department of Pharmaceutics and Industrial Pharmacy, Faculty of Pharmaceutical Sciences, Chulalongkorn University for their assistance and support on this thesis.

จุฬาลงกรณ์มหาวิทยาลัย
CHULALONGKORN UNIVERSITY

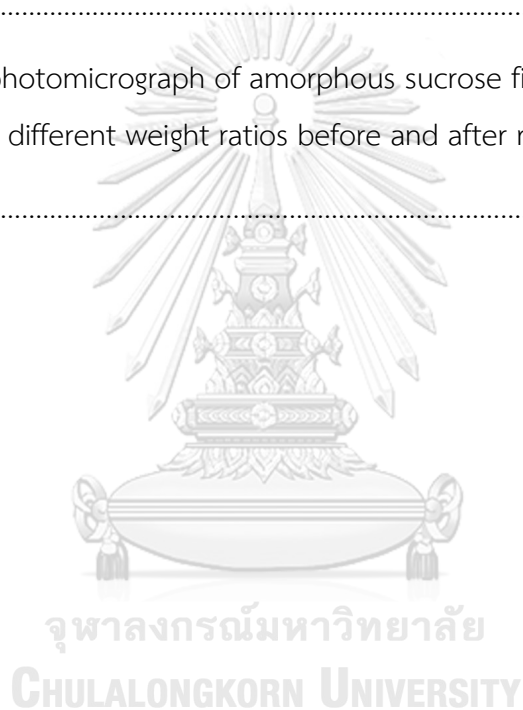
Pattama Donghontong

TABLE OF CONTENTS

	Page
ABSTRACT (THAI).....	iii
ABSTRACT (ENGLISH).....	iv
ACKNOWLEDGEMENTS	v
TABLE OF CONTENTS	vi
LIST OF FIGURES	ix
LIST OF TABLES.....	xv
LIST OF ABBREVIATIONS	xvii
CHAPTER I.....	1
INTRODUCTION.....	1
Objectives.....	2
CHAPTER II.....	3
LITERATURE REVIEW	3
CHAPTER III.....	18
MATERIALS AND METHODS.....	18
Materials.....	18
Equipments.....	18
Methods.....	20
1. Preparation of saccharide fiber using centrifugal spinner	20
2. Characterization of saccharide fiber	21
2.2 Solid state characterization of saccharide fiber	22
2.2.1 X-ray powder diffraction (XRPD)	22

2.2.2 Thermal analysis	22
Differential Scanning Calorimetric (DSC).....	22
Thermogravimetric analysis (TGA)	22
3. Molecular interaction among the component of saccharide fiber	22
4. Stability investigation of saccharide fiber	23
4.1 Volume reduction of saccharide fiber.....	23
4.2 Moisture sorption profile	23
CHAPTER IV	25
RESULTS AND DISCUSSIONS	25
Preparation of saccharide fiber	25
1. Monocomponent saccharide fiber	25
2. Binary component saccharide fiber.....	33
3. Effect of the amount of trehalose dihydrate on the glass transition temperature of spinning sucrose mixture fiber	41
CHAPTER V	63
CONCLUSIONS	63
REFERENCES	65
APPENDICES.....	74
Appendix 1	75
Glass transition temperature (T_g) of sucrose fiber containing different saccharides at weight ratio of 1:1	75
Appendix 2	76
Calculated and experimental $T_{g(mix)}$ of sucrose fiber containing trehalose dihydrate at different weight ratios	76
Appendix 3	82

Moisture sorption profile of amorphous sucrose fiber containing trehalose dihydrate at different weight ratios under storage condition of 30 ± 2 °C and $75\pm 5\%$ RH.....	82
Appendix 4.....	87
Moisture sorption profile of amorphous sucrose fiber containing trehalose dihydrate at different weight ratios under storage condition of 40 ± 2 °C and $75\pm 5\%$ RH.....	87
Appendix 5.....	93
Polarized light photomicrograph of amorphous sucrose fiber containing trehalose dihydrate at different weight ratios before and after recrystallization.....	93
VITA.....	98



LIST OF FIGURES

Figure 1 The classification of solid dispersions.....	3
Figure 2 Compartmental of centrifugal spinning equipment	7
Figure 3 The physical appearance of sucrose derived cotton candy produced by centrifugal spinning under different storage conditions.....	8
Figure 4 X-ray powder diffraction pattern of sucrose derived cotton candy under temperature of 23°C and 0% RH	8
Figure 5 X-ray diffraction pattern of sucrose cotton candy under temperature of 23°C and 45% RH	9
Figure 6 X-ray diffraction pattern of sucrose cotton candy under temperature of 23°C and 75% RH	10
Figure 7 DSC thermograms of freeze dry amorphous sucrose-trehalose mixtures containing various percentage of trehalose.....	12
Figure 8 X-ray diffraction pattern of an amorphous pure sucrose cotton candy mixture storage at 33% RH and 25°C	14
Figure 9 X-ray diffraction pattern of an amorphous 75% sucrose with 25% trehalose cotton candy after storage at 23% RH and 25°C	15
Figure 10 Zone of moisture sorption isotherm	17
Figure 11 Determination apparatus of the relatively change in volume reduction and height of saccharide fiber.....	23
Figure 12 Moisture sorption profile and determination of transition and recrystallization time of saccharide fiber.....	24
Figure 13 Physical appearance of saccharide fiber produced from different saccharide groups.....	27
Figure 14 DSC thermogram of sucrose fiber and trehalose anhydrous fiber	30

Figure 15 X-ray powder diffraction of (A) crystalline sucrose, (B) fiber produced from sucrose, (C)crystalline trehalose dihydrate and (D) fiber produced from trehalose dihydrate	30
Figure 16 ATR-FTIR spectra of crystalline sucrose (upper line) and sucrose fiber (lower line).....	31
Figure 17 ATR-FTIR spectra of crystalline trehalose dihydrate (upper line) and trehalose (anhydrous) fiber (lower line)	32
Figure 18 Physical appearance of the sucrose fiber during storage at temperature of 30 ± 2 °C, $75\pm 5\%$ RH over time	33
Figure 19 Physical appearance of the trehalose dihydrate fiber during storage at temperature of 30 ± 2 °C, $75\pm 5\%$ RH over time	33
Figure 20 Physical appearance (left panel) and Scanning electron photomicrograph (right panel) of sucrose fiber containing saccharides at weight ratio of 1:1. ((A) sucrose without any saccharides, (B) sucrose containing D-fructose, (C) sucrose containing D-glucose, (D) sucrose containing D-mannitol, (E) sucrose containing lactose anhydrous and (F) sucrose containing trehalose dihydrate).....	36
Figure 21 DSC thermogram of storage sucrose fiber at ambient	37
Figure 22 X-ray powder diffractogram of sucrose fiber containing different type of saccharides at weight ratio 1:1 (A – pure sucrose, B – sucrose and D-mannitol, C– sucrose and D-fructose, D – sucrose and D-glucose, E – sucrose and trehalose dihydrate, F – sucrose and lactose anhydrous).....	37
Figure 23 Estimated volume reduction of saccharide fiber upon storage at 30 ± 2 °C, $75\pm 5\%$ RH. (A) sucrose, (B) mixture of sucrose and trehalose dihydrate at 1:1 weight ratio and (C) trehalose anhydrous	40
Figure 24 Glass transition temperature of sucrose fiber containing trehalose dihydrate [$T_{g(mix)}$] at various weight ratio: (dash line) $T_{g(mix)}$ calculated from simple GT equation, (solid line) $T_{g(mix)}$ from experiment results	41

- Figure 25** Physical appearance of sucrose fiber containing trehalose dihydrate at different weight ratios (A) 100.0:0, (B) 87.5:12.5, (C) 75.0:25.0, (D) 62.5:37.5, (E) 50.0:50.0, (F) 37.5:62.5, (G) 25.0:75.0, (H) 12.5:87.5, and (I) 0:100.0 42
- Figure 26** Scanning electron photomicrograph of sucrose fiber containing trehalose dihydrate at different weight ratios (A) 100.0:0, (B) 87.5:12.5, (C) 75.0:25.0, (D) 62.5:37.5, (E) 50.0:50.0, (F) 37.5:62.5, (G) 25.0:75.0, (H) 12.5:87.5, and (I) 0:100.0 43
- Figure 27** X-ray diffractograms of sucrose fiber containing trehalose dihydrate at different weight ratios (A) 100.0:0, (B) 87.5:12.5, (C) 75.0:25.0, (D) 62.5:37.5, (E) 50.0:50.0, (F) 37.5:62.5, (G) 25.0:75.0, (H) 12.5:87.5, and (I) 0:100.0 44
- Figure 28** DSC and TGA thermograms of trehalose anhydrous fiber 47
- Figure 29** ATR-FTIR spectra of (A) crystalline sucrose, (B) crystalline trehalose dihydrate, (C) physical mixture of crystalline sucrose and crystalline trehalose dihydrate (25.0:75.0 by weight), and (D) sucrose fiber containing trehalose dihydrate (25.0:75.0 by weight) 49
- Figure 30** ATR-FTIR spectra of sucrose fiber containing trehalose dihydrate at different weight ratios (A) 100.0:0, (B) 75.0:25.0, (C) 50.0:50.0, (D) 25.0:75.0, and (E) 0:100.0 50
- Figure 31** Moisture sorption profile of amorphous sucrose fiber under storage condition of $30\pm 2^\circ\text{C}$ and $75\pm 5\%$ RH. (A – the transition time of amorphous glassy to rubbery state, B - the recrystallization time) 55
- Figure 32** The transition time of sucrose fiber containing trehalose dihydrate at different weight ratios under storage condition at temperature of $30\pm 2^\circ\text{C}$ and $75\pm 5\%$ RH 57
- Figure 33** The recrystallization time of sucrose fiber containing trehalose dihydrate at different ratios under storage condition at temperature of $30\pm 2^\circ\text{C}$ and $75\pm 5\%$ RH.. 58
- Figure 34** Photomicrographs of sucrose fiber containing trehalose dihydrate at weight ratio 75:25 at initial and after recrystallization (40×10 X) 59

Figure 35 Time period between “The transition time” and “The recrystallization time” (ΔT) as a function of weight ratios of sucrose fiber containing trehalose dihydrate	60
Figure 36 The transition time of sucrose fiber containing trehalose dihydrate at different ratios under storage condition at temperature of 40 ± 2 °C and $75\pm 5\%$ RH..	61
Figure 37 The recrystallization time sucrose fiber containing trehalose dihydrate at different ratios under storage condition at temperature of 40 ± 2 °C and $75\pm 5\%$ RH..	62
Figure 38 DSC thermograms of sucrose fiber containing the lower T_g saccharides at weight ratio of 1:1.....	75
Figure 39 DSC thermogram of sucrose fiber containing the higher T_g saccharide groups at weight ratio of 1:1	75
Figure 40 DSC thermograms of sucrose fiber containing trehalose dihydrate at weight ratio of 100.0 : 0	77
Figure 41 DSC thermograms of sucrose fiber containing trehalose dihydrate at weight ratio of 87.5 : 12.5	77
Figure 42 DSC thermograms of sucrose fiber containing trehalose dihydrate at weight ratio of 75.0 : 25.0	78
Figure 43 DSC thermograms of sucrose fiber containing trehalose dihydrate at weight ratio of 62.5 : 37.5	78
Figure 44 DSC thermograms of sucrose fiber containing trehalose dihydrate at weight ratio of 50.0 : 50.0	79
Figure 45 DSC thermograms of sucrose fiber containing trehalose dihydrate at weight ratio of 37.5 : 62.5	79
Figure 46 DSC thermograms of sucrose fiber containing trehalose dihydrate at weight ratio of 25.0 : 75.0	80
Figure 47 DSC thermograms of sucrose fiber containing trehalose dihydrate at weight ratio of 12.5 : 87.5	80

Figure 48 DSC thermograms of sucrose fiber containing trehalose dihydrate at weight ratio of 0 : 100.0.....	81
Figure 49 Moisture sorption profile of amorphous saccharide sucrose fiber.....	82
Figure 50 Moisture sorption profile of amorphous saccharide sucrose fiber containing trehalose dihydrate at weight ratio of 87.5 : 12.5	82
Figure 51 Moisture sorption profile of amorphous saccharide sucrose fiber containing trehalose dihydrate at weight ratio of 75.0 : 25.0	83
Figure 52 Moisture sorption profile of amorphous saccharide sucrose fiber containing trehalose dihydrate at weight ratio of 62.5 : 37.5	83
Figure 53 Moisture sorption profile of amorphous saccharide sucrose fiber containing trehalose dihydrate at weight ratio of 50.0 : 50.0	84
Figure 54 Moisture sorption profile of amorphous saccharide sucrose fiber containing trehalose dihydrate at weight ratio of 37.5 : 62.5	84
Figure 55 Moisture sorption profile of amorphous saccharide sucrose fiber containing trehalose dihydrate at weight ratio of 25.0 : 75.0	85
Figure 56 Moisture sorption profile of amorphous saccharide sucrose fiber containing trehalose dihydrate at weight ratio of 12.5 : 87.5	85
Figure 57 Moisture sorption profile of amorphous saccharide trehalose dihydrate fiber	86
Figure 58 Moisture sorption profile of amorphous saccharide sucrose fiber.....	88
Figure 59 Moisture sorption profile of amorphous saccharide sucrose fiber containing trehalose dihydrate at weight ratio of 87.5 : 12.5	88
Figure 60 Moisture sorption profile of amorphous saccharide sucrose fiber containing trehalose dihydrate at weight ratio of 75.0 : 25.0	89
Figure 61 Moisture sorption profile of amorphous saccharide sucrose fiber containing trehalose dihydrate at weight ratio of 62.5 : 37.5	89

Figure 62 Moisture sorption profile of amorphous saccharide sucrose fiber containing trehalose dihydrate at weight ratio of 50.0 : 50.0	90
Figure 63 Moisture sorption profile of amorphous saccharide sucrose fiber containing trehalose dihydrate at weight ratio of 37.5 : 62.5	90
Figure 64 Moisture sorption profile of amorphous saccharide sucrose fiber containing trehalose dihydrate at weight ratio of 25.0 : 75.0	91
Figure 65 Moisture sorption profile of amorphous saccharide sucrose fiber containing trehalose dihydrate at weight ratio of 12.5 : 87.5	91
Figure 66 Moisture sorption profile of amorphous saccharide trehalose dihydrate fiber	92
Figure 67 Photomicrographs of sucrose fiber containing trehalose dihydrate at different weight ratios (A)-(100.0:0), (B)-(87.5:12.5) (40*10 X).....	93
Figure 68 Photomicrographs of sucrose fiber containing trehalose dihydrate at different weight ratios (A)-(75.0:25.0), (B)-(62.5:37.5) (40*10 X).....	94
Figure 69 Photomicrographs of sucrose fiber containing trehalose dihydrate at different weight ratios (A)-(50.0:50.0), (B)-(37.5:62.5) (40*10 X).....	95
Figure 70 Photomicrographs of sucrose fiber containing trehalose dihydrate at different weight ratios (A)-(25.0:75.0), (B)-(12.5:87.5) (40*10 X).....	96
Figure 71 Photomicrographs of sucrose fiber containing trehalose dihydrate at different weight ratios (0:100.0) (trehalose dihydrate fiber) (40*10 X).....	97

LIST OF TABLES

Table 1 Fast dissolving product currently marketing.....	6
Table 2 Average onset of sucrose recrystallization time of sucrose fiber containing APIs stored under 11, 33, 53, and 75% RH at 25 °C.....	10
Table 3 Glass transition temperature (onset and endpoint) of pure sucrose cotton candy and sucrose cotton candy containing 5% raffinose as a function of %RH.....	13
Table 4 Time to crystallize for sucrose-trehalose cotton candy samples stored at different relative humidity.....	15
Table 5 Unit of control heating temperature and heating temperature using Infrared thermometer.....	20
Table 6 Melting temperature of saccharide.....	21
Table 7 Amorphous glass transition temperature of selected saccharides.....	28
Table 8 The calculated and experimental $T_{g(mix)}$ of sucrose fiber containing different saccharides at weight ratio of 1:1.....	38
Table 9 Physical stability of sucrose fiber containing trehalose dihydrate with different weight ratios under storage temperature of 30 ± 2 °C and $75\pm 5\%$ RH.....	45
Table 10 Physical stability of sucrose fiber containing trehalose dihydrate at different weight ratios under storage temperature of 40 ± 2 °C and $75\pm 5\%$ RH.....	52
Table 11 Physical stability of sucrose fiber containing trehalose dihydrate at different weight ratios under storage temperature of 2-8°C and $75\pm 5\%$ RH.....	53
Table 12 The transition time and the recrystallization time of sucrose/trehalose dihydrate fiber at various weight ratios under exposing temperature of 30 ± 2 °C and $75\pm 5\%$ RH.....	56
Table 13 Calculated and experimental $T_{g(mix)}$ of sucrose fiber containing trehalose dihydrate at different weight ratios.....	76

Table 14 The transition time and the recrystallization time of sucrose/trehalose dihydrate fiber with various weight ratios under exposing temperature of $40\pm 2^{\circ}\text{C}$ and $75\pm 5\%$ RH.....	87
--	----



LIST OF ABBREVIATIONS

API	Active Pharmaceutical Ingredient
BCS	Biopharmaceutical Classification System
XRPD	X-ray powder diffractometry
DSC	Differential Scanning Calorimetry
GT equation	Gordon-Taylor equation
TGA	Thermogravimetric Analysis
T_g	glass transition temperature
$T_{g(mix)}$	glass transition temperature of the mixture
$^{\circ}\text{C}$	degree Celsius (centigrade)
%	percentage
RH	Relative Humidity
min	minute (s)
Hr	hour (s)
μm	micrometre (s)
mg	milligram (s)
g	gram (s)
θ	theta angle
i.e.	that is
w/w	weight by weight
et al.	et al, and others
TREHA [®] ,TD	trehalose dihydrate
TH	trehalose
SC	sucrose
ATR-FTIR	Attenuated Total Reflection-Fourier Transform Infrared Spectroscop

CHAPTER I

INTRODUCTION

The major problem of BCS class II and IV API is poorly water soluble characters (1). It should be then possibly overcome by solid dispersion that is one of the most promising current techniques. The higher solubility of poorly water-soluble drugs obtained from solid dispersion approach resulting in higher dissolution and finally increasing their oral bioavailability (2, 3). The principle of solid dispersion is theoretically described that API is thoroughly dispersed in solid carrier. Method of preparation of solid dispersion involves the utilization of either solvent or melting. For solvent-assisted method, API and carriers are blended together with aid of solvent of interested. When the mixture is dissolved homogeneously, it is then converted to the solid form by removing the solvent. High volume of solvent usage with more time of removing is the disadvantages of this method (4). If the organic solvent is used, eco-friendly issue is critically concerned. Hence, solvent free method is seemed to be a good candidate of solid dispersion preparation.

Melting of saccharide carrier with dispersed API is classified as a solvent free method of solid dispersion preparation. Not only it provides the solid dispersion product, it can further generated in various forms such as powders, granules or fiber. In general, solid dispersion in the form of fiber offers more benefit than those of powders or granule. Solid dispersion as fiber form can be manufactured by several method. One of the popular methods is centrifugal spinning. It provides a high production rate and simple equipment setup. (4, 5). Briefly, such method of preparation involves the melting of API and solid carrier before gaining molten mixture. It is then spun by centrifugal force to form a small continues filament pattern. The molten liquid is then exposed with outside air temperature and solidified as fiber. It has a high surface area and may be porous. This is the reason why it can improve the dissolution of poorly aqueous soluble API.

Currently, the substance that is used as the solid dispersion carrier is polyethylene glycols, polyvinylpyrrolidone, hydroxymethyl propyl cellulose,

cellulose derivative, polyvinyl alcohol, poloxamers, urea and saccharide (6-9). Saccharide is one of most interesting carrier. It is due to the fact that it is easily available with reasonable price including widely utilization in the pharmaceutical industries. Moreover, there was a patent in the name of “flash dose technology” or “flash heat technology” by Fluisz in 1989 which related to the making solid dispersion using sugar as a carrier by spinning process (10-12). The saccharide fiber produced had a high surface area and porosity with amorphous solid state structure. Thus, it could enhance the water solubility of API dispersed. However, major disadvantage of saccharide fiber was related to the thermodynamic instability. It changed from glassy to rubbery amorphous solid state structure under exposing to high temperature and humidity. It was due to the moisture that acts as plasticizer. Moreover, surface defect was obviously occurred and had a direct effected on the moisture uptake. Hence, such fiber should be kept in tight and moisture-resistant container and stored at low temperature (below T_g). The problem solvings of the unstable saccharide fiber were offered differently. Optimizing T_g by adding other high T_g saccharide was then proposed. The blending of multicomponent to form homogeneous mixture yielded the new material with new T_g ($T_{g (mix)}$). Hence, the adjustment of T_g may improve stability of the fiber when exposing to high temperature and humidity.

Objectives

1. To prepare saccharide fiber produced by centrifugal spinning technique that would provide a better physical and physicochemical stability when exposed to high temperature and humidity.
2. To study the effect of saccharides on the physical and physicochemical property of saccharide fiber produced from sucrose.

CHAPTER II

LITERATURE REVIEW

Solid dispersion is a technique that can increase the solubility of poorly soluble drug. The principle of solid dispersion is regarding to the dispersion of API evenly in solid carrier. The characteristic of carrier used impacts on the performance of an improving solubility. In general, hydrophilic carrier can enhance the dissolution and bioavailability of poorly aqueous soluble drug. The advantages of solid dispersion are demonstrated as follows:

1. due to high surface area, it will rise the water solubility of low water solubility drug molecule (13)
2. increase wettability of poorly water soluble drug molecule (1, 14)
3. high porosity, resulting in an increasing of dissolution rate of drug molecule (2)
4. enhance water solubility of drug molecule via amorphization (1, 2). Poorly aqueous soluble drug molecule is mostly crystalline state but it becomes more soluble when amorphous state is developed.

Solid dispersion is commonly classified as three generations. The 1st generation of crystalline carriers, the 2nd generation of polymeric carriers (amorphous carriers) and the 3rd generation of the mixture of surfactants and polymers (Figure 1).

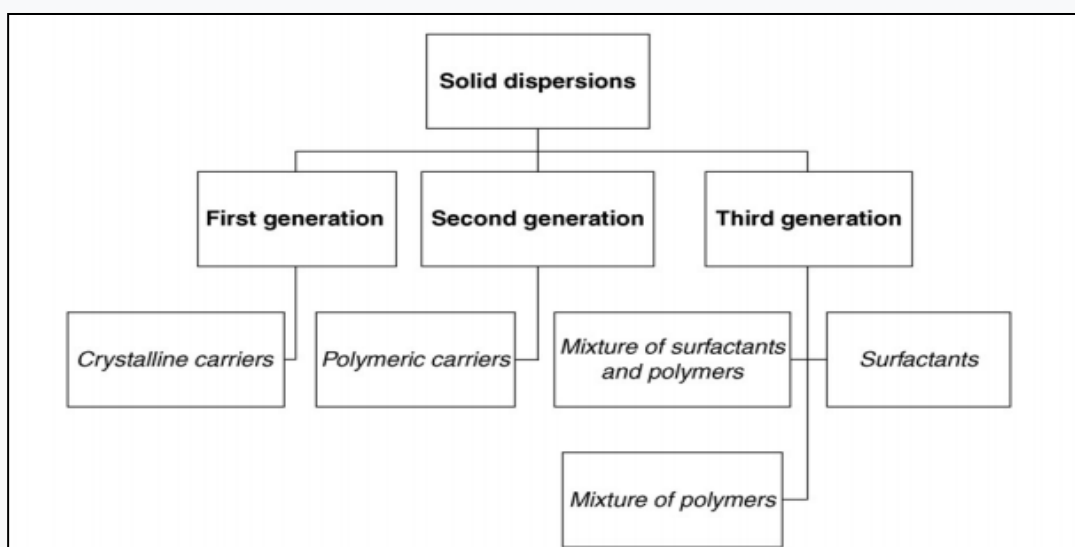


Figure 1 The classification of solid dispersions

For the first generation, solid dispersion uses crystalline carrier. Thus, the drug molecule embedded in crystalline carrier is not released as quickly as amorphous carrier. However, crystalline carrier will provide the higher thermodynamic stability of solid dispersion produced. Amorphous carrier or polymeric carrier in the second generation is working on the improving of the wettability and solubility of drug molecule. In the third generation, surfactant or a mixture of amorphous polymers and surfactants are utilized as carriers. This generation of solid dispersion can be accomplished with an increasing of the solubility, wettability and also gaining superior oral bioavailability of poorly soluble drug. Furthermore, It can control the drug release of poorly soluble drug (2, 14, 15).

When considering the type of carrier, one of the most promising carriers is goes to saccharide. It has been positioned as carrier in both first generation and second generation. It can be used as both crystalline and amorphous carrier. Advantage of saccharide carrier is shown herein after:

1. It contains or enriches with hydroxyl group in molecular structure, so it will give raises the high solubility of poorly aqueous soluble drug via the formation of hydrogen bonding or hydration (16).

2. It can give the high surface area of drug molecule and yield an improvement of wettability of poorly aqueous soluble drug (13, 16-18).

3. It can protect the self-agglomeration of drug molecule in solid dispersion during storage from steric hindrance effect (19).

In term of the usage of saccharide carrier, how to use the saccharide carrier in solid dispersion is mentioned. It can generally be categorized as two approaches solvent-assisted and non-solvent approach. Solvent-assisted method should include solvent evaporation, spray drying, freeze drying or lyophilization (7, 8, 20). Meanwhile, solvent free method covers hot melt extrusion, fusion, kneading, roll mixing and melting method (6, 21-24). Preparation of solid dispersion with saccharide carrier by solvent methods has several disadvantages. It needs high volume of organic or non-organic solvent in the manufacturing process and later the wasting of the time of removing. It is non-friendly with an environment (25). Thus, solvent free method becomes more interesting. Moreover, saccharide carrier with solvent free

method can be generated in various forms such as powders, granules, thread-like or networking of fiber.

In general, fiber can be manufactured by several preparation methods such as melt blowing, bi-component fiber spinning, phase separation, template synthesis, self-assembly including electrospinning. Among these methods, electrospinning is the most common method and has a wide variety of applications i.e. fabricating nanofiber, and tissue engineering. Nanofiber producing by electrospinning can control the release and delivery of several drugs such as antibiotic, anticancer, antimicrobial, anti-inflammatory, anti-histamine, gastrointestinal including macromolecule(26). Nanofiber of diclofenac sodium in Eudragit® polymer was developed and could control the drug release over time at small intestine (27). However, the disadvantage of electrospinning is still questionable. Such system need to put the voltage during manufacture to produce the continuous fiber from the different of electrical potential. In addition, it provides a low production rate and forms a fiber with only charged material. Thus, centrifugal spinning method is an alternative choice that has several advantages over electrospinning method. It can generate the nanofiber applied with organic materials, polymers including inorganic carbon. The production machine can be easily installed and provides high production rate. Furthermore, it takes a short time of production. As a result of short production time period, the material has less potential on the decomposition under the high temperature in process of manufacturing (4, 5).

Saccharide fiber produced by centrifugal spinning process has long been developed and manufactured. In the past, it was prepared as sweets that also known as “cotton candy” or “fairly floss”. The process of making drug loaded spinning fiber had been patented in the name of “Flash heat technology” or “Flash dose technology”. It used the principle of the making of partial recrystallization of saccharide carrier and later milling as powders or granules. It was then mixed with active substances before compress as a tablet. This techniques could be further applied for the preparation of fast dissolving system (11, 12). Above system was suitable for several patients who had suffered from the difficulty of swallowing medicine such as unconscious, pediatric, elderly including schizophrenic patients. It

was due to the good ability of rapid disintegrating with small amount of liquid and later easily dissolved in oral cavity. Currently, there are the marketed product of fast dissolving system with Flash heat technology such as Paroxetine FD (Table 1) (28).

Preparation of centrifugal spinning saccharide fiber uses the principle of the dispersion of API in the molten saccharides before spinning and congealing as a solid material. The molten mixture of API and carrier solidify as a high porous fiber when upon contact with environmental condition. Furthermore, it has high surface area with amorphous structure of both API and carrier. Thus, it can increase the solubility of poorly water soluble API effectively.

Table 1 Fast dissolving product currently marketing (28)

Drug Products	Active Ingredient	Indication	Company	Technology	Technology Company
Claritin RediTabs	Loratadine	Allergy	Schering-Plough		
Clarinet x RediTabs	Desloratadine	Allergy	Schering-Plough		
Dimetapp	Brompheniramine, phenylpropanolymine	Cold, allergy	Wyeth		
Feldene Melt	Piroxicam	NSAID, pain	Pfizer		
Imodium Lingual	Loperamide	Antidiarrhea	J&J		
Innovace Melt	Enalapril maleate	Hypertension	Merck	Zydis	Cardinal Health
Maxalt-MLT	Rizatriptan benzoate	Migraine	Merck		
Motilium	Domperidone maleate	Motion sickness	J&J		
Pepcid RPD	Famotidine	Antiulcer	Merck		
Seresta Expidet	Oxazepam	Tranquilizer	Wyeth		
Zofran ODT	Ondansetron	Nausea (cancer chemo induced)	GSK		
Zyprexa VeloTab®	Olanzapine	Antipsychotic	Eli Lilly		
Seglor Lyoc	Dihydroergotamine mesylate	Migraine	Sanofi	Lyoc	Cephalon
Propulsid QuickSolv	Cisapride monohydrate	Gastroesophageal reflux disease	Janssen (J&J)		
Risperdal M-TAB/ Quicklet	Risperidone	Schizophrenia, bipolar mania	Janssen (J&J)	QuickSolv	Janssen (J&J)
Fazalco	Clozapine	Schizophrenia	Alamo		
Remeron SolTab	Mirtazapine	Antidepressant	Organon, Solvay	OraSolv	
Tempra® Quicklets/ FirsTabs	Acetaminophen	Analgesic	BMS		Cima (Cephalon)
Alavert	Loratadine	Allergy	Wyeth		
Nulev	Hyoscyamine sulfate	Irritable bowel	Schwarz Pharma	DuraSolv	
Zomig ZMT	Zolmitriptan	Antimigraine	AstraZeneca		
Benadryl Fastmelt	Diphenhydramine pseudoephedrine	Allergy, cold, sinus	Johnson & Johnson	WOW Tab	Yamanouchi (Astellas)
Paroxetine FD	Fluoxetine	Depression, obsessive compulsive disorder	Biovail	Flashdose	Biovail
Zolpidem FD	Zolpidem tartrate	Insomnia	Biovail		
Excedrin Quicktabs	Acetaminophen, caffeine	Pain	BMS		
Febrectol & DolFlash	Acetaminophen	Pain, antipyretic	Ethypharm	FlashTab	Ethypharm
Prevacid SoluTab	Lansoprazole	Duodenal ulcer	TAP		

The preparation of saccharide spinning fiber has two major concerning factors of centrifugal spinning equipment and the type of saccharide used as a carrier.

For spinning equipment, It consists of aluminium spinneret which generates axial centrifugal spinning force, heating element that supplies heat in order to achieve the high temperature for melting, and the collector that is used as collecting or harvesting compartment. In general, the spinning process is carried out by initial

pouring material used into spinneret head. Next, it will be heated until homogeneous mixture was developed. The molten liquid in spinneret is then transferred or delivered through small orifice as a streamline of molten material. Solidification is subsequently occurred after the streamline contact with air and yields the high porous amorphous fiber. The final product is collected via the rolling of the wood stick over the harvesting compartment. The centrifugal spinning velocity is approximately set up at around 2,000-13,000 rpm (Figure 2) (29-31).



Figure 2 Compartmental of centrifugal spinning equipment (4)

When considering the type of saccharide chosen as a carrier in the preparation of saccharide fiber, it can be monosaccharide, disaccharide, polysaccharide and sugar alcohol etc. Sucrose is the most common material for preparing spinning fiber as cotton candy from the past to present (Figure 3). It is an interesting saccharide because of easy to find and inexpensive price. It consists of glucose and fructose that are linked together via glycosidic bond. Sucrose spinning fiber was found to be amorphous nature that was seen from halo X-ray diffraction pattern without any Bragg's respond peaks (Figure 4). It was also appeared in glassy solid state structure. Hence, it could increase the dissolution of poorly aqueous soluble API. Developing of sucrose carrier microfiber loaded with three selected BCS class II (itraconazole, olanzapine and piroxicam) was performed. The result from sucrose carrier microfiber showed the higher dissolution of all APIs compared to either drug particle itself or the physical mixtures of them (4, 32). Furthermore,

amorphous sucrose fiber loaded with olanzapine and piroxicam indicated the higher rate and extent of drug release at absorption site. It would result in an enhancing their oral bioavailability (9).



Figure 3 The physical appearance of sucrose derived cotton candy produced by centrifugal spinning under different storage conditions (33)

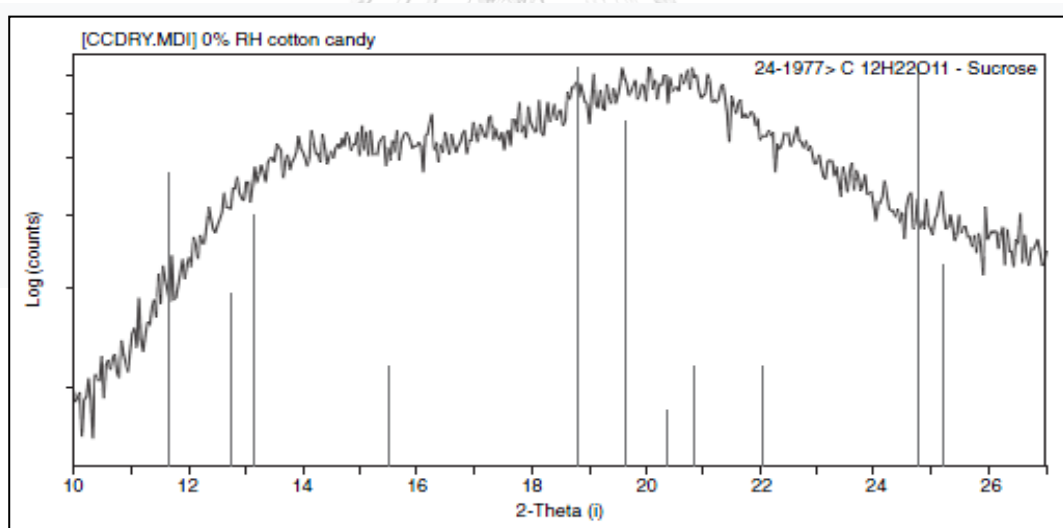


Figure 4 X-ray powder diffraction pattern of sucrose derived cotton candy under temperature of 23°C and 0% RH (33)

Sucrose has two polymorphic forms of I and II. Form I is a stable polymorphic form with high melting point of approximately 185-190°C. Meanwhile, the metastable polymorph of form II shows the melting point around 150-160 °C (34). As described earlier, sucrose is possibly used for producing the fiber. It can be used only itself as saccharide carrier that known as “single floss” or “unit floss” while the combination

between two or more saccharide carriers called “dual floss” or “binder floss” Although sucrose carrier could elevate the dissolution of drug in dosage form, the structure of floss was unstable after exposing with high temperature and humidity. For example, cotton candy or sucrose fiber was prone to hygroscopic and more physically unstable. It would collapse shortly after exposing with high relative humidity (Figure 3). It began recrystallized after keeping in high humidity that shown in distinguished Bragg’s peaks in X-ray diffraction pattern (Figure 5 and Figure 6).

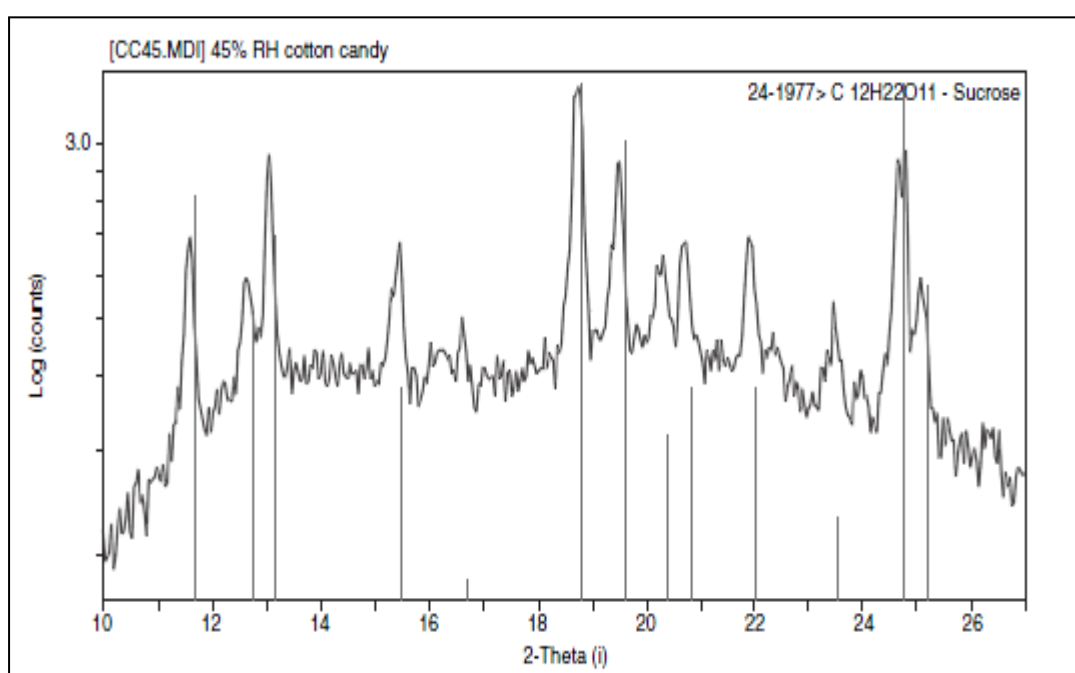


Figure 5 X-ray diffraction pattern of sucrose cotton candy under temperature of 23°C and 45% RH(33)

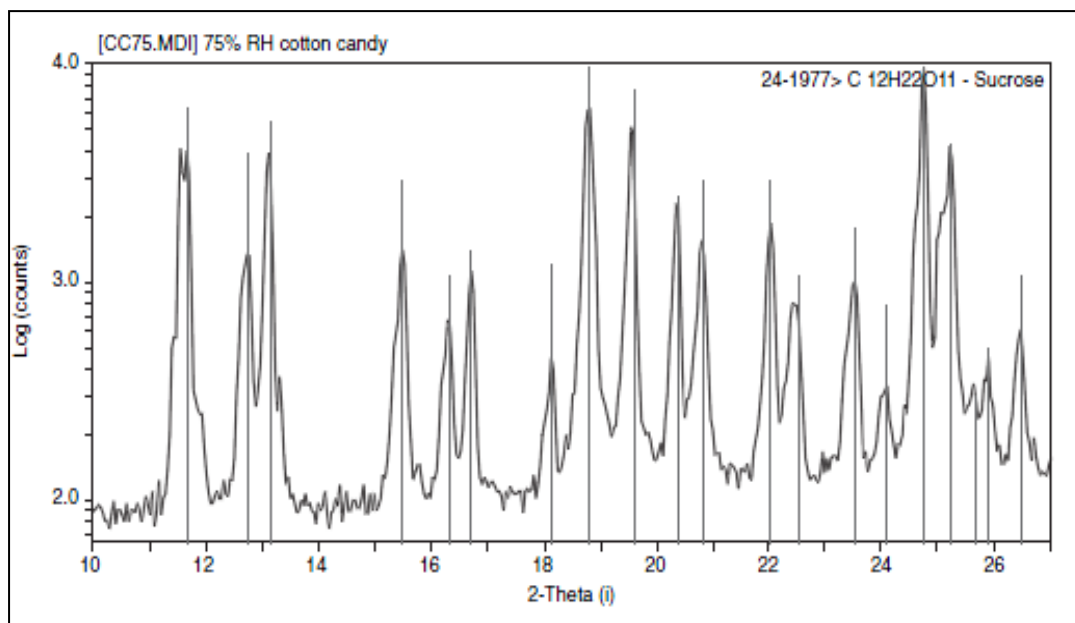


Figure 6 X-ray diffraction pattern of sucrose cotton candy under temperature of 23°C and 75% RH (33)

Disadvantage of sucrose spinning fiber is the high thermodynamically unstable that finally recrystallized of aged sample. It had been demonstrated in case of sucrose fiber loaded olanzapine and piroxicam under high moisture content. The more rapid onset of sucrose recrystallization time containing drugs was investigated when they were kept under higher moisture condition (Table 2).

Table 2 Average onset of sucrose recrystallization time of sucrose fiber containing APIs stored under 11, 33, 53, and 75% RH at 25 °C (9)

sample	relative humidity (%)	XRPD profiles	T_g (mean \pm SD) (°C)	onset of sucrose recrystallization time (mean \pm SD) (days)
sucrose fibers	11	halo pattern	71.1 \pm 4.3	n.o.
	33	sucrose Bragg peaks	n.o.	2.1 \pm 0.8
	53	sucrose Bragg peaks	n.o.	0.8 \pm 0.2 (<1 day)
	75	sucrose Bragg peaks	n.o.	0.7 \pm 0.1 (<1 day)
OLZ–sucrose fibers	11	halo pattern	73.9 \pm 2.1	n.o.
	33	sucrose Bragg peaks	n.o.	23.5 \pm 2.6
	53	sucrose Bragg peaks	n.o.	1.1 \pm 0.2
	75	sucrose Bragg peaks	n.o.	0.9 \pm 0.1
PRX–sucrose fibers	11	halo pattern	69.6 \pm 1.4	n.o.
	33	sucrose Bragg peaks	n.o.	9.0 \pm 1.6
	53	sucrose Bragg peaks	n.o.	1.0 \pm 0.2
	75	sucrose Bragg peaks	n.o.	0.8 \pm 0.1
ITZ–sucrose fibers	11	halo pattern	74.3 \pm 1.9	n.o.
	33	halo pattern	74.1 \pm 2.1	n.o.
	53	sucrose Bragg peaks	n.o.	1.7 \pm 0.8
	75	sucrose Bragg peaks	n.o.	1.1 \pm 0.1

^aBold values highlight significant differences ($p < 0.05$) in the sucrose recrystallization times under 33% RH. n.o. = not observed. Crystalline sucrose 2θ angle peaks: 11.64°, 13.10°, 18.78°, 19.56°, and 24.70°.

Thermodynamically unstable of saccharide spinning fiber from sucrose or cotton candy involved with three major factors of (33, 35-38)

1. T_g , it will be changed from glassy amorphous state to rubbery amorphous state when lower T_g was gained. (33).

2. Amorphous content, it more favored to absorb moisture when more amorphous content was developed (36).

3. Defect on the surface, it was more readily absorb the moisture when more energetic surface defect and resulted in less stability (35, 37, 38).

Aspect of T_g

T_g is the pronouncing factor on the stability of cotton candy. When T_g was lower than temperature of storage condition, it would be changed from glassy amorphous state to rubbery amorphous state. Stickiness from rubbery state was usually found. One of the problem-solving methods was the adjustment of T_g of system. In general, the optimal T_g of system can be attained by mixing two or more compatible components. The mixing of multicomponent to form the homogeneous mixture yields the new material with new T_g ($T_{g(mix)}$). $T_{g(mix)}$ can be simply explained by the relationship of Gordon Taylor (GT) equation as shown herein (39-41).

$$T_{g(mix)} = \frac{[(w_1 T_{g1}) + (kw_2 T_{g2})]}{[w_1 + kw_2]}$$

W_1 and W_2 are the weight fraction of component 1 and component 2, respectively.

T_{g1} and T_{g2} are the T_g of component 1 and component 2, respectively.

K is constant that depends on the interaction between components.

$T_{g(mix)}$ of multicomponent system is based on the interaction between components, weight fraction and T_g of each component. From the above equation, if both substances do not have any interactions with each other. The constant are not taken into account or it takes 1 for calculation.

Crystalline trehalose dihydrate is an interesting saccharide that a high T_g around 74-125°C (42-48). It was therefore selected to mix with sucrose in order to observe the new T_g or $T_{g(mix)}$. Roe and Labuza (2005) determined the $T_{g(mix)}$ of freeze-dried sucrose and trahalose dihydrate system using DSC. They found that the

higher $T_{g(mix)}$ were achieved with the increment of trehalose dihydrate at 4 to 12% by weight. They also concluded that trehalose dihydrate effectively inhibited the recrystallization of sucrose in amorphous freeze-dried product (Figure 7).

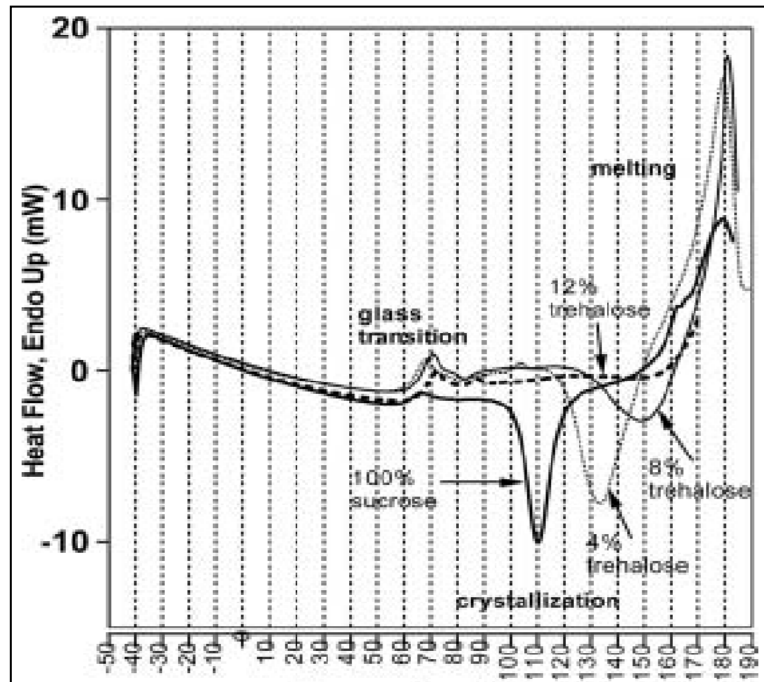


Figure 7 DSC thermograms of freeze dry amorphous sucrose-trehalose mixtures containing various percentage of trehalose (40)

Moreover, Leinen and Labuza (2006) found that the adding of raffinose in spinning sucrose fiber would change the T_g of fiber produced ($T_{g(mix)}$). Pure raffinose (5% w/w) with sucrose (95% w/w) was prepared as fiber and then determined its thermal properties. Fiber produced showed slightly higher $T_{g(mix)}$ compared to that of pure sucrose even kept in different storage condition (Table 3) (49). It was due to the fact that the higher T_g of pure raffinose (around 102-120°C) influenced on the $T_{g(mix)}$ of sucrose fiber composing of raffinose(43, 47, 50). In addition, raffinose could inhibit the recrystallization of sucrose (51). It was explained that raffinose molecule was able to attach with sucrose molecule and directly effect on the formation of sucrose crystal. The plasticizer volume was then lost resulted in slower sucrose crystal growth rate (51).

Table 3 Glass transition temperature (onset and endpoint) of pure sucrose cotton candy and sucrose cotton candy containing 5% raffinose as a function of %RH (49)

System	T_g		Sun <i>et al.</i> (1996)
	Onset (°C)	End (°C)	
11%RH, 100% sucrose	52	65	~ 52
11%RH, 5% raffinose and 95% sucrose	52	67	
33%RH, 100% sucrose	19	27	~26 to 27
33%RH, 5% raffinose and 95% sucrose	22	30	
43%RH, 100% sucrose	7	4	~15
43%RH, 5% raffinose and 95% sucrose	<-20	<-20	

Another method for solving the low T_g of sucrose fiber was goes to the selection of proper storage condition. The suitable storage condition for sucrose fiber should be able to maintain the structure integrity. It should be kept away from excess moisture by impermeable packaging materials of construction e.g aluminium pouch. In addition, the temperature of storage was another importance issue regarding to the T_g . Bhandari and Roos (2016) recommended that amorphous sugar should be placed at the temperature below its T_g in order to preserve the glassy amorphous state. It was due to the slower rate of molecular mobility of sugar molecule at the lower temperature than its T_g . It was then harder to form nuclei and provided the longer progression of nucleation and crystal growth later on.

Aspect of amorphous nature and content

Amorphous content is an important factor on the stability of sucrose fiber. More amorphous content may absorb more moisture due to the more energetic entropy (36, 52). Adding of some surfactants, lecithin, polyethylene glycol (PEG), propylene glycol (PPG), dextrose might be act as crystallization enhancer(11). Subsequently, crystallization was partially occurred and less of amorphous region was remained. The mechanism of crystallization enhancer related to the molecular structure of the surfactant incorporated in the crystal structure of sucrose molecule by hydrophobic and hydrophilic interaction (53). They would delay the nucleation and crystal growth of sucrose molecule. The different size of molecular structure of

surfactant might effect on the delaying of crystallization of sucrose fiber(54). Thus, it would be able to employ surfactants for solving the amorphous-relating problem on the fiber stability (11, 55, 56). The common surfactants used for stabilization of fiber were polyethoxylated sorbitan esters and sorbitan esters, respectively (11).

Cotton candy or spinning fiber of sucrose was amorphous nature (Figure 4) with less stability. The physical structure would collapse with in short time after storage regarding to the recrystallization. At the end of storage, the interconversion of amorphous to crystalline state of sucrose was found at 33% RH and 25°C for 11 days as shown in Figure 8(40). When trehalose dihydrate (25%) was incorporated within sucrose (75%), the fiber produced was also found to be amorphous as shown in Figure 9. However, the longer stability was gained under the same previous storage condition (Table 4). Furthermore, the higher the added amount of trehalose dihydrate the longer the recrystallization time when kept it at higher moisture condition of 54% RH (Table 4).

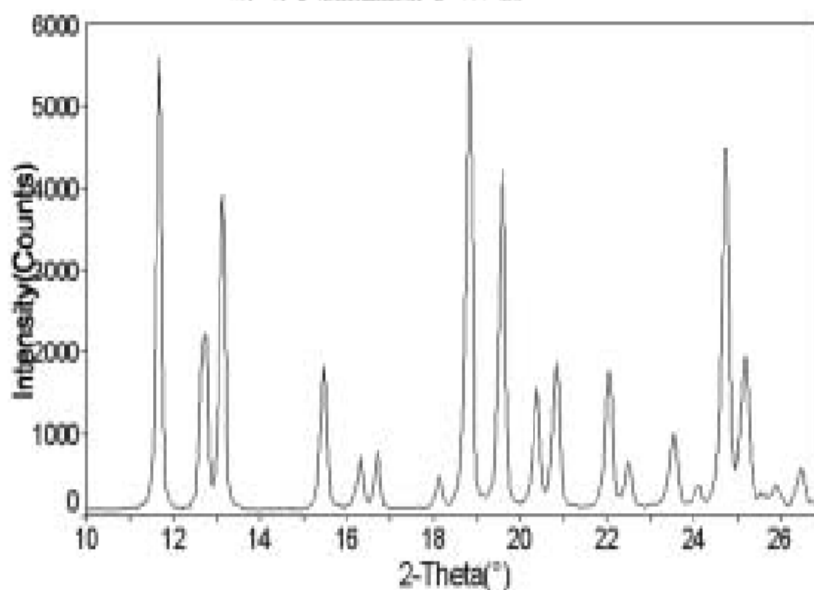


Figure 8 X-ray diffraction pattern of an amorphous pure sucrose cotton candy mixture storage at 33% RH and 25°C(40)

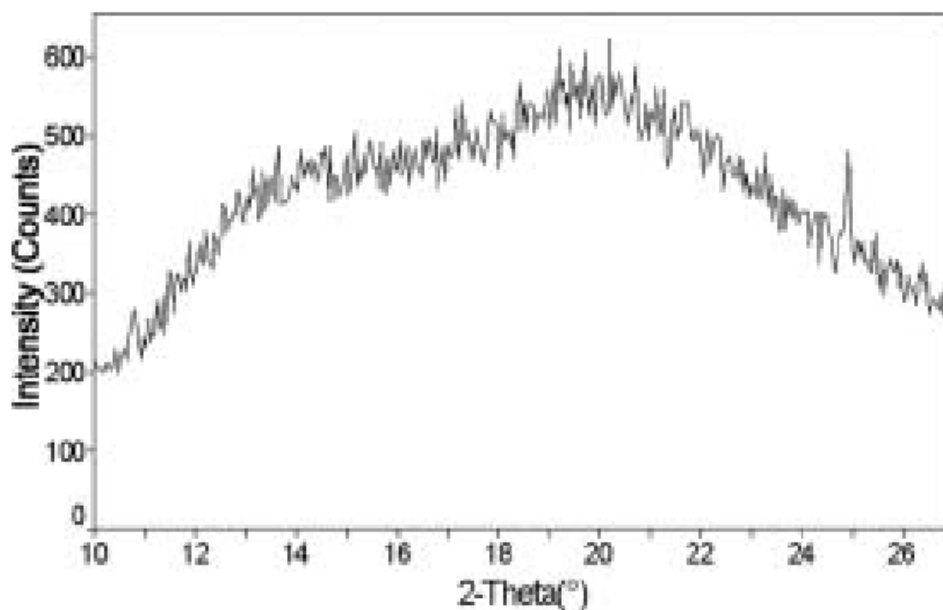


Figure 9 X-ray diffraction pattern of an amorphous 75% sucrose with 25% trehalose cotton candy after storage at 23% RH and 25°C (40)

Table 4 Time to crystallize for sucrose-trehalose cotton candy samples stored at different relative humidity (40)

Storage Humidity	100% sucrose	75% sucrose 25% trehalose	50% sucrose 50% trehalose	100% trehalose
23%	>30 days	>30 days	>30 days	>30 days
33%	11 days	>30 days	>30 days	>30 days
54%	<48 hours	<120 hours	~120 hours	~20 hours

Aspect of surface defect

More defects on the fiber surface induced the less stability on moisture sorption (35, 37, 38). Moisture would be deposited at the high energetic site particularly the defect point on the surface. The adsorbed moisture would be then plasticizer the fiber and resulting in lower T_g , more molecular mobility and less stability. For solving this problem, surface coating with polymer was suggested.

Furthermore, increasing mechanical properties of fiber by nanostructured coating layer could figure out this problem (57). Moreover, surface finishing with zeolite particles of Ultem® 1000 polyetherimide of spinning fiber provide a smoother fiber surface (58). It should be noted that less defect or smooth surface would absorb less moisture (59).

In order to evaluate the level of smoothness of fiber, surface morphology was primarily carried out. Scanning electron microscope was routinely used for such determination. However, it should be employed roughly to discriminate between different fiber surface. Therefore, indirect method of surface smoothness determination based on the ability of moisture sorption of different surface defect was then employed.

Generally, moisture sorption of amorphous materials such as amorphous carbohydrate or lipid showed a specific character. Roudaut and Debeaufort (2011) described that an amorphous saccharide in food more sensitive to moisture. The mechanism of moisture uptake related to an elevating of %RH of an environment and degree of amorphization. Interested system should initially uptake moisture rapidly until water saturated and later provided more molecular mobility of active substance molecule. Seeding or nucleation of active molecule would then occur and excess of water molecule from moisture saturated was subsequently impeded. Therefore, nuclei of active molecule was progressively initiated and eventually recrystallized. Changing of weight as a function of %RH was known as moisture sorption profile. Moisture sorption profile or isotherm was theoretically divided as three zones (Figure 10)

Zone 1: Water molecule from moisture began to be absorbed through pore or channel on the surface of substrate. The arrangement of water molecule was a monomolecular monolayer via Van der Waals interaction.

Zone 2: After saturation of water molecule was achieved, pluri-molecular adsorption on surface monolayer was later occurred. All water molecule adsorbed were held in solid matrix. Weight increase of substance would be found.

Zone 3: Excess water molecule was repelled from matrix. Finally, weight of substance was decreased.

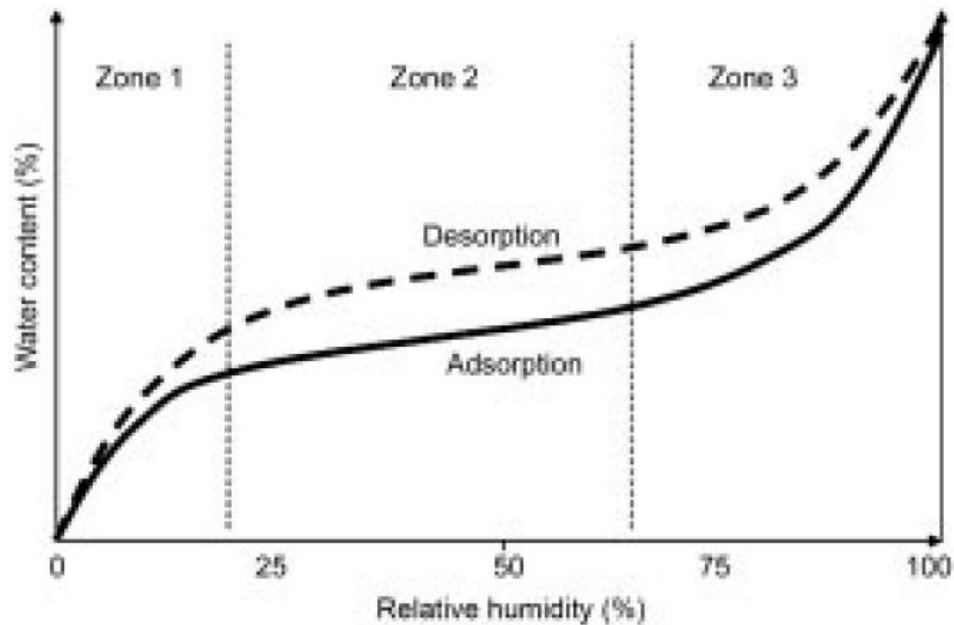


Figure 10 Zone of moisture sorption isotherm (60)

Different patterns of moisture sorption profile were able to relatively compared and implied to the level of surface smoothness. It was due to the fact that the more surface defect usually provided the faster moisture uptake because of more energetic site of defect. Not only water sorption was faster but recrystallization was also faster.

CHAPTER III

MATERIALS AND METHODS

Materials

- crystalline sucrose Lot.25071692 (Mitr Phol Sugar Corp., LTD, Thailand)
- crystalline sucrose Lot.140715102 (Mitr Phol Sugar Corp., LTD, Thailand)
- D-sorbitol Batch no.1405168772 (Ajax fine chem pty., LTD, New Zealand)
- D-fructose Batch no. 0707276 (Asia Pacific Specialty Limited, Australia)
- D-glucose Batch no. AF612114 (Ajax fine chem pty., LTD, New Zealand)
- D-mannitol Batch no. 160712554 (KGaA, Germany)
- D-galactose Batch no. 0120726 (Sigma-Aldrich, United States)
- D-xylitol Batch no.1408772 (Ajax fine chem pty., LTD, New Zealand)
- matodextrin dextrose equivalence 20 Batch no. MFCD00146679 (Sigma-Aldrich, United States)
- lactose anhydrous Batch no.632752 (DOMO[®], Netherlands)
- sodium chloride Batch no.1409179263 (Ajax finechem pty.,LTD New Zealand)
- TREHA[®] or trehalose dihydrate Lot. 6D04 (Hayashibara Co.,Ltd, Japan)

Equipments

- Analytical balance (model MT044, Mettler Toledo, Schwarzenbach, Switzerland)
- Analytical balance (XP205, Mettler Toledo, Schwarzenbach, Switzerland)
- Blender mixer (ROH-FP 135, Ronic Corporation SAS, France)
- Centrifugal spinner (model M500, China)
- Differential scanning calorimetry (Model 822^e, Mettler Toledo, Columbus, USA)
- Thermogravimetric analyzer (TGA/SDTA851^e, Mettler Toledo, Columbus, USA)

- Digital camera (Model EOS 700D, Canon, Tokyo, Japan)
- Fourier Transform Infrared Spectrometer (Model Spectrum one, Perkin Elmer, Massachusetts, United states of America)
- Thermohygrometer (thermometer jumbo electronic Max Min, S. Brannan & Sons Ltd, Cumbria, UK)
- Hot-stage microscope (Model FP82HT, Mettler Toledo, Columbus, United States of America)
- Infrared Thermometer (Type TFI 250, Part No. 1340-1753, ebro®, Germany)
- Polarized Light Microscope (Nikon Eclipse E200, Nikon, Japan)
- Scanning Electron Microscope (SEM model JSM-6400, Jeol Ltd., Tokyo, Japan)
- Scanning Electron Microscope and Energy Dispersive X-ray Spectrometer (SEM model JSM-6610LV and Oxford, X-MaxN 50, Jeol Ltd., Tokyo, Japan)
- X-ray diffractometer (Model Miniflex II, Rigaku, Tokyo, Japan)



Methods

1. Preparation of saccharide fiber using centrifugal spinner

Saccharide fiber was prepared by using centrifugal spinner with the controlling of an environment condition of 22-25 °C and 38-42% RH. Approximate of 20 grams of saccharide material was weighed and transferred into pre-heating pan. Pre-heating temperature of the pan was set up at above melting temperature of saccharide material (not exceeding 3-5 °C). The pan's temperature was monitored using Infrared thermometer. Melting the saccharide with continuously stirred was then performed. After that, molten saccharide was introduced into pre-heating spinneret of spinning head. Centrifugal spinning was then processed. The small and continuous stream of molten saccharide was formed and solidified when contacting with ambient condition. A cluster of solid saccharide fiber was therefore harvested by rolling the wood stick over the collector chamber. It was stored in tightly sealed aluminum foil pouch. The controlling of heating temperature of centrifugal spinning was 4 units analogue-operating. Each unit of analogue-operating was relatively calibrated as temperature using infrared thermometer (10 minutes of heating). Data are shown in Table 5.

Table 5 Calibrating the controlling of heating temperature and heating temperature using Infrared thermometer

Unit of control heating level	Heating temperature (°C)
1	61.4
2	118.7
3	181.5
4	246.3

In case of binary component system, sucrose was utilized as a main component. Meanwhile, another saccharide was added into system as minor component. Sucrose and another saccharide were melted together by sequential melting process in pre-heating pan. The higher melting point saccharide was primarily loaded and

melted until completely molten liquid was gained. Later, the lower one was added and evenly stirred. Molten mixture was then processed with centrifugal spinner as same as mentioned above. Melting temperature of individual saccharides were shown in Table 6.

Table 6 Melting temperature of saccharide

Saccharide	Melting temperature (°C)	References
D-galactose	163-169	(61)
D-glucose	146-165	(34)
D-fructose	102-132	(34)
D-xylitol	92.7	(54)
D-mannitol	162.15-167.8	(62)
D-sorbitol	99.5	(62)
sucrose	140-191	(62)
trehalose dihydrate	215	(63, 64)
maltodextrin DE 20	220-240	(65)

2. Characterization of saccharide fiber

2.1 Fiber morphology

Physical appearance of saccharide fiber was determined by visual observation. Scanning electron microscope (SEM) was additionally performed to observe the morphology and surface of saccharide fiber. The sample was cut in to small pieces and attached on adhesive stub. It was then coated with gold sputter coater at a condition of 15 mA for 3 minutes. The photomicrograph of sample fiber was taken at an acceleration voltage of 15 kV.

Preliminary investigation of non-crystalline state of saccharide fiber was carried out by polarized microscope. A small amount of cutting fiber was placed on glass slide and subjected on stage of microscope. Polarized light setting device was set up in order to investigate the birefringence of saccharide fiber.

2.2 Solid state characterization of saccharide fiber

2.2.1 X-ray powder diffraction (XRPD)

XRPD was used to observe the crystallinity of the saccharide fiber. One gram of fiber was weighed and packed into a low background quartz sample holder. The surface of sample needs to be smoothed by placing the cover glass over the sample with gentle pressing. The experimental condition was indicated as following: $\text{CuK}\alpha$, scan range of $5\text{-}27^\circ 2\theta$ and scan speed at $2.0^\circ 2\theta/\text{min}$.

2.2.2 Thermal analysis

Differential Scanning Calorimetric (DSC)

DSC was used to investigate the thermal history and determined the glass transition temperature of sample fiber. Saccharide fiber of 5-10 mg was weighed in aluminum sample pan $40\ \mu\text{L}$ and hermetically sealed with pin holed lid to allow the evaporation of any volatile residuals. The temperature scan range was -20 to 230°C with the heating rate of $10^\circ\text{C}/\text{min}$. The flow rate at $60\ \text{ml}/\text{min}$ of nitrogen gas was employed as purge gas. STAR^e evaluation software was used for data analysis. The calibration was performed by using indium(66).

Thermogravimetric analysis (TGA)

TGA was employed to examine thermal history and stability of fiber. Saccharide fiber of 5-10 mg was weighed in alumina crucibles $70\ \mu\text{L}$ with pierced lid and was heated from 25°C to 230°C at the rate of $10^\circ\text{C}/\text{min}$. The flow rate at $20\ \text{ml}/\text{min}$ of nitrogen gas was employed as purge gas. STAR^e evaluation software was also used for data analysis. The calibration was also carried out the same as DSC.

3. Molecular interaction among the component of saccharide fiber

Attenuated Total Reflectance Fourier Transform Infrared Spectroscopy (ATR-FTIR) was employed to observe the molecular interaction between saccharides in the system. Sample saccharide fiber was placed on the window of ATR sampling accessory. The detection was carried out within the scan range from 400 to

4000 cm^{-1} . Spectral setup was the average of 64 scans at 4 cm^{-1} resolution. OMNIC software was used for data analysis.

4. Stability investigation of saccharide fiber

4.1 Volume reduction of saccharide fiber

The sample of saccharide fiber around 500 mg were kept in polystyrene plastic bottle without closure. It was then stored in humidity chamber of 75% RH with saturated sodium chloride solution at different temperature of $30\pm 2^\circ\text{C}$, $40\pm 2^\circ\text{C}$ and $2-8^\circ\text{C}$, respectively. The appearances of sample were observed in term of the relatively change in volume and height of a cluster of fiber compared with initial appearance using the scale attached with polystyrene bottle (Figure 11).



Figure 11 Determination apparatus of the relatively change in volume reduction and height of saccharide fiber.

4.2 Moisture sorption profile

The sample was prepared as same as described in 4.1. Periodical determination of weight change as a function of storage time was carried out. The storage condition of 75% RH with at different temperature of $30\pm 2^\circ\text{C}$, $40\pm 2^\circ\text{C}$ was utilized in order to observe the effect of temperature on moisture sorption ability. Correlation between weight changing over storage time was constructed. It was theoretically divided into three phases: initial weight gaining (moisture sorption), moisture saturation plateau, and declination of weight from recrystallization. Determination of the intersection points amidst phases was then performed by using

tangential line of each phase. The first intersection time point (A) between initial moisture sorption and saturation plateau was stated as “transition time” whereas, the second intersection time point (B) between saturation plateau and recrystallization was expressed as “recrystallization time” (Figure 12).

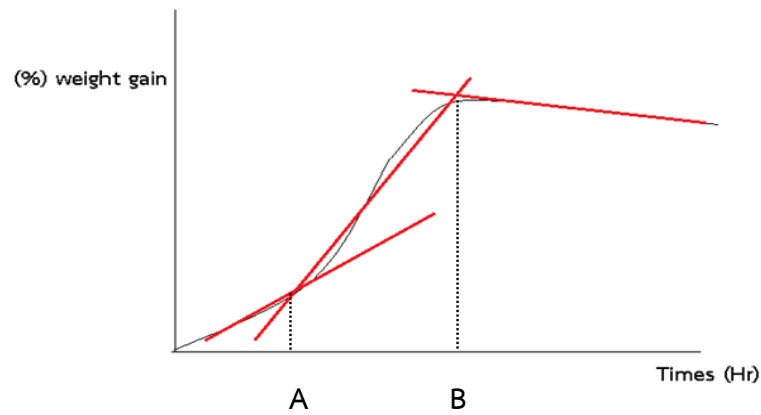


Figure 12 Moisture sorption profile and the determination of transition and recrystallization time of saccharide fiber

CHAPTER IV

RESULTS AND DISCUSSIONS

Preparation of saccharide fiber

1. Monocomponent saccharide fiber

Saccharides used in this study were categorized in four groups: monosaccharide, disaccharide, polysaccharide and sugar alcohol. Monosaccharides were D-galactose, D-glucose and D-fructose. Meanwhile, sucrose, trehalose dihydrate and lactose anhydrous were utilized as disaccharide representatives. Maltodextrin DE 20 as polysaccharide was also employed. In addition, D-xylitol, D-mannitol and D-sorbitol were selected and represented the sugar alcohol. Saccharide of choice was transformed in the form of fiber via centrifugal spinning process. Briefly, molten state of saccharide was prepared by heating and then flowed through the pin of spinneret head. The continuous stream of molten saccharide was generated and exposed to the air at ambient temperature. Subsequently, it was rapidly recrystallized and eventually resulted in the form of solid thread-like matter. It was then harvested and kept in the air-tight container.

All fibers produced from monosaccharide were not able to fabricate. They adhered around collector chamber after spinning as shown in Figure 13. It might be due to the low glass transition temperature (T_g) (lower than ambient temperature). Raw materials of monosaccharide used were generally as a crystalline material (without T_g). If they were converted to amorphous counterpart, their amorphous T_g were found to be nearly or lower than room temperature as shown in Table 7.

Amorphous rubbery state of fiber produced from monosaccharide should be therefore occurred. They were not possibly form the stable fiber due to the lower T_g . On the one hand, all sugar alcohols provided the same results as monosaccharides. The fibers were not able to collect because of the rubbery like appearance. It was expected that the lower T_g of amorphous fiber produced was obtained(67-69). In

addition, imprecisely controlled moisture during preparation also played a crucial role on the lowering of amorphous T_g due to plasticization effect(35). It should be therefore taken into account for the ability of fiber formation.

Theoretically, the fiber of maltodextrin should be formed because amorphous T_g of freeze dried maltodextrin was around 141°C that obviously higher than room temperature (Table 7). Unfortunately, the brownish molten liquid of melt maltodextrin was investigated before spinning and did not able to generate fiber successfully. The melting decomposition of maltodextrin was then proposed as a major concern. Maltodextrin is naturally derived material from starch which has the melting point of 240 °C. Thermal analysis (thermogravimetry, TGA) of maltodextrin showed two consecutive weight losses of moisture evaporation at around 70-100 °C followed with flash decomposition (200-350 °C)(32). The pronounced of secondary weight loss directly determined an irreversible decomposition. Hence, it was in good agreement that decomposition of maltodextrin affected on the formation of spinning fiber.

In case of disaccharides, spinning fiber of lactose anhydrous was not able to fabricate even it had a higher T_g of 101 °C(70). It might due to the decomposition of anhydrous lactose at temperature of melting (around 240 °C) that could be investigated from the caramelization as brownish color as shown in Figure 13(C1). It was the good supporting evidence on the non-forming fiber produced from lactose anhydrous. Thermal analysis (DSC) of anhydrous β -lactose revealed only single endotherm of melting followed with obvious decomposition at 234 °C that could be seen from significant weight change during TGA (71). The heating energy consumption with the disappearing of mass indicated the combustion of matter. Therefore, it should be concluded that lactose anhydrous decomposed during centrifugal spinning process. On the other hand, sucrose and trehalose dihydrate could be utilized to form spinning fiber [Figure 13(C2 and C3)]. They provided a fluffy with continuous fiber character and stable after freshly prepare.



Figure 13 Physical appearance of saccharide fiber produced from different saccharide groups. (A) monosaccharide (B) sugar alcohol (C) disaccharide and (D) polysaccharide

Table 7 Amorphous glass transition temperature of selected saccharides

Type of saccharide	Amorphous T_g (°C)	References
Monosaccharide		
D-galactose	32	Bhandari B.R., et al.1999. (72)
D-glucose	31	Athanasia G.M., 2017. (73)
D-fructose	16	Truong V. et al. 2004. (74)
Disaccharide		
sucrose	52 62 67 75	Leinen K.M., et al. 2005. (49), Athanasia G.M., 2017. (73), Martinez M.L., et al. 2011. (46), Shamblin S.L., et al. 1996. (48),
trehalose dihydrate	74 115	Chen (45) T., et al. 2002. (45), Martinez M.L., et al. 2011. (46),
lactose anhydrous	120 101	Shamblin (48) S.L., et al. 1996. (48) Roos Y., et al. 1991.(70)
Polysaccharide		
Maltodextrin 20 DE	141	Bhandari B.R., et al. 1999. (72)
Sugar alcohol		
D-xylitol	-29	Roos Y. 1993. (67)
D-mannitol	-7.4	Yoshinari T., et al. 2003. (68)
D-sorbitol	-3.4	Yu L.,et al. 1998.(69)

According to the T_g viewpoint, two major factors of the amorphous content and the plasticization (from environmental moisture) were taken into consideration. T_g of fiber produced should be influenced from both governing factors. The DSC results showed that T_g of sucrose fiber and trehalose anhydrous fiber were found to be 58.13 and 60.10°C, respectively (Figure 14). They were higher than ambient temperature that glassy state should be obtained. They were therefore possible to form stable fiber. Nevertheless, they eventually collapsed within an hour under uncontrolled ambient condition. It was due to fact that the microstructure of fiber

produced was non-ordered molecular arrangement or amorphous state (Figure 15(B)). XRPD patterns of raw sucrose and trehalose dihydrate powder exhibited sharp and intense Bragg's peaks which strongly indicated well-ordered internal structure of crystalline state (Figure 15(A)). Meanwhile, diffused XRPD patterns were observed in case of sucrose and trehalose anhydrous spinning fiber. Thus, crystalline sucrose and trehalose dihydrate were transformed to amorphous sucrose and trehalose anhydrous form via centrifugal spinning process. Generally, amorphous could absorb moisture faster than its crystalline counterpart due to the plasticization effect of ambient moisture (75, 76). When focusing on the ability of moisture in environment as a plasticizer, the chemical interaction between amorphous fiber and water molecule should be investigated. As a result of ATR-FTIR, band broadening ($3200\text{--}3600\text{ cm}^{-1}$ representing OH stretching) was determined in both sucrose fiber and trehalose anhydrous fiber (Figure 16 and Figure 17)(77). It revealed the interaction between water molecule from moisture and amorphous state of disaccharide used in fiber produced via hydrogen bonding (78-80). Furthermore, the disappearing of characteristics bending peak of water of crystallization at 1688 cm^{-1} of trehalose dihydrate was also observed (81). Two more peaks of $998, 957\text{ cm}^{-1}$ that represented CO stretching and CCH stretching of trehalose molecule also slightly downward shifted (Figure 17) (82-84). All of this finding confirmed an anhydrate state of trehalose after spinning. It could be concluded that hydrogen bonding was formed when moisture interacted with amorphous sucrose fiber or amorphous anhydrous trehalose fiber.

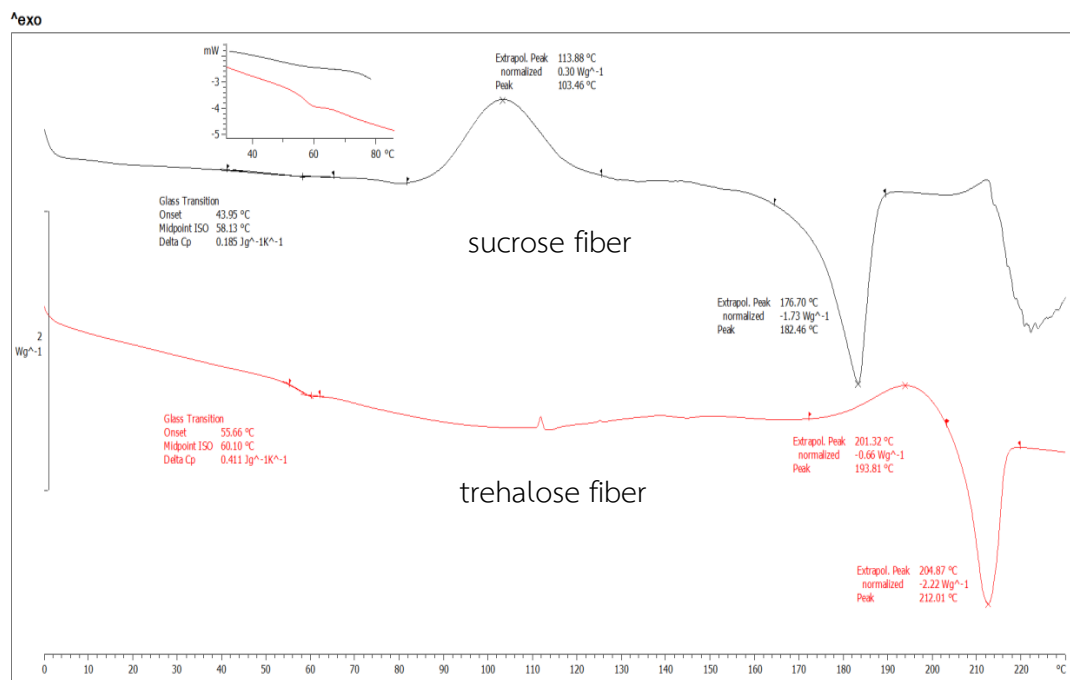


Figure 14 DSC thermogram of sucrose fiber and trehalose anhydrous fiber

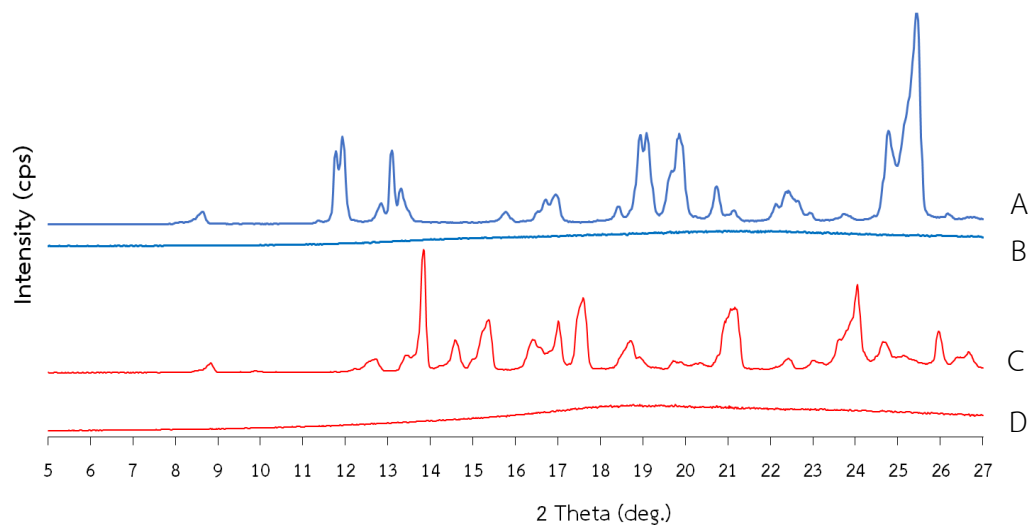


Figure 15 X-ray powder diffraction of (A) crystalline sucrose, (B) fiber produced from sucrose, (C) crystalline trehalose dihydrate and (D) fiber produced from trehalose dihydrate

The possibility of fiber preparation from saccharide was closely related to the molten ability that should not decompose after melting. It was due to the fact that the melting with decomposition of saccharide demonstrated non-fibered appearance. Not only the stability of molten saccharide but T_g of saccharide was also taken into consideration for fiber formation. Because of the lowering of T_g of fiber produced after centrifugal spinning, the high T_g saccharide should be used as starting material in order to gain a stable fiber with specified T_g over ambient temperature that would exhibit the glassy state.

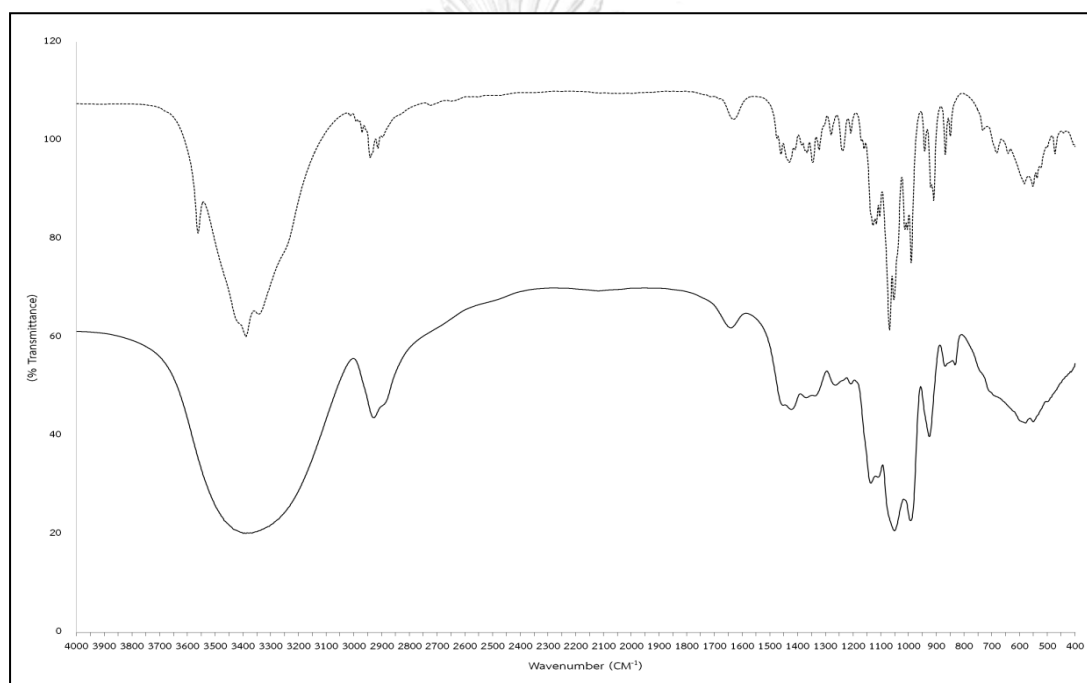


Figure 16 ATR-FTIR spectra of crystalline sucrose (upper line) and sucrose fiber (lower line)

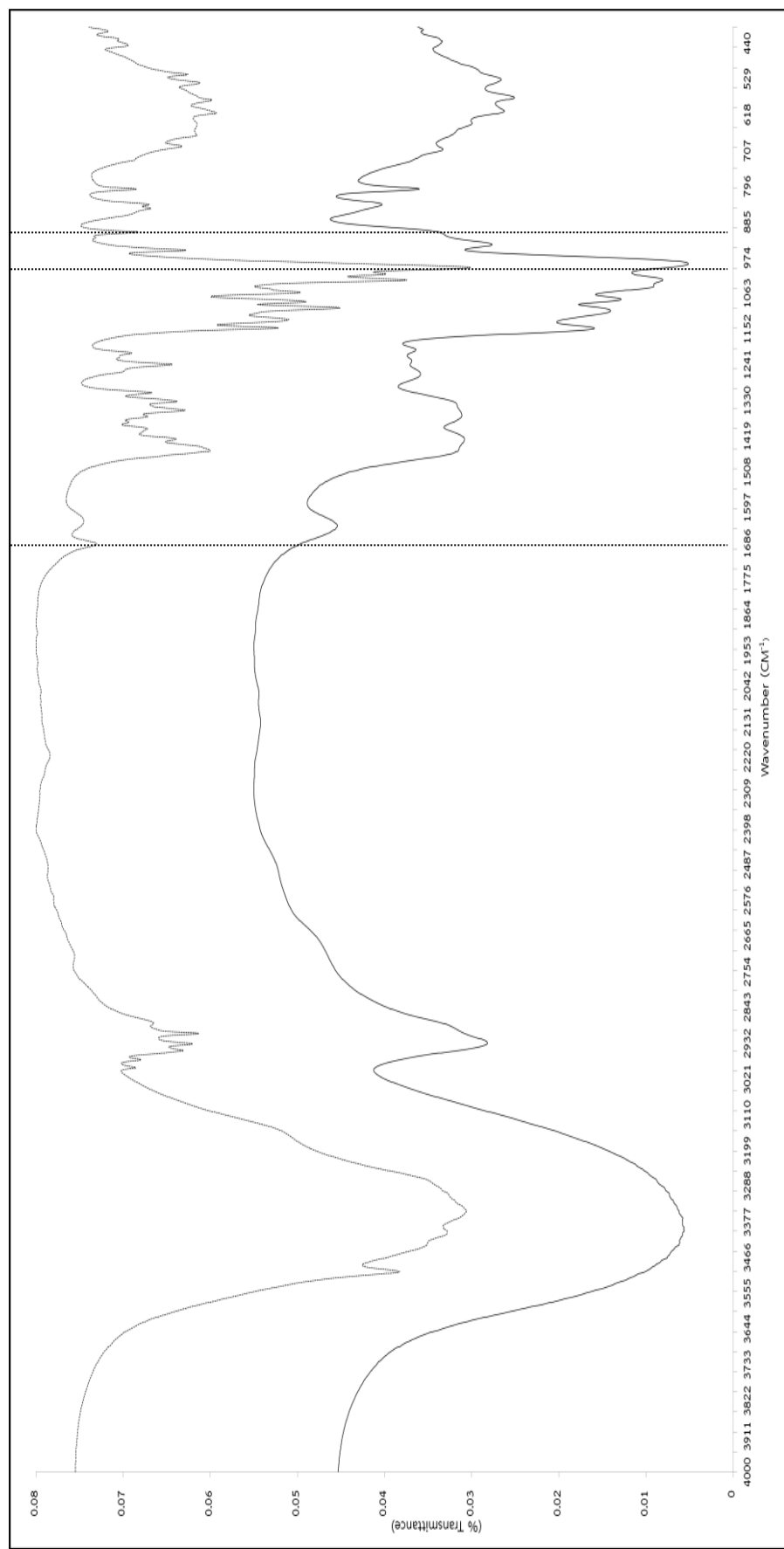


Figure 17 ATR-FTIR spectra of crystalline trehalose dihydrate (upper line) and trehalose (anhydrous) fiber (lower line)

2. Binary component saccharide fiber

From previous studies, it should be considered that sucrose and trehalose dihydrate were the good choices for fabricating centrifugal spinning fiber. It was due to an acceptable physical stability that would be seen from non-fusing fiber after contact with moisture at temperature of 30 ± 2 °C, $75\pm 5\%$ RH within an hour (Figure 18 and Figure 19). Upon reconsideration, sucrose provided more benefits over trehalose dihydrate such as readily water soluble, commercial availability and reasonable price. It would be then used as major component of spinning fiber in this study. Nevertheless, sucrose fiber produced collapsed or fused within short term period (around 1 hour) that too short for handling.

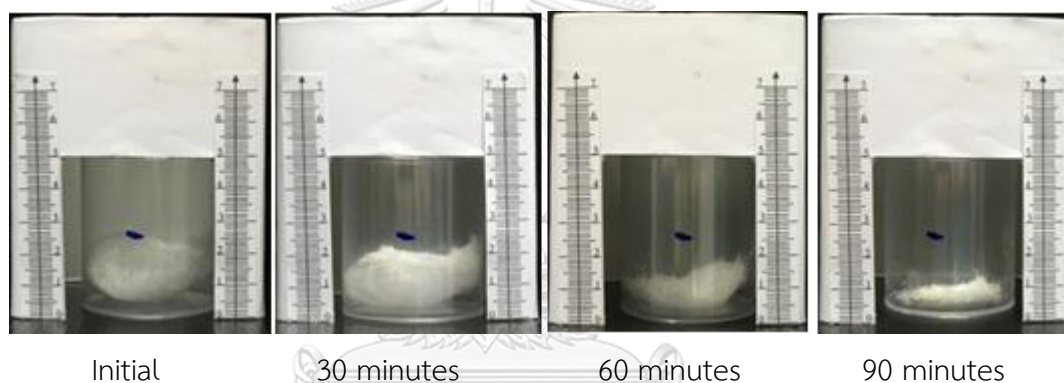


Figure 18 Physical appearance of the sucrose fiber during storage at temperature of 30 ± 2 °C, $75\pm 5\%$ RH over time

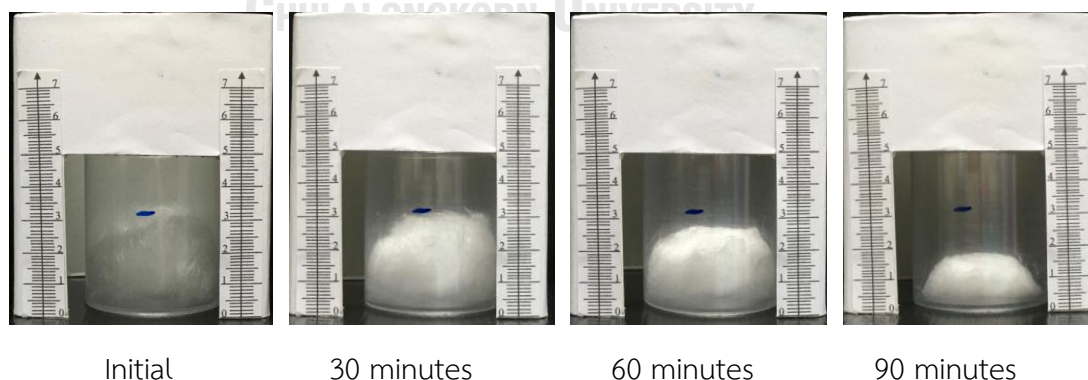


Figure 19 Physical appearance of the trehalose dihydrate fiber during storage at temperature of 30 ± 2 °C, $75\pm 5\%$ RH over time

It would be hypothesized that thermodynamically unstable state of spinning fiber from sucrose was achieved (33, 35-38). Three major critical factors involved the instability of fiber were as follows:

1. The lower the T_g the more the chance of rubbery amorphous state (33)
2. The higher the amorphous content the more the moisture sorption (36)
3. The higher the more defect of surface area the less the stability (35, 37, 38)

One of the most promising approaches for overcoming the instability of fiber produced was the elevation of the T_g of amorphous saccharide system. Theoretically, the mixture of different components would show the T_g of system ($T_{g(mix)}$) regarding to both weight fraction (w) and their own individual T_g as described in Gordon-Taylor (GT) equation (11, 40, 51). More recent development of GT equation, the interaction between components (K) was reconsidered and shown below as modified GT equation (eq 1 (39)).

$$T_{g(mix)} = \frac{[(w_1 T_{g1}) + (K w_2 T_{g2})]}{[w_1 + K w_2]} \quad \text{Equation 1}$$

where w_1 and w_2 are the weight fraction of component 1 and 2

T_{g1} and T_{g2} are T_g of component 1 and 2

K is interaction between component 1 and 2

In this study, no interaction between components was assumed and K was therefore equal to be 1. Simple GT equation was then used as a model. For getting higher T_g of amorphous sucrose fiber produced, higher T_g saccharides (compared with T_g of sucrose) were chosen and incorporated into sucrose component. However, lower T_g saccharides were also investigated to confirm the changing of $T_{g(mix)}$ as ascribed in eq 1. Either lower or higher T_g saccharide was mixed with sucrose at weight ratio of 1:1. The evaluation of such blending saccharides with sucrose was primarily determined by the finding of $T_{g(mix)}$. In addition, the structural integrity of fiber produced was further assessed by both crystallinity and physical appearance determination.

The lower T_g saccharides were selected and found to be D-mannitol, D-fructose and D-glucose whereas the higher one were lactose anhydrous and

trehalose dihydrate (40, 68, 73, 74). After freshly prepared fiber via centrifugal spinning process, the pure sucrose fiber was continuous length and fluffy fiber (Figure 20A). It showed the T_g of 58.13°C that would be an amorphous glassy state (Figure 14). Therefore, it should retain its structural integrity and stable for longer period after storage. Unfortunately, it collapsed and fused together until dense fiber structure was achieved after exposing at 30±2°C, 75±5% RH for 90 minutes (Figure 18). T_g was thus not found to be only the main factor governing on the stability of sucrose fiber. Surface morphology of sucrose fiber was then focused and observed. It was clearly seen that rough and more defect of surface of sucrose fiber was occurred after fiber formation (Figure 20B,C and D). The more the defects the more the ability to get absorbs moisture(59). Owing to the surface roughness with quickly absorbed moisture(59), absorbed water strongly impacted on both plasticization and increased the molecular mobility of sucrose molecule in fiber (35, 38). Subsequently, the T_g of storage sucrose fiber downward shifted to 41.22°C (Figure 21) which lower than that of former structure. However, the physical appearance was unchanged.

For binary component, the saccharides that had a lower T_g were mixed with sucrose and spun to form fiber. All fiber produced were sticky and collapsed within a few seconds (Figure 20B,C and D). They appeared as amorphous that would be seen from halo pattern without any Bragg's peak responses of XRPD (Figure 22). As a result of $T_{g(mix)}$ determination, T_g of sucrose fiber containing D-mannitol, D-glucose and D-fructose were found to be 4.54, 2.42 and -3.15°C that obviously lower than ambient temperature (Table 8). Hence, they were well agreed on the instability of fiber due to the rubbery amorphous characters. In addition, surface defect of all samples supported the plasticization effect dealing with more absorbed water from surrounding that eventually increased molecular mobility of sucrose in fiber. Even focusing on the sucrose-D-glucose system (Figure 22D), it would argue that partial crystalline was appeared as seen from few Bragg's peaks at 21 and 26 °2 θ but it still showed a more nature of amorphous including lower T_g and more defect surface. It would hence totally provide less stable fiber. Conclusively, mixture between sucrose and lower T_g saccharides provided an unstable spinning fiber that would be the

result of three mentioned factors of low T_g (mix), rubbery amorphous in conjunction with surface roughness.

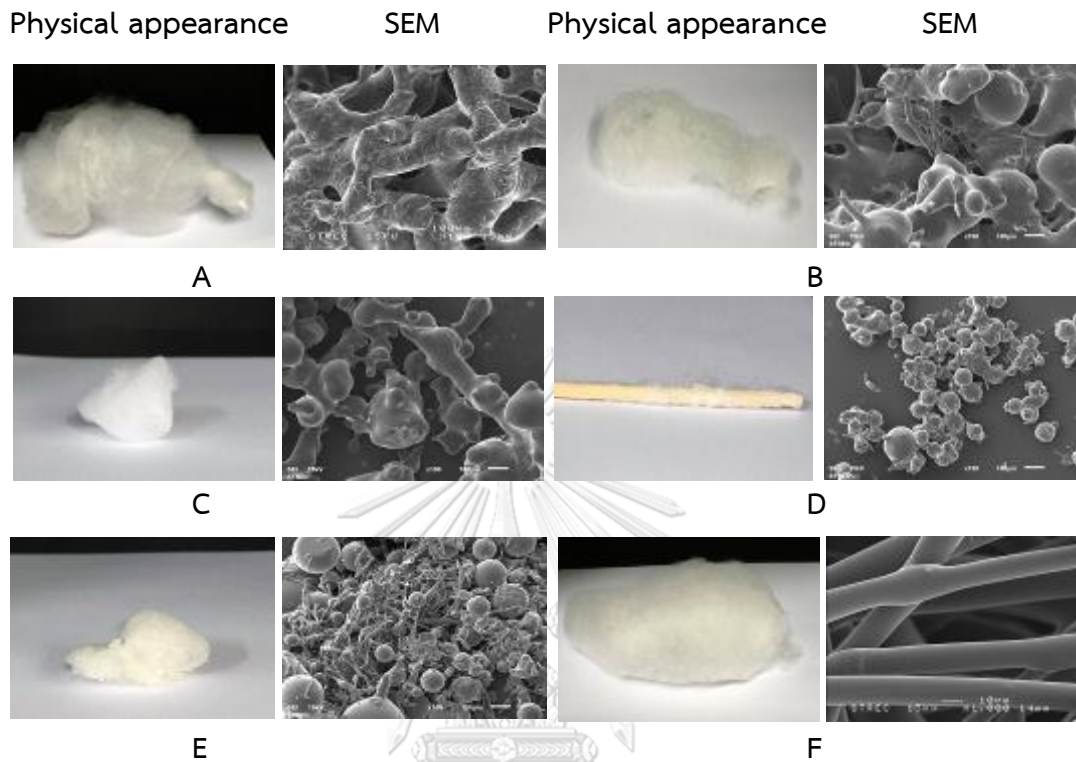


Figure 20 Physical appearance (left panel) and Scanning electron photomicrograph (right panel) of sucrose fiber containing saccharides at weight ratio of 1:1. ((A) sucrose without any saccharides, (B) sucrose containing D-fructose, (C) sucrose containing D-glucose, (D) sucrose containing D-mannitol, (E) sucrose containing lactose anhydrous and (F) sucrose containing trehalose dihydrate)

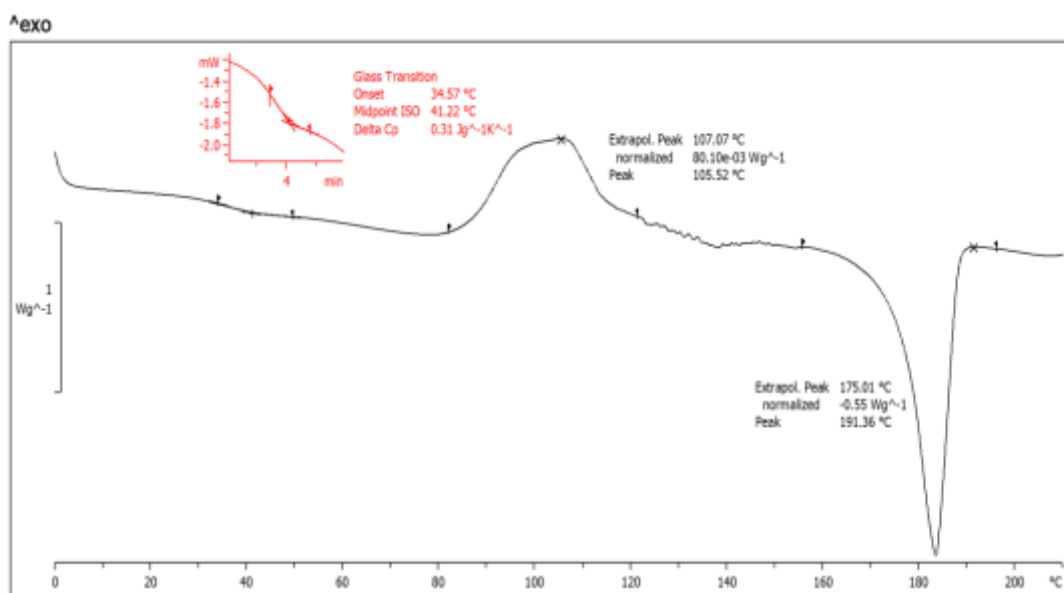


Figure 21 DSC thermogram of storage sucrose fiber at ambient condition for 3 days

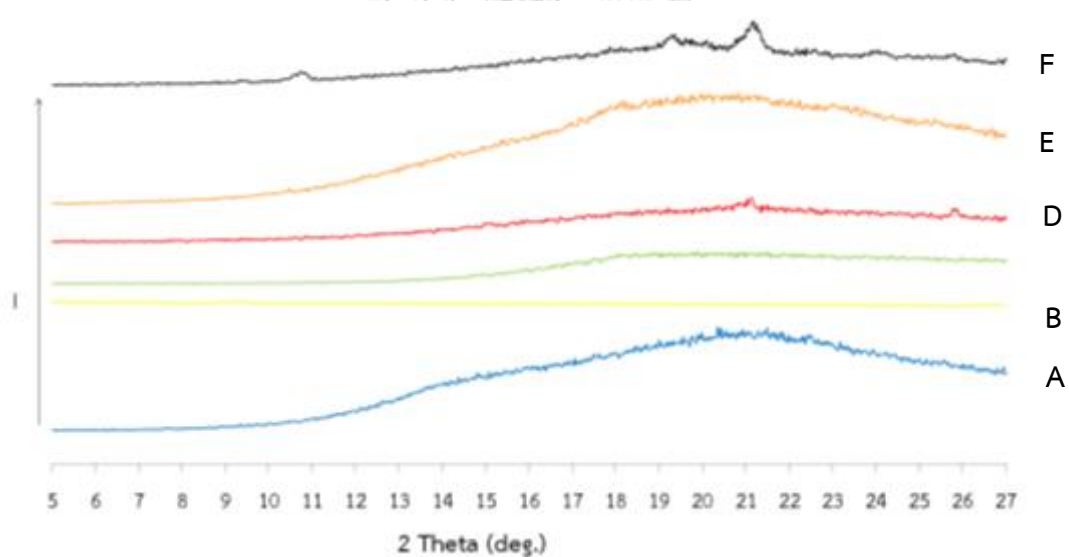


Figure 22 X-ray powder diffractograms of sucrose fiber containing different type of saccharides at weight ratio 1:1 (A – pure sucrose, B – sucrose and D-mannitol, C– sucrose and D-fructose, D – sucrose and D-glucose, E – sucrose and trehalose dihydrate, F – sucrose and lactose anhydrous)

Table 8 The calculated and experimental $T_{g (mix)}$ of sucrose fiber containing different saccharides at weight ratio of 1:1

Saccharides	T_g (°C)	$T_{g (mix)}$ (°C)	
		Calculated*	Experimental ^{***}
D-mannitol	-7.4	32.77	4.54
D-glucose	31.0	44.57	2.42
D-fructose	16.0	37.07	-3.15
lactose anhydrous	101.0	79.57	8.57
trehalose dihydrate	60.1 ^{**}	60.12	44.16

* Calculating from simple GT equation

** From the experimental of centrifugal spinning fiber produced

*** See appendix 1

Remark: T_g of sucrose fiber was 58.13 °C

On the other hand, higher T_g saccharides either trehalose dihydrate or lactose anhydrous was also mixed with sucrose at weight ratio of 1:1 to form spinning fiber. The results revealed that sucrose fiber containing trehalose was found to be fluffy appearance with more physically stable. It would be easily prepared and harvested. Meanwhile, the sucrose fiber containing lactose anhydrous was not easy to fabricate and handle. It seemed to be a sticky thread that collapsed within a few seconds after preparation (Figure 20E). $T_{g (mix)}$ of sucrose fiber containing trehalose and lactose anhydrous were found to be 44.16 and 8.57°C, respectively (Table 8). However, sucrose fiber containing lactose anhydrous showed the remarkable differentiation in term of T_g compared to that of trehalose. $T_{g (mix)}$ of fiber containing lactose anhydrous was lower whereas fiber containing trehalose was higher than ambient temperature. Therefore, the addition of trehalose dihydrate into spinning sucrose fiber provided the $T_{g (mix)}$ that higher than ambient temperature. It should thus be existing as glassy nature with appreciable stability.

When considering the solid state structure aspect, amorphous state of fiber would be a great of interest. Sucrose fiber containing trehalose revealed non-ordered

molecular arrangement as seen from the amorphous halo pattern (Figure 22E). Whilst amorphous containing some of crystalline was found in case of sucrose with lactose anhydrous fiber. It would be the result of non-homogeneous blending between sucrose and lactose anhydrous at higher temperature during molten step before spinning. Solid crystal of lactose anhydrous still existed in molten sucrose even higher temperature of blending was achieved. Thus, seed nucleation or also known as “seeding” of lactose would be proposed after gaining the fiber. It induced the nucleation of crystalline solid by reducing the activation energy of the barrier for nucleation and crystal growth (85, 86). Recrystallization would be then observed in XRPD (Figure 22F).

Fiber morphology was further assessed in order to evaluate the physical stability. Smooth surface was acquired in case of trehalose whereas lactose anhydrous yielded rougher fiber surface with non-continuing thread nature (Figure 20E and F). Therefore, sucrose fiber containing trehalose should be more stable than that of lactose anhydrous due to the less of moisture sorption ability from less energetic site of defected surface. In conclusion, the important factors affecting the physical stability of binary component of higher T_g saccharides were the $T_{g(mix)}$ and the surface defect of fiber produced.

Binary mixture between sucrose (major component) with different saccharides (minor component) obviously provided various characters of spinning fiber. The saccharide with lower T_g allowed the less structural stability but the higher one should give the more stable fiber. Furthermore, the more surface defect of saccharide fiber showed the faster moisture sorption (38, 59). The most promising of fiber produced from binary component in this study was goes to the mixture between sucrose and trehalose with T_g of 44.16 °C, amorphous nature including smooth surface. Nevertheless, binary component at 1:1 weight ratio would not provide the better fiber in term of physical stability comparing to that of mono component of trehalose anhydrous fiber. It could be seen from the reduction of estimated volume of fiber produced upon storage (Figure 23).

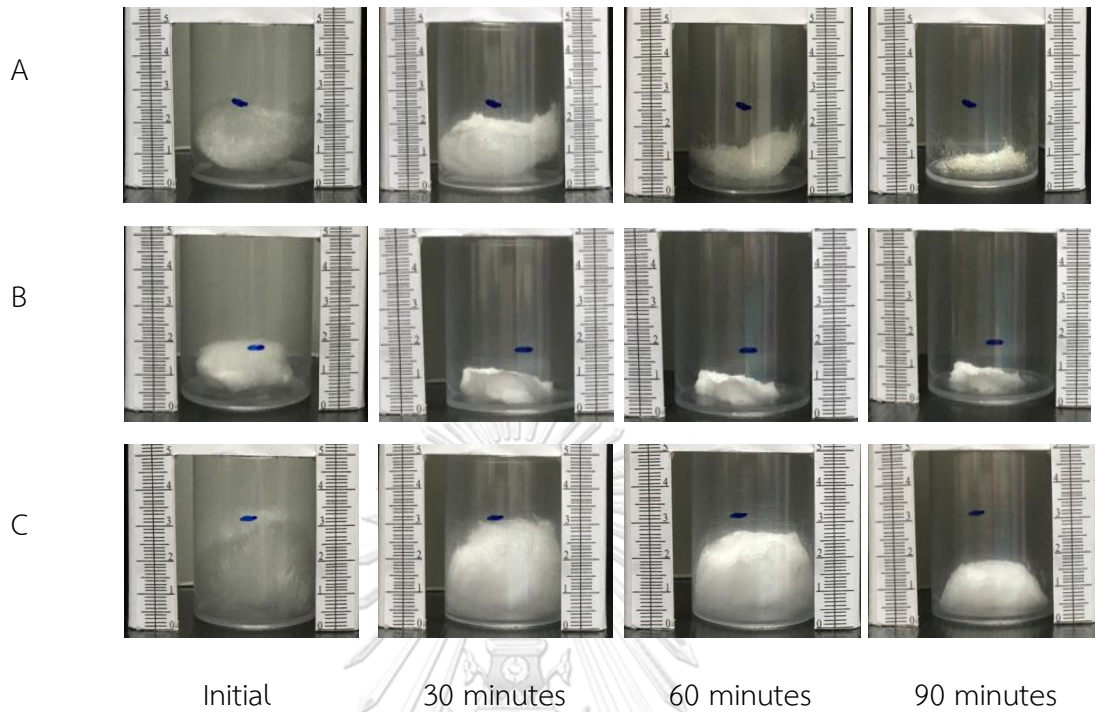


Figure 23 Estimated volume reduction of saccharide fiber upon storage at $30\pm 2^\circ\text{C}$, $75\pm 5\%$ RH. (A) sucrose, (B) mixture of sucrose and trehalose dihydrate at 1:1 weight ratio and (C) trehalose anhydrous

3. Effect of the amount of trehalose dihydrate on the glass transition temperature of spinning sucrose mixture fiber

From previous studies, blending between trehalose dihydrate with sucrose at 1:1 weight ratio resulted in less stable physical appearance of fiber upon storage (Figure 23B). It was expected that $T_{g(mix)}$ of system would be lower or rubbery state might be formed. Therefore, the effect of different weight ratios between sucrose and trehalose dihydrate on the $T_{g(mix)}$ was investigated. According to simple GT equation, blending of two components without any interaction should provide a linear relationship of $T_{g(mix)}$ as a function of weight fraction and T_g of each component. The mixing of various amounts of trehalose dihydrate into sucrose system should thus reveal a value of $T_{g(mix)}$ as presented in Figure 24 (dash line). Unfortunately, non-linear (curvature) relationship between $T_{g(mix)}$ and weight ratio between sucrose and trehalose dihydrate was observed in this study. (Figure 24)

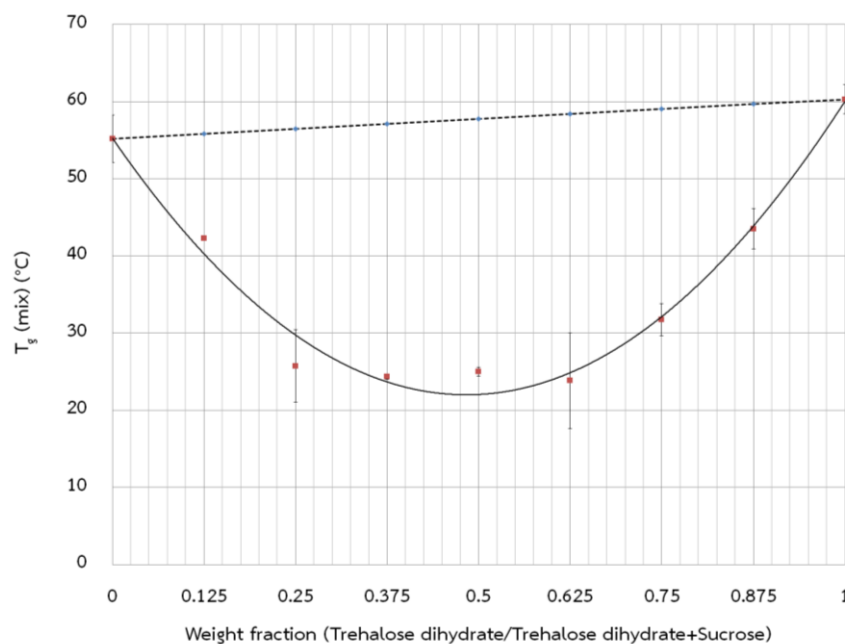


Figure 24 Glass transition temperature of sucrose fiber containing trehalose dihydrate [$T_{g(mix)}$] at various weight ratios: (dash line) $T_{g(mix)}$ calculated from simple GT equation, (solid line) $T_{g(mix)}$ from experiment results

Data are shown as mean \pm sd in Table 11 (Appendix 2)

Trehalose dihydrate was incorporated into sucrose fiber at the different weight ratios of 0, 12.5, 25.0, 37.5, 50.0, 62.5, 87.5 and 100.0 in order to investigate the stability of fiber after exposing with high temperature and humidity. They were acquired as continuous length fiber with less defect on the surface compared to that of pure sucrose fiber (Figure 25 and Figure 26). The smoother of fiber surface did not depend upon “how much trehalose dihydrate was added” because the lowest concentration incorporated of trehalose dihydrate (12.5% w/w) still provided less defect and smooth texture. In addition, they were existed as amorphous which were seen from XRPD halo pattern (Figure 27).

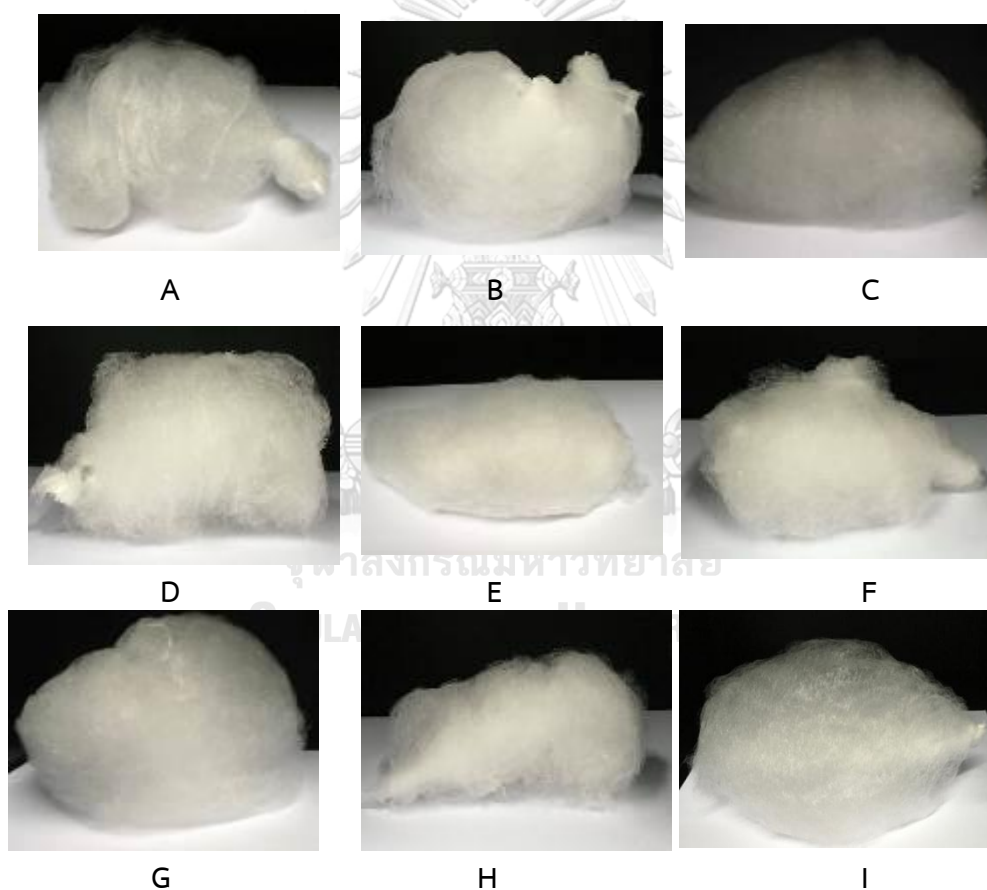


Figure 25 Physical appearance of sucrose fiber containing trehalose dihydrate at different weight ratios (A) 100.0:0, (B) 87.5:12.5, (C) 75.0:25.0, (D) 62.5:37.5, (E) 50.0:50.0, (F) 37.5:62.5, (G) 25.0:75.0, (H) 12.5:87.5, and (I) 0:100.0

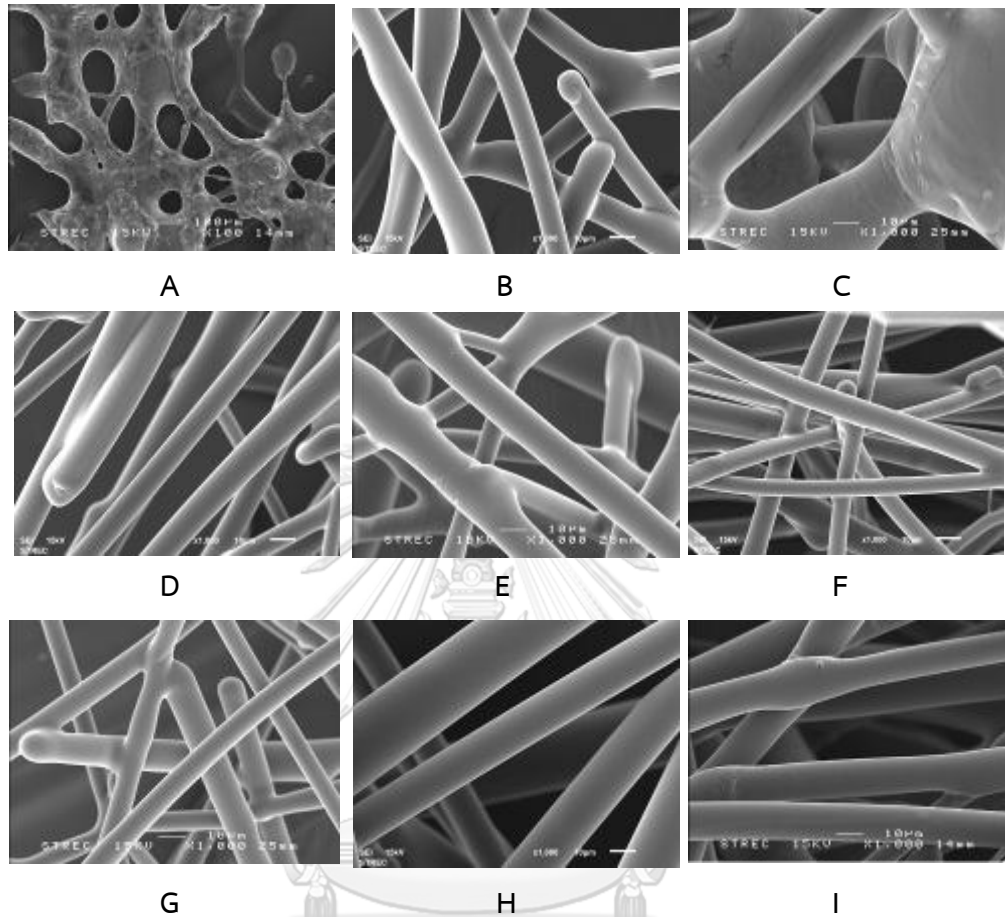


Figure 26 Scanning electron photomicrograph of sucrose fiber containing trehalose dihydrate at different weight ratios (A) 100.0:0, (B) 87.5:12.5, (C) 75.0:25.0, (D) 62.5:37.5, (E) 50.0:50.0, (F) 37.5:62.5, (G) 25.0:75.0, (H) 12.5:87.5, and (I) 0:100.0

From Figure 24, the decrement of T_g (mix) demonstrated the physically unstable of fiber upon storage at temperature of 30 ± 2 °C and $75 \pm 5\%$ RH. The physical instability of fiber was seen from the volume changing of fiber or the collapsible nature under specified storage condition (Table 9). All fibers showed the lower T_g which were nearly ambient temperature that reflected the existing of rubbery state. They should theoretical collapse due to the more molecular mobility and interaction with moisture.

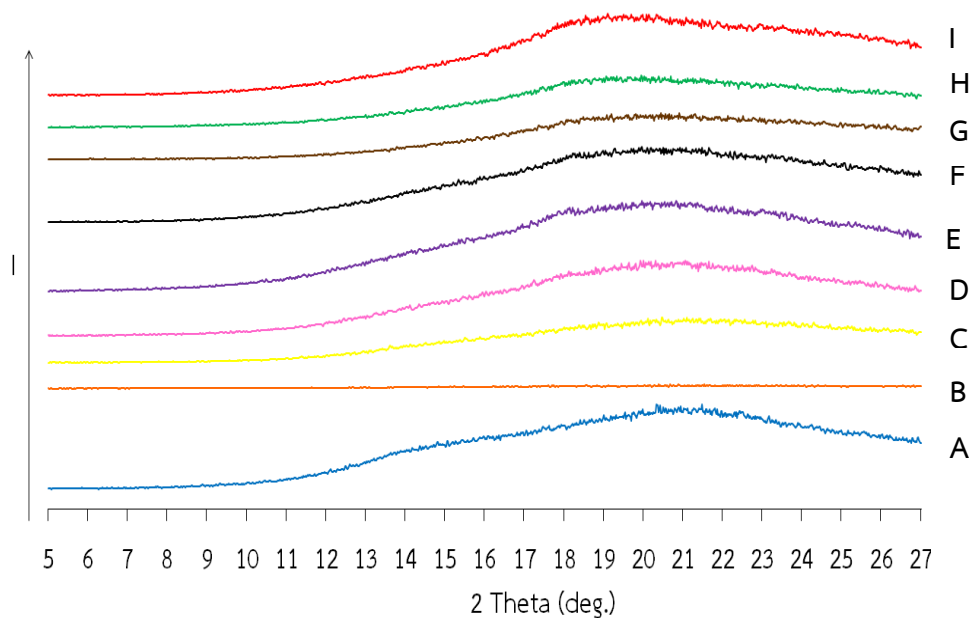
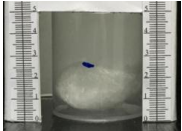

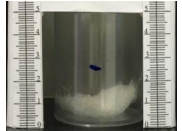
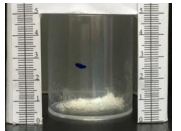
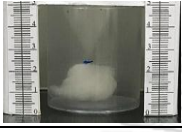

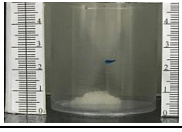
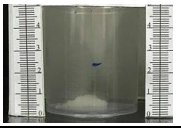
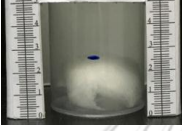

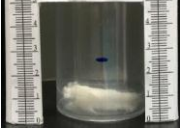

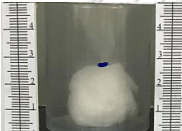


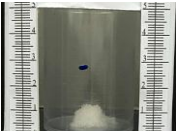
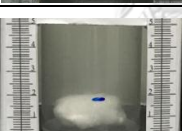

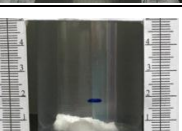

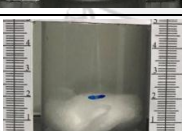
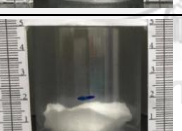

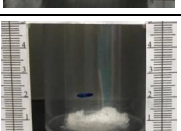
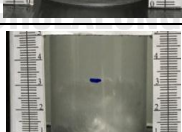
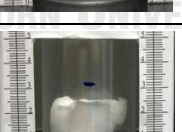
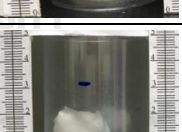
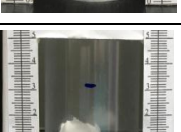
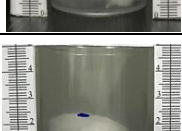
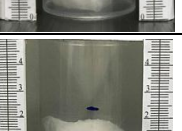
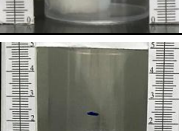
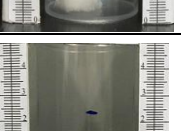
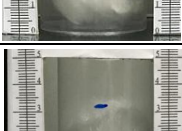
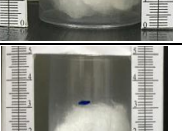
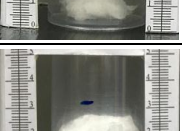
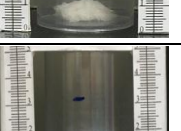


Figure 27 X-ray diffractograms of sucrose fiber containing trehalose dihydrate at different weight ratios (A) 100.0:0, (B) 87.5:12.5, (C) 75.0:25.0, (D) 62.5:37.5, (E) 50.0:50.0, (F) 37.5:62.5, (G) 25.0:75.0, (H) 12.5:87.5, and (I) 0:100.0

Table 9 Physical stability of sucrose fiber containing trehalose dihydrate with different weight ratios under storage temperature of 30 ± 2 °C and $75\pm 5\%$ RH

Weight ratios of sucrose:trehalose dihydrate	Relative volume changing of fiber at different storage time			
	Initial	30 minutes	60 minutes	90 minutes
100.0 : 0 (pure sucrose)				
87.5 : 12.5				
75.0 : 25.0				
62.5 : 37.5				
50.0 : 50.0				
37.5 : 62.5				
25.0 : 75.0				
12.5 : 87.5				
0 : 100.0 (pure trehalose dihydrate)				

From above result, the major factors affecting on the stability of saccharide fiber were relating to amorphous, T_g including surface defect. In case of sucrose, amorphous content and defect of surface played a key role on its stability whereas trehalose dihydrate fiber was affected by only amorphous content. When two of above saccharides were mixed, instability of such fiber was mainly impacted by $T_{g(mix)}$.

Changing of $T_{g(mix)}$ should be the result from the component interaction because T_g of compounded fiber were not found to obey simple GT equation ($K=1$). Therefore, chemical interaction between sucrose and trehalose dihydrate should play an important role on the $T_{g(mix)}$ of fiber. Finding relationship comprised of two different stages: initial phase of decrement (plasticization) and later phase of increment (antiplasticization). During initial negative deviation (the concentration of trehalose dihydrate up to 50%w/w), lower $T_{g(mix)}$ was observed (compared to calculated $T_{g(mix)}$ with simple GT equation). It was due to the interaction of any species in the system with sucrose molecule that might be either moisture in an environment or trehalose dihydrate. It was also known as plasticization. Generally, plasticization particularly in food system containing carbohydrates, lipids, proteins and fiber mainly occurred regarding to an internal water or external atmospheric water (35, 87). Nevertheless, polyol including disaccharide could promote a lowering of both T_g and temperature of melting (T_m) of powdered porcine gelatin via hydrogen bonding. It was because of the enriched hydroxyl group in polyols and disaccharide. Thus, trehalose dihydrate (a type of disaccharide with enrich hydroxyl group) might react with sucrose via hydroxyl group interaction (88, 89).

On the other hand, the increasing of trehalose dihydrate (more than 50% w/w) revealed the elevating of $T_{g(mix)}$ as non-linear positive deviation (Figure 24). The higher the concentration of trehalose dihydrate the higher the $T_{g(mix)}$. In this situation, trehalose dihydrate showed antiplasticization effect. However, $T_{g(mix)}$ in this concentration range still lower than that of calculated $T_{g(mix)}$. It might due to either the ability to fill in free volume of amorphous matrix or the reactivity with matrix molecules (90). As seen from above T_g determination results, trehalose dihydrate could be acting as either plasticizer or antiplasticizer. Theoretically, the $T_{g(mix)}$ of

blending component depended upon several factors such as enthalpy of mixing, volume of mixing, quality size, shape, structure, molecular weight including hydrogen bonding of plasticizer (41, 90-92)

In order to investigate the possibility of reactive functional group between sucrose and trehalose dihydrate in centrifugal spinning fiber, FT-IR was carried out. In addition, thermal analysis was also performed to support the existence of bimolecular water of crystallization in trehalose dihydrate.

DSC thermograms of trehalose anhydrous fiber (Figure 28) indicated the T_g at 60.10°C. The first broad endothermic peak (80-110 °C) was found and followed with the second exothermic peak (180-210 °C). Sharp endothermic peak response at 210-220 °C was investigated at the end. To clearly demonstrate such thermal event, TGA was synchronously carried out. The first broad endothermic peak corresponded to the weight loss around 4% w/w that should correlate with the removal of moisture absorbed on surface. The second and third thermal event displayed the sharp exothermic (195 °C) and endothermic peaks (210 °C) which were the recrystallization and melting of trehalose anhydrous, respectively.

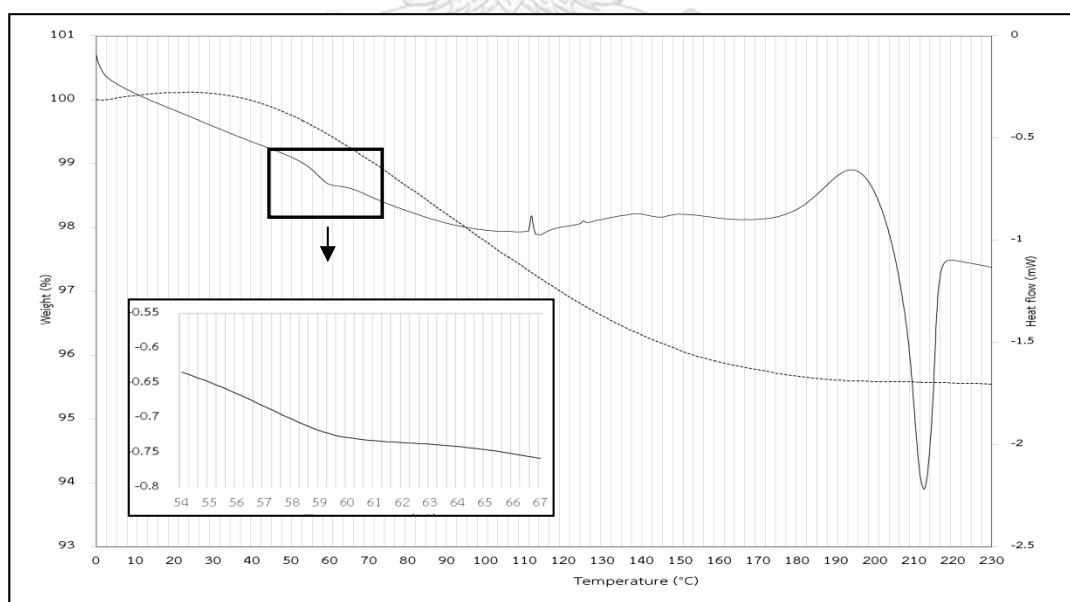


Figure 28 DSC and TGA thermograms of trehalose anhydrous fiber

In order to prove the existence of starting materials of sucrose and trehalose dihydrate in fiber produced, FT-IR method was also employed. All spectra were

compared and illustrated in Figure 29. Focusing on the IR spectra of fiber produced in 800-1200 cm^{-1} range, the group of 848, 940, 987, 1050 and 1106 cm^{-1} appeared that agreed well with crystalline sucrose spectra(93, 94). In addition, both respond peaks of 800 and 1150 cm^{-1} were also found and correlated to trehalose dihydrate spectra. Therefore, fiber obtained conclusively comprised of sucrose and trehalose. Fortunately, IR peak at 1688 cm^{-1} that represented the crystal water of trehalose dihydrate was not observed. This finding correlated with previous results of the effect of spinning process on the disappearing of water of crystallization of trehalose fiber. In conclusion, fiber obtained was composed of sucrose and anhydrous trehalose.

As the presence of both starting materials in fiber produced was described above, it might have any interactions between them. Thus, the change of any responded peaks of FT-IR spectra would possibly reflect the chemical interaction. Crystalline trehalose dihydrate showed the major peak with absorption band in the range of 3200-3500 cm^{-1} and 1688 cm^{-1} that representing O-H stretching and O-H bending of two crystal water molecules (via hydrogen bonding), respectively. Physical mixture between crystalline sucrose and trehalose dihydrate at the weight ratio of 25:75 showed the existing peak of crystal water of trehalose dihydrate at 1688 cm^{-1} (Figure 29). It indicated no interaction between two solid components of sucrose and trehalose dihydrate after physical blending. However, the FT-IR spectra of sucrose-trehalose fiber illustrated the disappearing of 1688 cm^{-1} peak which inferred to the impeding of both water molecules of crystallization of trehalose dihydrate during centrifugal spinning process (Figure 29). Moreover, the chemical interaction between sucrose and trehalose dihydrate in fiber was concentration independent (Figure 30).

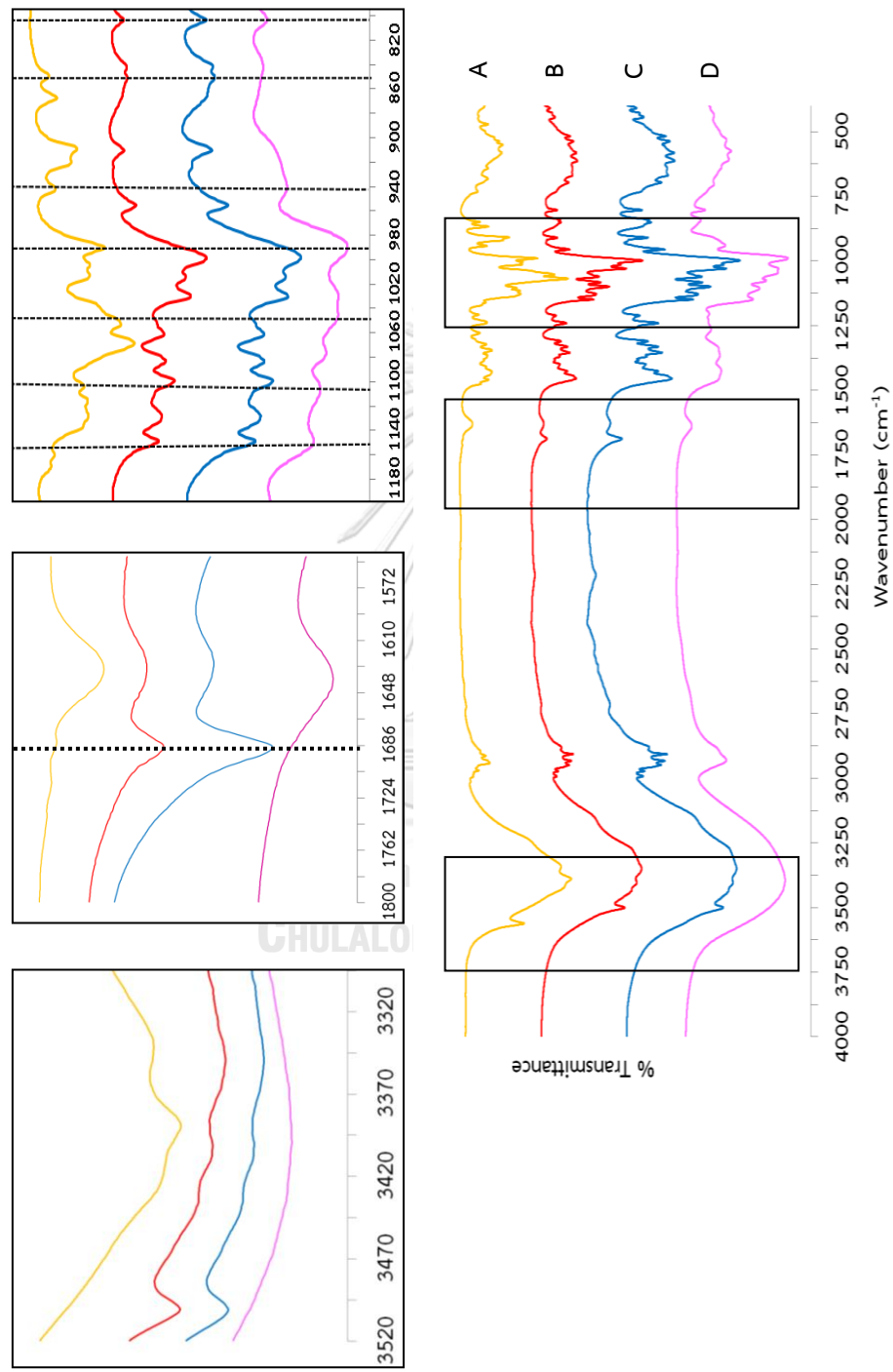


Figure 29 ATR-FTIR spectra of (A) crystalline sucrose, (B) crystalline trehalose dihydrate, (C) physical mixture of crystalline sucrose and crystalline trehalose dihydrate (25.0:75.0 by weight), and (D) sucrose fiber containing trehalose dihydrate (25.0:75.0 by weight)

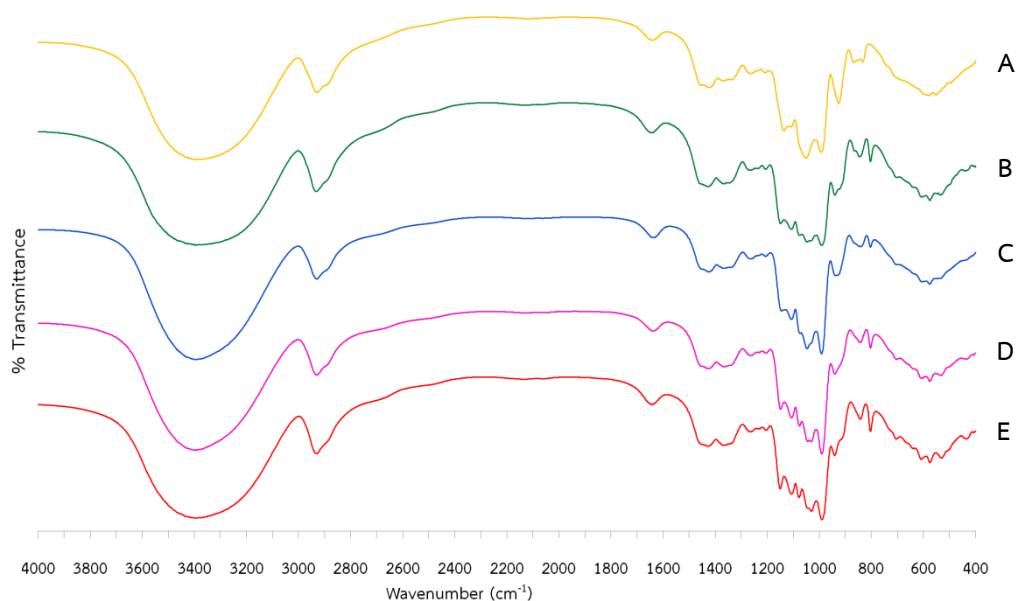


Figure 30 ATR-FTIR spectra of sucrose fiber containing trehalose dihydrate at different weight ratios (A) 100.0:0, (B) 75.0:25.0, (C) 50.0:50.0, (D) 25.0:75.0, and (E) 0:100.0

The mixing of trehalose dihydrate into sucrose fiber affected on mainly $T_{g(mix)}$ of fiber. Meanwhile, the state of amorphous and surface morphology of fiber were not significantly different (Figure 26 and Figure 27). Hence, the stability of sucrose mixture fiber importantly relied on $T_{g(mix)}$.

From experimental results, $T_{g(mix)}$ of sucrose fiber containing trehalose dihydrate at weight ratio 50.0:50.0 was found to be 25.00°C that was not close to the $T_{g(mix)}$ determined from previous study as 44.16°C (Table 8). It was due to the fact that T_g mostly depended on either source of material, sample preparation method, equipment used or method of determination (74). In this research, there were two different batches of crystalline sucrose. Batch number of 140715102 was used in the study of “the effect of the amount of trehalose dihydrate on the T_g of spinning sucrose mixture fiber” whereas the previous one of batch number 25071692 was utilized in the aspect of “structural integrity determination of higher or lower T_g saccharides blend in sucrose fiber”.

When T_g of system was considered, the temperature of storage might provide the different impacts on stability of fiber. If the storage temperature was higher than T_g , the fiber should be in rubbery state or presented the sticky nature. On the other hand, if the temperature of storage was lower than T_g , the glassy state was developed. Therefore, the physical appearance of all fibers under storage temperature of 40 ± 2 °C and $75 \pm 5\%$ RH was found to be sticky because of the lower T_g (between 20 °C to 40 °C) (Table 10). They were further investigated and found the relatively faster in volume reduction than that of ambient temperature. In turn, the storage temperature in between 2 °C to 8 °C and $75 \pm 5\%$ RH provided the longer time of collapse (Table 11). It should well agree with above finding as a result of the better preservation of glassy state. It could be explained with the aspect of molecular mobility and nucleation growth of molecule at the low temperature. Yoshioka et al (1994) found that crystallization rate of amorphous indomethacin samples occurred through rotational molecular mobility, nucleation and crystal growth. They were a stable polymorphic form over several days when stored below its T_g (50 °C) due to the insufficient molecular mobility (high viscosity) for nucleation site. In the mean time, the rate of crystallization was increased regarding the greater mobility at storage of temperature near or above T_g (95). However, all mixture fiber finally collapsed because of the effect of moisture saturation. In conclusion, controlled temperature of storage demonstrated the impact on the stability of fiber regarding to the molecular motion. The lower the temperature the less the molecular mobility.

Table 10 Physical stability of sucrose fiber containing trehalose dihydrate at different weight ratios under storage temperature of 40 ± 2 °C and $75\pm 5\%$ RH

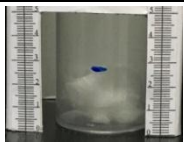
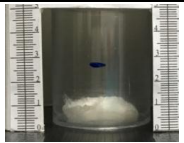
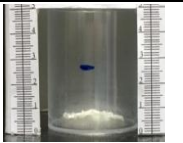
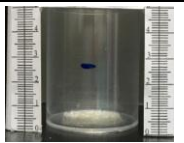
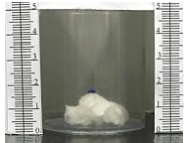




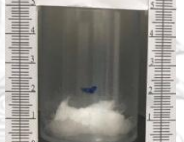
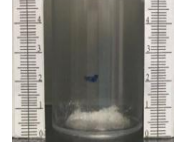

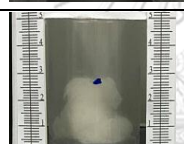

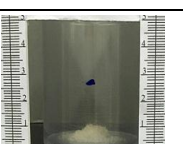
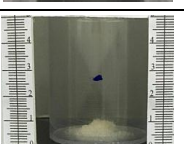
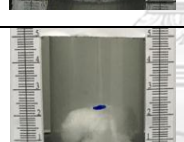
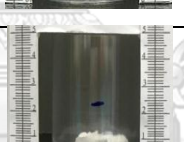
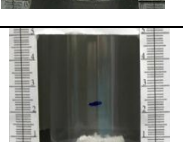

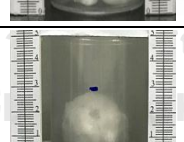
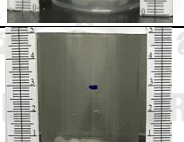
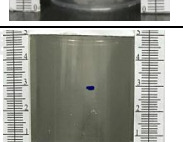
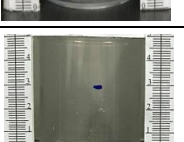
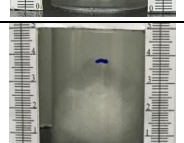
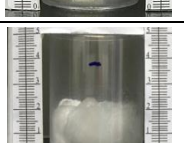
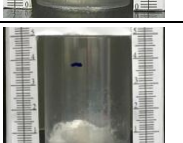
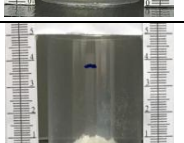
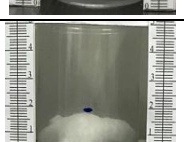

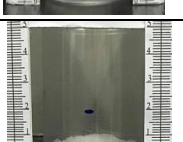

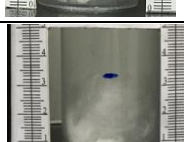
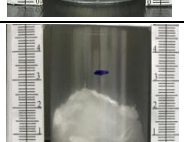
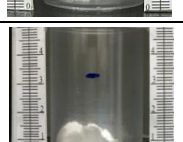
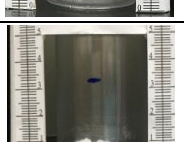
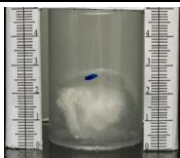
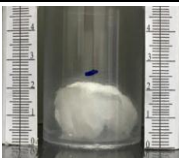
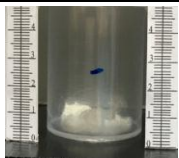
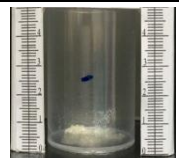
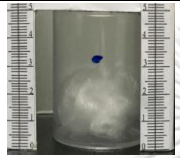
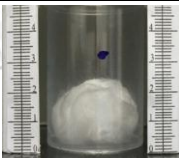
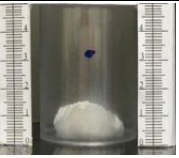
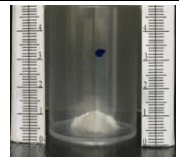




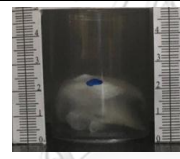
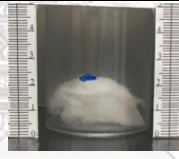

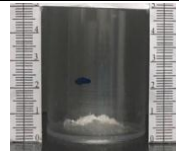
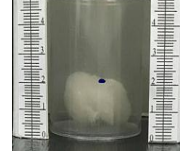




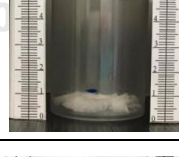
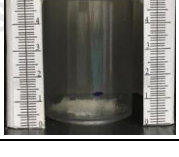
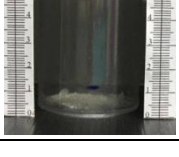
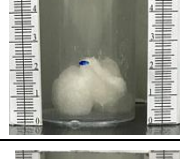


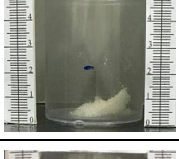
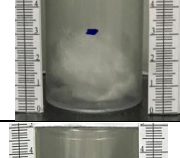
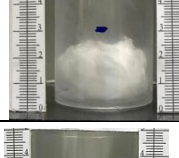
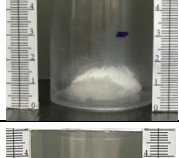
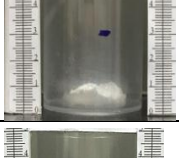


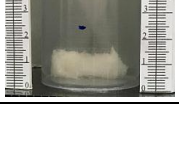
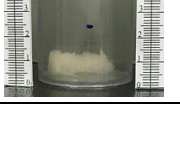
Weight ratios of sucrose:trehalose dihydrate	Relative volume changing of fiber at different storage time			
	Initial	30 minutes	60 minutes	90 minutes
100.0 : 0 (pure sucrose)				
87.5 : 12.5				
75.0 : 25.0				
62.5 : 37.5				
50.0 : 50.0				
37.5 : 62.5				
25.0 : 75.0				
12.5 : 87.5				
0 : 100.0 (pure trehalose dihydrate)				

Table 11 Physical stability of sucrose fiber containing trehalose dihydrate at different weight ratios under storage temperature of 2-8°C and 75±5% RH

Weight ratios of sucrose:trehalose dihydrate	Relative volume changing of fiber at different storage time			
	Initial	60 minutes	120 minutes	180 minutes
100.0 : 0 (pure sucrose)				
87.5 : 12.5				
75.0 : 25.0				
62.5 : 37.5				
50.0 : 50.0				
37.5 : 62.5				
25.0 : 75.0				
12.5 : 87.5				
0 : 100.0 (pure trehalose dihydrate)				

The critical main factors affecting on the stability of the sucrose/trehalose fiber were T_g , amorphous content and surface defect. Previous results noticed the existence of amorphous including a smoother of fiber surface while the difference of T_g were achieved. It was thus indicated that T_g obviously affected on stability of fiber. However, not only T_g was a great concern but the level of surface defect was also an important factor. Generally, the defect on surface such as pore, channel, and roughness of surface could potentially absorb moisture from environment. Absorbed water might plasticize the amorphous saccharide and resulting in softer, less integrity, more collapse, stickier and caking of structure finally (60, 75). Visualization of the fiber's morphology using SEM revealed the smoother surface after trehalose dihydrate was incorporated at all concentrations (Figure 26). Nevertheless, the degree of smoothness or defect on surface could not be distinguished from only SEM results. The study of moisture sorption profile of saccharide fiber could be further employed for the differentiation of the degree of surface defect.

The defect on the surface of amorphous material could quickly absorb moisture owing to its high energetic site that eventually yielded the rubbery state. Weight gaining was remarkably happened over time. Unchanged of weight was then achieved regarding to the moisture saturation. The transition between two of above time periods was defined as "the transition time of amorphous glassy to rubbery state". After the saturation of moisture, molecules of saccharide had a more molecular mobility (supersaturate solution) and subsequently collided together. They would be lead to form the nuclei or seed entire the system. Progression of nucleation affected on the repelling of water molecules throughout the matrix. Therefore, water molecules would diffuse out to the environment resulting in the disappearing of certain weight (60). The starting point of weight decrease was defined as "the recrystallization time" (Figure 31).

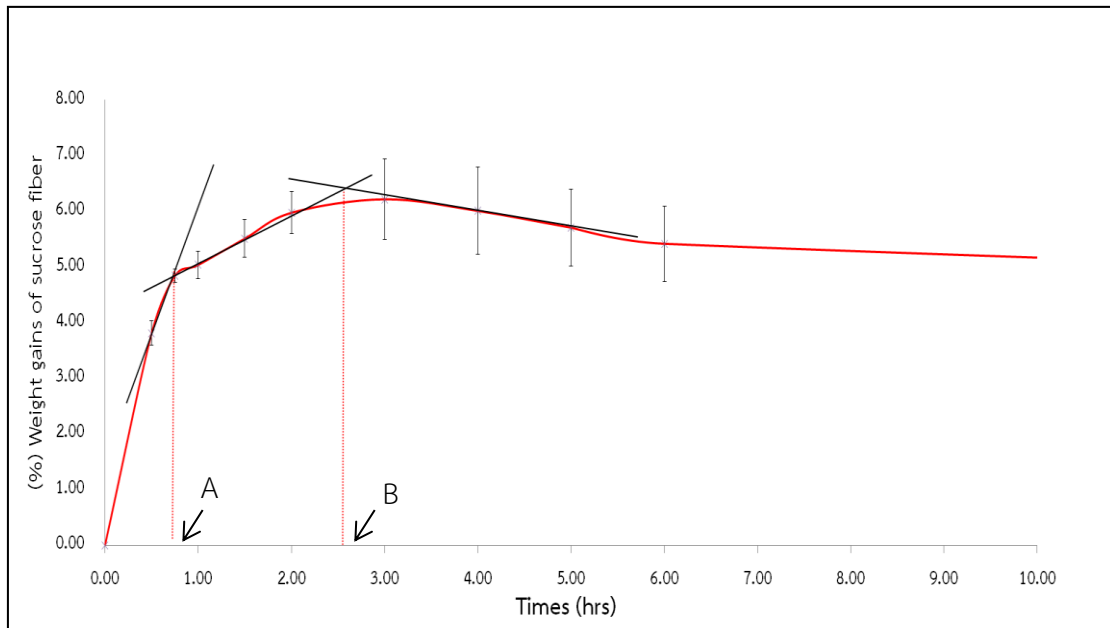


Figure 31 Moisture sorption profile of amorphous sucrose fiber under storage condition of $30\pm 2^{\circ}\text{C}$ and $75\pm 5\%$ RH. (A – the transition time of amorphous glassy to rubbery state, B - the recrystallization time)

Therefore, the more the defect sites the shorter the transition time. Moreover, the interconversion rate between the amorphous rubbery to new crystalline form was faster as a function of the defect content.

The determination of “the transition time” and “the recrystallization time” of sample fibers after storage under relatively high moisture content were conducted. The results of both times were summarized and tabulated as shown in Table 12.

Table 12 The transition time and the recrystallization time of sucrose/trehalose dihydrate fiber at various weight ratios under exposing temperature of 30 ± 2 °C and $75\pm 5\%$ RH

Weight ratios of sucrose : trehalose dihydrate	Transition time (hrs)			Recrystallization time (hrs)				
	#1	#2	#3	average \pm sd	#1	#2	#3	average \pm sd
100.0 : 0	0.93	0.74	0.68	0.78 \pm 0.13	3.55	2.60	2.02	2.66 \pm 0.67
87.5 : 12.5	1.05	1.13	1.25	1.14 \pm 0.10	2.83	3.39	3.10	3.11 \pm 0.28
75.0 : 25.0	2.08	2.69	3.71	2.89 \pm 0.74	11.64	11.99	11.36	11.66 \pm 0.32
62.5 : 37.5	3.41	4.16	4.70	4.09 \pm 0.65	9.41	9.45	10.06	9.64 \pm 0.36
50.0 : 50.0	4.21	4.59	5.66	4.82 \pm 0.75	10.08	13.94	13.87	12.63 \pm 2.21
37.5 : 62.5	5.91	5.34	5.68	5.64 \pm 0.29	13.41	12.00	11.94	11.98 \pm 0.03
25.0 : 75.0	5.33	5.18	5.23	5.25 \pm 0.08	14.00	14.22	14.21	14.14 \pm 0.12
12.5 : 87.5	4.00	4.00	4.00	4.00 \pm 0.00	8.76	8.82	9.35	8.98 \pm 0.32
0 : 100.0	1.50	1.12	1.23	1.28 \pm 0.20	3.09	3.77	3.55	3.47 \pm 0.35

* Moisture sorption profile of amorphous sucrose fiber containing trehalose dihydrate at different weight ratios were shown in Appendix 3

The shortest transition time was observed in case of sucrose fiber. It was due to the most defect of surface as could be seen from SEM (Figure 26A). When the adding amount of trehalose dihydrate went up to 62.5% by weight, transition time was linearly longer as a function of the added amount of trehalose dihydrate. It should be primarily concluded that the higher amount of trehalose dihydrate provided the smoother surface eventhough SEMs did not show any significance different of fiber surface (Figure 32). Focusing on the weight ratio in between 62.5-75% by weight, the transition times were not significantly different at an alpha level of 0.05. The recrystallization time showed the tendency as same as the transition time (Figure 33).

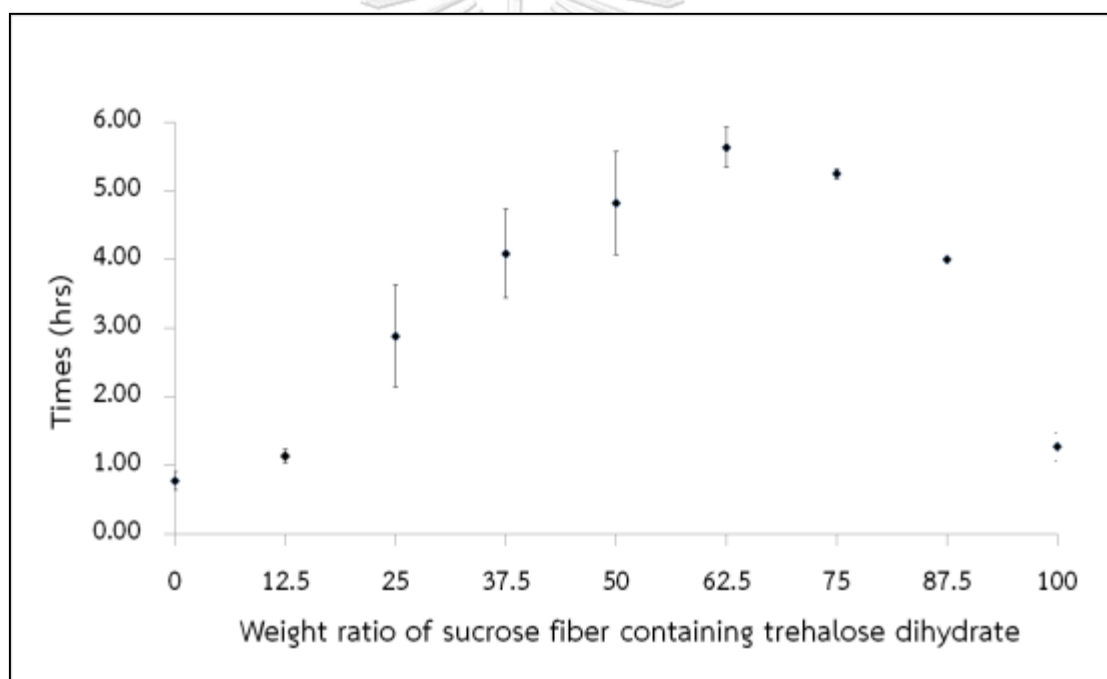


Figure 32 The transition time of sucrose fiber containing trehalose dihydrate at different weight ratios under storage condition at temperature of 30 ± 2 °C and $75\pm 5\%$ RH

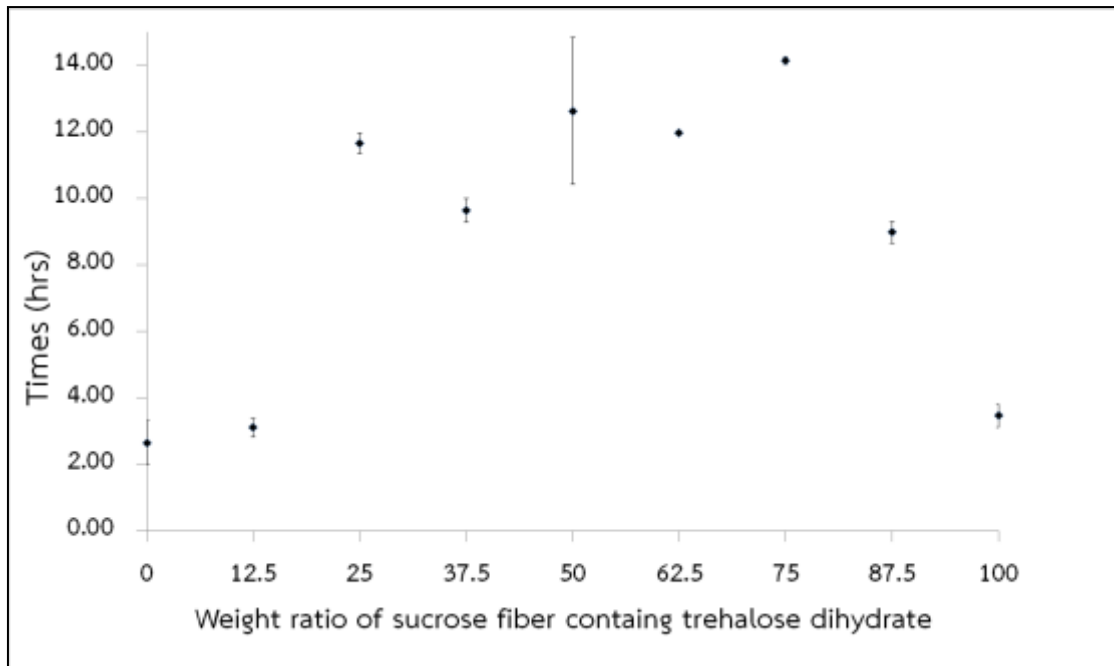


Figure 33 The recrystallization time of sucrose fiber containing trehalose dihydrate at different ratios under storage condition at temperature of 30 ± 2 °C and $75\pm 5\%$ RH

Supporting evidence on recrystallization of fiber are shown in Figure 34. The polarized light photomicrograph indicated the birefringence of aged sample after recrystallization. It revealed the crystallization of saccharide fiber upon moisture sorption. The time period between the transition time and the recrystallization time (Δt) might be useful to determine “which phenomenon played more an important role on the stability of fiber”. They were calculated and illustrated in Table 12 and Figure 35. If the comparable Δt were obtained, it should reflect the more pronouncing effect of “transition of glassy to rubbery” over “the recrystallization” on the stability of fiber. The results showed incomparable Δt that meant to both phenomena had the influence on the stability of sample fiber.

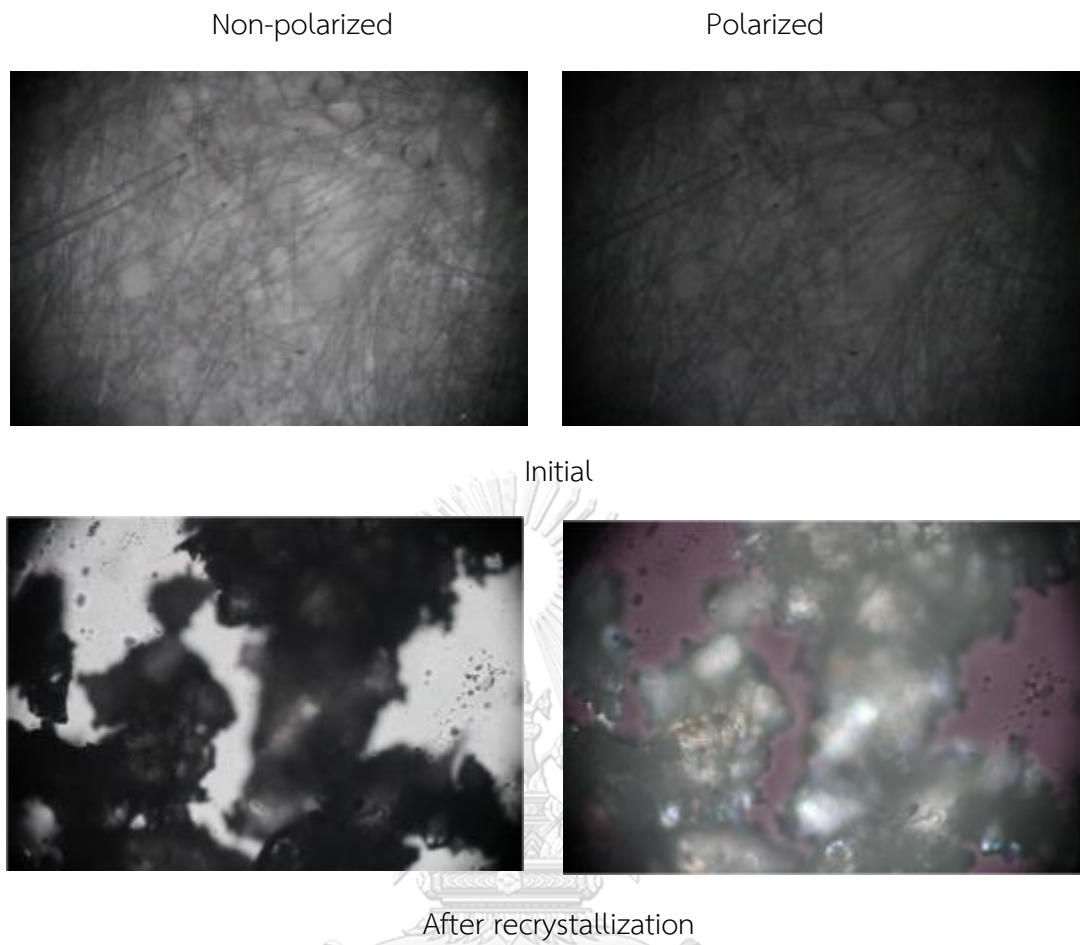


Figure 34 Photomicrographs of sucrose fiber containing trehalose dihydrate at weight ratio 75:25 at initial and after recrystallization under polarized and non-polarized light (40*10 X)

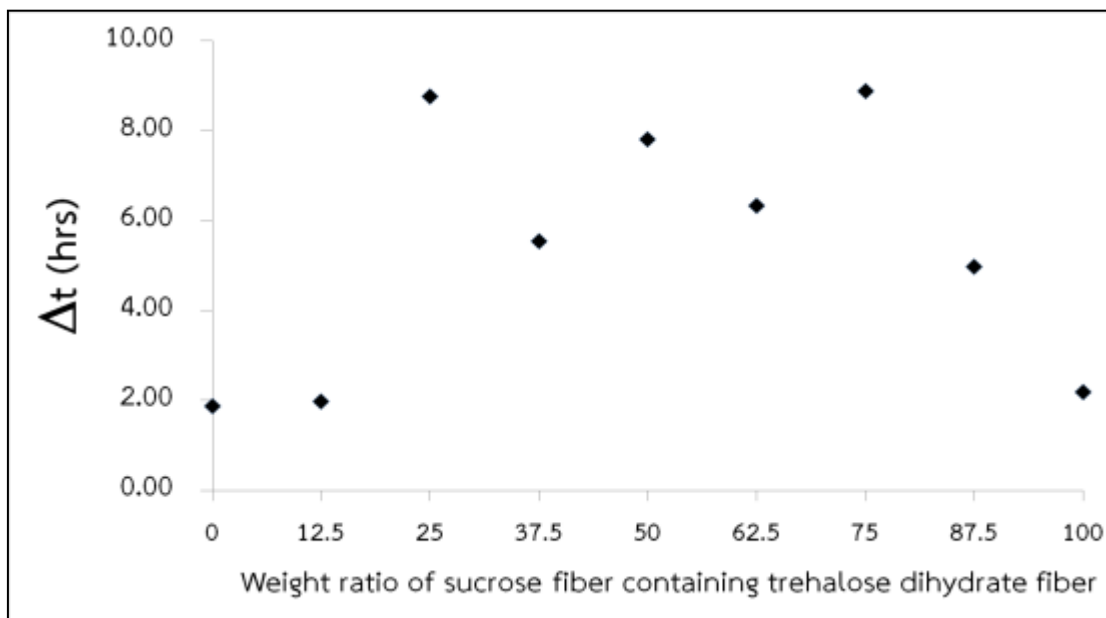


Figure 35 Time period between “The transition time” and “The recrystallization time” (ΔT) as a function of weight ratios of sucrose fiber containing trehalose dihydrate

Surprisingly, the shorter transition and recrystallization time were investigated at the higher level of trehalose dihydrate added (87.5%w/w). Although the surface defect seems to be an important factor in this case, other factors of T_g and amorphous should also be taken into account. Previous result of this fiber showed the T_g of 43.51°C which indicated the existing of glassy amorphous state under experimental storage condition of 30°C (Figure 24). Thus, amorphous content was probably an interesting point for the faster moisture sorption in this situation.

Conclusively, the longer transition time of fiber was acquired with the addition of trehalose dihydrate at weight ratio of up to 75.0% w/w. It was due to the less defect of surface. However, shorter transition time with higher T_g was determined at higher concentration of 87.5% w/w with smooth surface. Therefore, it contradicted with above finding. Amorphous content might be therefore another relating factor on the stability of fiber.

Temperature of environment might also influence on stability of fiber because of the T_g of system. If all samples were storage at near or below their T_g , they were found to exist in rubbery state. The results showed that trend and value of “the transition time” and “the recrystallization time” were negligible different under different storage condition at $40\pm 2^\circ\text{C}$ and $30\pm 2^\circ\text{C}$. Added trehalose dihydrate of up to 87.5 %w/w provided longer transition time and recrystallization time (Figure 36 and Figure 37). Thus, the longer transition time and recrystallization time at $40\pm 2^\circ\text{C}$ was consistent with $30\pm 2^\circ\text{C}$. Interestingly, at highest concentration of 87.5%, the higher value of transition time and recrystallization time were found that did not correlated with observed data of $30\pm 2^\circ\text{C}$ condition. Above finding should relate to the vicinity of T_g of fiber and storage temperature. In this case, amorphous rubbery should mainly govern on the ability of moisture sorption. Somehow, surface defect and amorphous content should also be considered.

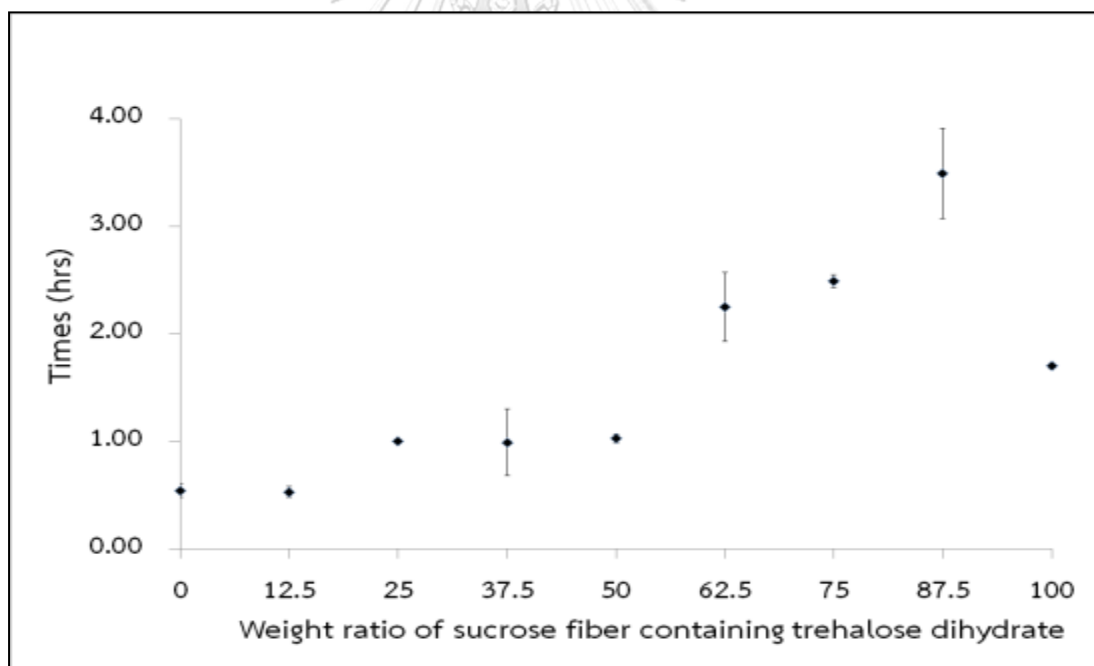


Figure 36 The transition time of sucrose fiber containing trehalose dihydrate at different ratios under storage condition at temperature of $40\pm 2^\circ\text{C}$ and $75\pm 5\%$ RH
 Remark: data are shown as mean \pm sd in Table 14 and moisture sorption profile of amorphous sucrose fiber containing trehalose dihydrate at different weight ratios were shown in Appendix 4.

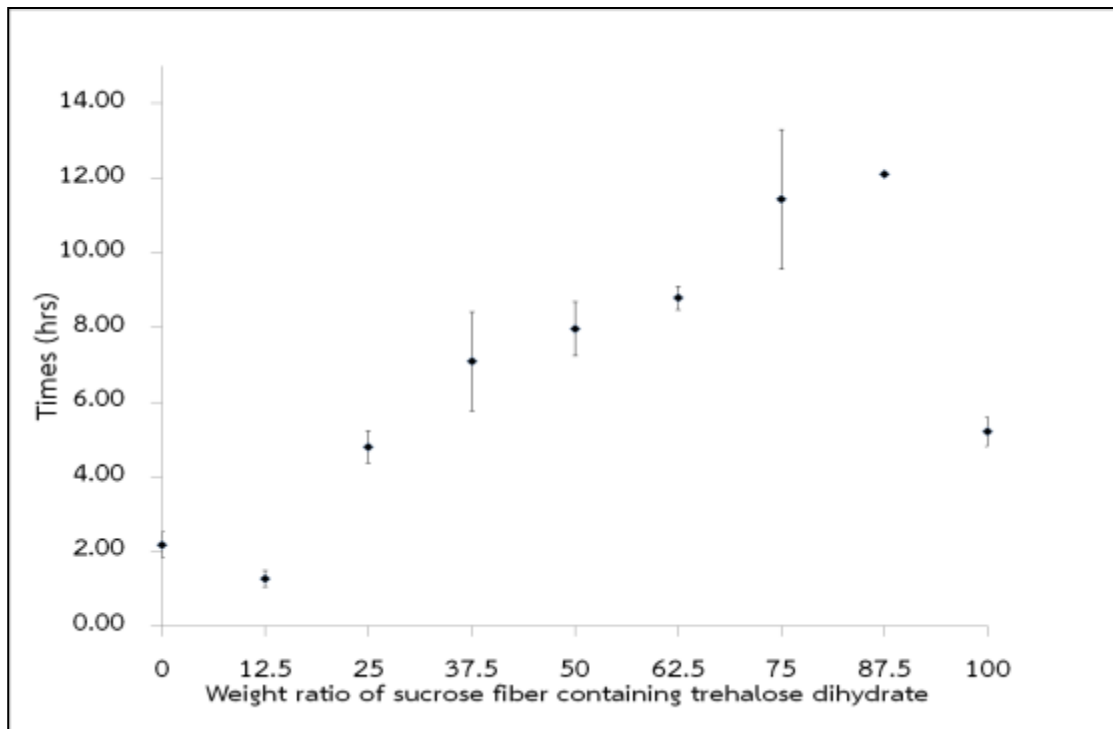


Figure 37 The recrystallization time sucrose fiber containing trehalose dihydrate at different ratios under storage condition at temperature of 40 ± 2 °C and $75\pm 5\%$ RH

CHAPTER V

CONCLUSIONS

Sucrose and trehalose dihydrate were successfully prepared as centrifugal spinning fiber whereas lactose anhydrous was not able to form such fiber. In the group of monosaccharide (D-galactose, D-glucose and D-fructose), sugar alcohol (D-xylitol, D-mannitol and D-sorbitol) and polysaccharide of maltodextrin 20 DE could not also be generated as a fiber form. They were due to the low T_g compared to ambient temperature that eventually resulted in rubbery amorphous with fusible nature. Although lactose anhydrous and maltodextrin showed the higher T_g , their decomposition were occurred (after melting) at the temperature below processing temperature. Thus, the preparation of centrifugal spinning fiber from saccharide should be possible depending upon T_g of saccharide and their stability after melting.

As mentioned above, sucrose and trehalose dihydrate were the candidate for using as starting material of spinning fiber with centrifugal method. However, sucrose was more appropriate than trehalose dihydrate due to several advantages. It was later utilized as a major component of fiber preparation. Even though sucrose could be generated as spinning fiber, it would start to collapse within an hour. Blending sucrose with other saccharides should provide different T_g ($T_{g(mix)}$). Adding of low T_g saccharide resulted in lower $T_{g(mix)}$ while high T_g saccharide gained the higher $T_{g(mix)}$.

The adjusting of T_g of sucrose fiber was a pronouncing method of choices in order to provide more structural integrity. As described by GT equation, the increasing of T_g was achieved with the addition of higher T_g saccharide. $T_{g(mix)}$ of sucrose with trehalose dihydrate related to modified GT equation with non-linear relationship (K not equal 1). Meanwhile, the effect lactose anhydrous on $T_{g(mix)}$ was not concluded. It was due to the fact that there was an existence of crystalline solid of lactose anhydrous in the amorphous mixture between sucrose and lactose anhydrous matrix. Focusing on the impaction of added trehalose dihydrate on $T_{g(mix)}$, negative and positive deviation was occurred due to the plasticization and antiplasticization, respectively.

Fiber produced from the blending between trehalose dihydrate and sucrose system yielded the acceptable physical appearance. However, the stability of fiber under stress condition with high humidity was not appreciable. It should be the results from three different factors of T_g , amorphous content and defect on the surface. $T_{g(mix)}$ played a key role on stability. It directly regarded with the state of glassy or rubbery. Low $T_{g(mix)}$ provided the rubbery state that potentiated the interaction of moisture and saccharide. Plasticization was then occurred. Amorphous content has also important issue due to the high thermodynamically unstable. The more the completeness of amorphous state the less the structural integrity. Not only $T_{g(mix)}$ and amorphous that strongly impacted on the fiber stability but surface defect also a promising element. The defect of surface affected on the moisture sorption of fiber. The more defect point on surface provided the higher and faster moisture sorption. Direct measuring of surface defect of fiber using SEM was not able to distinguish the relative level of defect. Therefore, indirect measuring with the moisture sorption profile was employed. The longer of “the transition time” and “the recrystallization time” were observed when adding trehalose dihydrate into sucrose system. It hence reflected the less of defect on the surface.

In conclusion, the saccharide fiber made with high T_g sacchride could be produced by centrifugal spinning. Molten ability with non decomposition should be considered in order to produce stable saccharide fiber. Factors affecting on the stability of saccharide fiber were T_g , amorphous content including defect of surface. In order to stabilize the fiber produced, some chemical materials should be added such as crystallization enhancer. The storage temperature was also another aspect of improving more stability of fiber. Handling the fiber at lower temperature might prolong the glassy state with more stability. They would be further studied in such given details.

REFERENCES

1. Nikghalb A. L., Singh G., Singh G., Kahkeshan F.K. Solid dispersion: methods and polymers to increase the solubility of poorly soluble drugs. *J Appl Pharm Sci.* 2012;2(10):170-175.
2. Allawadi D., Singh N., Singh S., S. A. Solid dispersion: a review on drug delivery system and solubility enhancement. *Pak J Pharm Sci.* 2009;22(2):234-246.
3. Torre D. P., Torrado S, Torrado S. Preparation, dissolution and characterization of praziquantel solid dispersions. *Chem Pharm Bull.* 1999;47(1):1629-1633.
4. Marano S. , Barker A.S. , Raimiabraham T.B., Missaghi S. , RajabiSiahboomi A., Craig Q.M. D. Development of microfibrinous solid dispersions of poorly water-soluble drugs in sucrose using temperature-controlled centrifugal spinning. *Eur J Pharm Biopharm.* 2016;103:84-94.
5. Zhang X., Lu Y. Centrifugal spinning: an alternative approach to fabricate nanofibers at high speed and low cost. *Polym Rev.* 2014;54(4):677-701.
6. Siahi-Shadbad R.M., Ghanbarzadeh S., Barzegar-Jalali M., Valizadeh H., Taherpoor A., Mohammadi G., et al. Development and characterization of solid dispersion for dissolution improvement of furosemide by cogrinding method. *Adv Pharm Bull.* 2014;4(4):391-399.
7. Hamidi A. H., Edwards A. A., Mohammad A M., Nokhodchi A. To enhance dissolution rate of poorly water-soluble drugs: Glucosamine hydrochloride as a potential carrier in solid dispersion formulations. *Colloids Surf B Biointerfaces.* 2010;76(1):170-178.
8. Karavas E., Georgarakis E., Sigalas M.P., Avgoustakis K., D. B. Investigation of the release mechanism of a sparingly water-soluble drug from solid dispersions in hydrophilic carriers based on physical state of drug, particle size distribution and drug-polymer interactions. *Eur J Pharm Biopharm.* 2007;66(3):334-347.
9. Marano S. , Barker A.S. , Raimiabraham T.B., Missaghi S. , RajabiSiahboomi A., Aliev A. E., et al. Microfibrinous solid dispersions of poorly water-soluble drugs produced via centrifugal spinning: unexpected dissolution behavior on recrystallization. *Mol*

Pharm. 2017;14(5):1666-1680.

10. Getz J.J., Frisbee S.E., Misra T.K., Sisak J.R., Sanghvi P.P., inventors; Biovai Technologies Ltd., assignee. Sachet formulations. patent US 6,270,804. 1998 Oct 30.
11. Raiden M.G., Sanghvi P.P., Misra T.K., Currington J.W., Kamath S.V., inventors; Fuisz Technologies Ltd., assignee. Self binding shearform compositions. patent US 5,980,941. 1998 Jun 19.
12. Richard C., inventor; Fuisz Technologies Ltd, assignee. Saccharide-based matrix. patent US. 5,429,836. 1993 Jul 29.
13. Saffoon N., Uddin R., Huda H.N., Sutradhar B.K. Enhancement of oral bioavailability and solid dispersion: a review. *J Appl Pharm Sci.* 2011;07:13-20.
14. Francois H., Lyes M., Malika L., Skiba, Youssef A., Mohamed S. Solid dispersions for oral administration: an overview of the methods for their preparation. *Curr Pharm Des.* 2016;22(32):4942-4958.
15. Vasconcelos T., Sarmento B., Costa P. Solid dispersions as strategy to improve oral bioavailability of poor water soluble drugs. *Drug Discov Today.* 2007;12(23):1068-1075.
16. Okonogi S., Puttipipatkachorn S. Dissolution improvement of high drug-loaded solid dispersion. *AAPS PharmSciTech.* 2006;7(2):E148-E153.
17. Jachowicz R. Dissolution rates of partially water-soluble drugs from solid dispersion systems. I. Prednisolone. *Int J Pharm.* 1987;35(1):1-5.
18. Ali A.A., Gorashi A.S. Absorption and dissolution of nitrofurantoin from different experimental formulations. *Int J Pharm.* 1984;19(3):297-306.
19. Fasano A. Innovative strategies for the oral delivery of drugs and peptides. *Trends Biotechnol.* 1998;16(4):152-157.
20. Herbrink M., Schellens H.M.J., Beijnen H.J., B. N. Improving the solubility of nilotinib through novel spray-dried solid dispersions. *Int J Pharm.* 2017;529(1):294-302.
21. Ghareeb M. M., Abdulrasool A. A., Hussein A. A., Noordin I.M. Kneading technique for preparation of binary solid dispersion of meloxicam with poloxamer 188. *AAPS PharmSciTech.* 2009;10(4):1206-1215.
22. Liu J., Cao F., Zhang C., Ping Q. Use of polymer combinations in the preparation

of solid dispersions of a thermally unstable drug by hot-melt extrusion. *Acta Pharm Sin B*. 2013;3(4):263-272.

23. Uejo F., Limwikrant W., Moribe K., Yamamoto K. Dissolution improvement of fenofibrate by melting inclusion in mesoporous silica. *Asian J Pharm*. 2013;8(6):329-335.

24. Saito M., Ugajin T., Nozawa Y., Sadzuka Y., Miyagishima A., Sonobe T. Preparation and dissolution characteristics of griseofulvin solid dispersions with saccharides. *Int J Pharm*. 2002;249(1):71-79.

25. Baghel S., Cathcart H., O'Reilly N.J. Polymeric amorphous solid dispersions: a review of amorphization, crystallization, stabilization, solid-state characterization, and aqueous solubilization of biopharmaceutical classification system class II drugs. *J Pharm Sci*. 2016;105(9):2527-2544.

26. Torres-Martinez E. J., Cornejo Bravo J. M., Serrano M. A., Pérez Gonzalez G. L., Villarreal G.J. A summary of electrospun nanofibers as drug delivery system: drugs loaded and biopolymers used as matrices. *Curr Drug Deliv*. 2018;15(10):1360-1374.

27. Shen X., Yu D., Zhu L., Branford-White C., White K., Chatterton N.P. Electrospun diclofenac sodium loaded Eudragit® L 100-55 nanofibers for colon-targeted drug delivery. *Int J Pharm*. 2011;408(1):200-207.

28. Jeong S.H., et. a. *Fast disintegrating tablets. Oral controlled release formulation design and drug delivery*: John Wiley & Sons; 2010.

29. Nikghalb L.A., Singh G., Singh G., Kahkeshan F.K. Solid dispersion: methods and polymers to increase the solubility of poorly soluble drugs. *J Appl Pharm Sci*. 2012;2(10):170-175.

30. Joe J.H., Lee W.M., Park Y.J., Joe K.H., Oh D.H., Seo Y.G., et al. Effect of the solid dispersion method on the solubility and crystalline property of tacrolimus. *Int J Pharm*. 2010;395(1-2):161-166.

31. DiNunzio J.C., Brough C., Hughey J.R., Miller D.A., Williams Iii R.O., McGinity J.W. Fusion production of solid dispersions containing a heat-sensitive active ingredient by hot melt extrusion and Kinetisol® dispersing. *Eur J Pharm Biopharm*. 2010;74(2):340-351.

32. Saavedra Z., Porras L.C., Sandra A.D., Alberto T.T., Anahi B.E. Technological

application of maltodextrins according to the degree of polymerization. *Molecules*. 2015;20(12):21067–21081.

33. Labuza T.P., Labuza P.S. Influence of temperature and relative humidity on the physical states of cotton candy. *J Food Process Preserv*. 2004;28(4):274-287.

34. Tu L., Yu S.L., inventors; National Central University, Taoyuan(TW), assignee. Method of obtaining conformational polymorph of sucrose patent US 8,202,987B2. 2012.

35. Wang Y., Truong T. Chapter 7: glass transition and crystallization in foods. Woodhead Publishing: Elsevier Ltd; 2017.

36. Yu X., Kappes S.M., Bello-Perez L.A., Schmidt S.J. Investigating the moisture sorption behavior of amorphous sucrose using a dynamic humidity generating instrument. *J Food Sci*. 2008;73(1):E25-E35.

37. Dickmann R., Strasburg G., Romsos D., Wilson L., Lai G., Huang H. Particle size, surface area, and amorphous content as predictors of solubility and bioavailability for five commercial sources of ferric orthophosphate in ready-to-eat cereal. *Nutrients*. 2016;8(3):129.

38. Costantino H.R., Pikal M.J. Lyophilization of biopharmaceuticals. United States of America: Springer science & business media; 2004.

39. Seo J.A., Oh J., Kim H.K., Hwang Y.H. Study of glass transition temperatures in sugar mixtures. *J Korean Phys Soc*. 2005;46(3):606-609.

40. Roe K.D., T.P L. Glass transition and crystallization of amorphous trehalose-sucrose mixtures. *Int J Food Prop*. 2005;8(3):559-574.

41. Seo J., Kim S.J., Kwon H.J., Yang Y.S., Kim H.K., Hwang Y.H. The glass transition temperatures of sugar mixtures. *Carbohydr Res*. 2006;341(15):2516-2520.

42. Surana R., Pyne A., Suryanarayanan R. Effect of preparation method on physical properties of amorphous trehalose. *Pharm Res*. 2004;21(7):1167-1176.

43. Ógáin O.N., Li J., Tajber L., Corrigan O.I., Healy A.M. Particle engineering of materials for oral inhalation by dry powder inhalers. I—Particles of sugar excipients (trehalose and raffinose) for protein delivery. *Int J Pharm*. 2011;405(1):23-35.

44. Xin Y., Zhang M., Adhikari B. Effect of trehalose and ultrasound-assisted osmotic

dehydration on the state of water and glass transition temperature of broccoli. *J Food Eng.* 2013;119(3):640-647.

45. Chen T., Bhowmick S., Sutteck A., Fowler A., Toner M. The glass transition temperature of mixtures of trehalose and hydroxyethyl starch. *Cryobiology.* 2002;44(3):301-306.

46. Martinez M.L., Videa M., Mederos F., Yane M.D. Preservation effect of vitreous non reducing carbohydrates on the enzymatic activity, denaturation temperature and retention of native structure of lysozyme. *J Mex Chem Soc* 2011;55(3):185-189.

47. Hinch D.K., Zuther E., Heyer A.G. The preservation of liposomes by raffinose family oligosaccharides during drying is mediated by effects on fusion and lipid phase transitions. *Biochim Biophys Acta.* 2003;1612(2):172-177.

48. Shamblin S.L., Taylor L.S., Zografi G. Mixing behavior of colyophilized binary systems. *J Pharm Sci.* 1998;87(6):694-701.

49. Leinen K.M., Labuza T.P. Crystallization inhibition of an amorphous sucrose system using raffinose. *J Zhejiang Univ Sci B.* 2006;7(7):85-89.

50. Hogan S.E., Buckton G. Water sorption/desorption—near IR and calorimetric study of crystalline and amorphous raffinose. *Int J Pharm.* 2001;227(1):57-69.

51. Belcourt L.A., Labuza T.P. Effect of raffinose on sucrose recrystallization and textural changes in soft cookies. *J Food Sci.* 2007;72(1):C065-C071.

52. Graeser K.A., Patterson J.E., Zeitler J.A., Rades T. The Role of Configurational Entropy in Amorphous Systems. *Pharmaceutics.* 2010;2(2):224-244.

53. Akoh C.C. *Food lipids:chemistry, nutrition, and biotechnology.* fourth ed: Taylor&Francis; 2017.

54. Cottrell T., Peij V.J. Sorbitan Esters and Polysorbates. In: Norn V, editor. *Emulsifiers in Food Technology.* United States: John Wiley & Sons, Ltd; 2014.

55. Szafraniec J., Antosik A., Justyna K.-K., Chmiel K., Kurek M., Gawlak K., et al. The self-assembly phenomenon of poloxamers and its effect on the dissolution of a poorly soluble drug from solid dispersions obtained by solvent methods. *Pharmaceutics.* 2019;11(3):130.

56. Abutaleb A., Lolla D., Aljuhani A., Shin H.U., Rajala J.W., Chase G.G. Effects of

surfactants on the morphology and properties of electrospun polyetherimide fibers. *Fibers*. 2017;5(3):33.

57. Gao S.L., Mäder E., Plonka R. Nanocomposite coatings for healing surface defects of glass fibers and improving interfacial adhesion. *Compos Sci Technol*. 2008;68(14):2892-2901.

58. Husain S., Koros W.J. Mixed matrix hollow fiber membranes made with modified HSSZ-13 zeolite in polyetherimide polymer matrix for gas separation. *J Membrane Sci*. 2007;288(1):195-207.

59. Migneault S., Koubaa A., Erchiqui F., Chaala A., Englund K., Wolcott M.P. Effects of processing method and fiber size on the structure and properties of wood-plastic composites. *Compos Part A Appl Sci Manuf*. 2009;40(1):80-85.

60. Roudaut G., Debeaufort F. 3 - Moisture loss, gain and migration in foods. In: Kilcast D, Subramaniam P, editors. *Food and beverage stability and shelf life*: Woodhead Publishing; 2011.

61. Preedy V.R. *Dietary sugars: chemistry, analysis, function and effects*. Great Britain CPI group (UK) Ltd: Royal Society of Chemistry; 2012.

62. Seo J.-A., Kim S.J., Kwon H.-J., Yang Y.S., Kim H.K., Hwang Y.-H. The glass transition temperatures of sugar mixtures. *Carbohydr Res*. 2006;341(15):2516-2520.

63. Sussich F., Cesaro A. Trehalose amorphization and recrystallization. *Carbohydr Res*. 2008;343(15):2667-2674.

64. Cesaro A., De Giacomo O., Sussich F. Water interplay in trehalose polymorphism. *Food Chem*. 2008;106(4):1318-1328.

65. Ba K., Blecker C., Danthine S., Tine E., Destain J., Thonart P. Physicochemical characterization of dextrans prepared with amylases from sorghum malt. *STARCH-STARKE*. 2013;65:962-968.

66. Drebuschak V.A. Calibration coefficient of a heat-flow DSC; Part II. Optimal calibration procedure. *J Therm Anal Calorim*. 2005;79(1):213-218.

67. Roos Y. Melting and glass transitions of low molecular weight carbohydrates. *Carbohydr Res*. 1993;238(Supplement C):39-48.

68. Yoshinari T., Forbes R.T., York P., Kawashima Y. Crystallisation of amorphous

mannitol is retarded using boric acid. *Int J Pharm.* 2003;258(1):109-120.

69. Yu Lian, Mishra D. S., Rigsbee D. R. Determination of the glass properties of d-mannitol using sorbitol as an impurity. *J Pharm Sci.* 1998;87(6):774-777.

70. Roos Y., Karel M. Plasticizing effect of water on thermal behavior and crystallization of amorphous food models. *J Food Sci.* 1991;56(1):38-43.

71. Listiohadi Y., Hourigan J., Sleigh R., John Steele R. Thermal analysis of amorphous lactose and alpha-lactose monohydrate. *Dairy Sci Technol.* 2009;89:43-67.

72. Bhandari B.R., Howes T. Implication of glass transition for the drying and stability of dried foods. *J Food Sci Eng.* 1999;40(1):71-79.

73. Athanasia G.M. Implications of non-equilibrium state glass transitions in spray-dried sugar-rich foods. Greece: Elsevier Ltd; 2017.

74. Truong V., Bhandari B.R., Howes T., Adhikari B. Glass transition behaviour of fructose. *Int J Food Sci Technol.* 2004;39(5):569-578.

75. Hancock B.C., Shamblin S.L. Water vapour sorption by pharmaceutical sugars. *Pharm Sci Technolo Today.* 1998;1(8):345-351.

76. Hancock B.C., Zografi G. The relationship between the glass transition temperature and the water content of amorphous pharmaceutical solids. *Pharm Res.* 1994;11(4):471-477.

77. Wolkers W.F., Oldenhof H., Alberda M., Hoekstra F.A. A Fourier transform infrared microspectroscopy study of sugar glasses: application to anhydrobiotic higher plant cells. *Biochimica et Biophysica Acta (BBA) - General Subjects.* 1998;1379(1):83-96.

78. Frédéric Roig, Eric Dantras, Jany Dandurand, Lacabanne. C. Influence of hydrogen bonds on glass transition and dielectric relaxations of cellulose. *J Phys D Appl Phys.* 2011;44:1-12.

79. Levine H., Slade L. Water as a plasticizer: physico-chemical aspects of low-moisture polymeric systems. In: Franks F, editor. *Water Science Reviews 3: Water Dynamics.* Water Science Review. 3. Cambridge: Cambridge University Press; 1988. p. 79-185.

80. Seow C.C., Cheah P.B., Chang Y.P. Antiplasticization by water in reduced-moisture food systems. *J Food Sci.* 1999;64(4):576-581.

81. Raimi-Abraham T.B., Moffat G. J., Belton S. P., Barker A. S., Craig D. Generation and characterization of standardized forms of trehalose dihydrate and their associated solid-state behavior. *Cryst Growth Des.* 2014;14:4955-4967.
82. Hsieh W. H., Cheng W. T., Chen L. C., Lin H. L., Lin S.Y. Non-isothermal dehydration kinetics of glucose monohydrate, maltose monohydrate and trehalose dihydrate by thermal analysis and DSC-FTIR study. *J Biomed Pharm Sci.* 2018;1:101.
83. Akao K., Okubo Y., Asakawa N., Inoue Y., Sakurai M. Infrared spectroscopic study on the properties of the anhydrous form II of trehalose. Implications for the functional mechanism of trehalose as a biostabilizer. *Carbohydr Res.* 2001;334(3):233-241.
84. Nikonenko N.A., Buslov D.K., Sushko N.I., Zhbakov R.G. Investigation of stretching vibrations of glycosidic linkages in disaccharides and polysaccharides with use of IR spectra deconvolution. *Biopolymers.* 2000;57(4):257-262.
85. Stieger Nicole, Wilna. L. Recrystallization of active pharmaceutical ingredients 2012. Available from: <https://www.intechopen.com/books/crystallization-science-and-technology/recrystallization-of-active-pharmaceutical-ingredients>.
86. Price R., Young P.M. Visualization of the crystallization of lactose from the amorphous state. *J Pharm Sci.* 2004;93(1):155-164.
87. Meste M.L., Champion D., Roudaut G., Blond G., Simatos D. Glass transition and food technology: a critical appraisal. *J Food Sci.* 2002;67(7):2444-2458.
88. D'Cruz N.M., Bell L.N. Thermal unfolding of gelatin in solids as affected by the glass transition. *J Food Sci.* 2005;70(2):E64-E68.
89. Hickey A.J., da Rocha S.R. *Pharmaceutical inhalation aerosol technology*, third edition: CRC Press; 2019.
90. Job U. Plasticization and antiplasticization in amorphous food systems. *Curr Opin Food Sci.* 2018;21:72-78.
91. Lu X., Weiss R.A. Relationship between the glass transition temperature and the interaction parameter of miscible binary polymer blends. *Macromolecules.* 1992;25(12):3242-3246.
92. Kalogeras I.M. Description and molecular interpretations of anomalous compositional dependences of the glass transition temperatures in binary organic

mixtures. *Thermochimica Acta*. 2010;509(1):135-146.

93. Wiercigroch E., Szafraniec E., Czamara K., Pacia M.Z., Majzner K., Kochan K., et al. Raman and infrared spectroscopy of carbohydrates: A review. *Spectrochim Acta A Mol Biomol Spectrosc*. 2017;185:317-335.

94. Zhibankov R.G., Andrianov V.M., Marchewka M.K. Fourier transform IR and Raman spectroscopy and structure of carbohydrates. *J Mol Struct*. 1997;436-437:637-654.

95. Yoshioka M., Hancock B.C., Zografi G. Crystallization of indomethacin from the amorphous state below and above its glass transition temperature. *J Pharm Sci*. 1994;83(12):1700-1705.





APPENDICES

จุฬาลงกรณ์มหาวิทยาลัย
CHULALONGKORN UNIVERSITY

Appendix 1

Glass transition temperature (T_g) of sucrose fiber containing different saccharides at weight ratio of 1:1

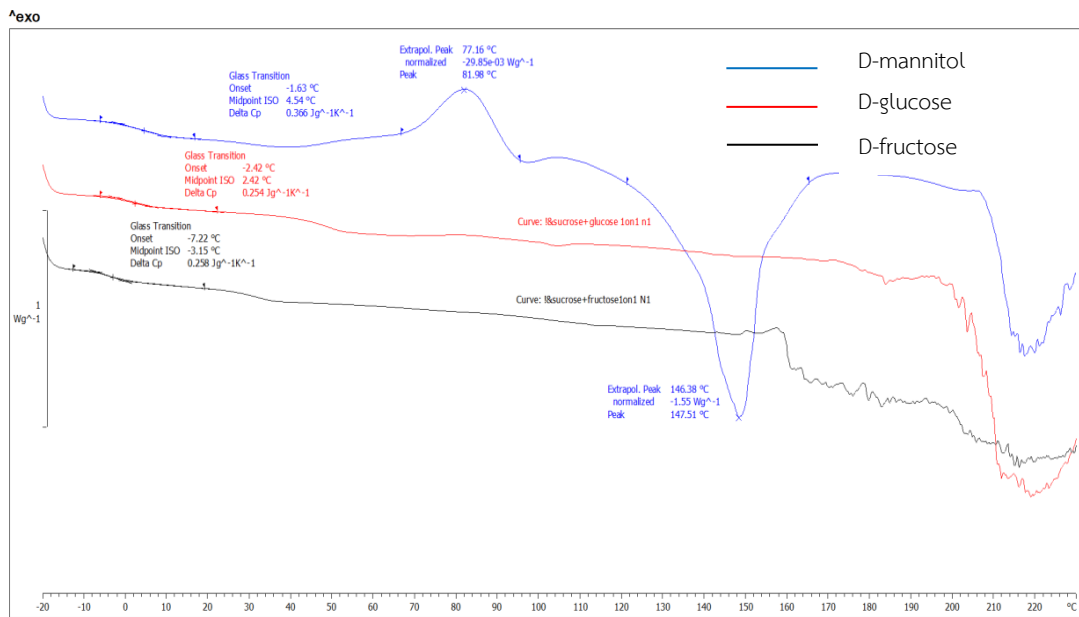


Figure 38 DSC thermograms of sucrose fiber containing the lower T_g saccharides at weight ratio of 1:1

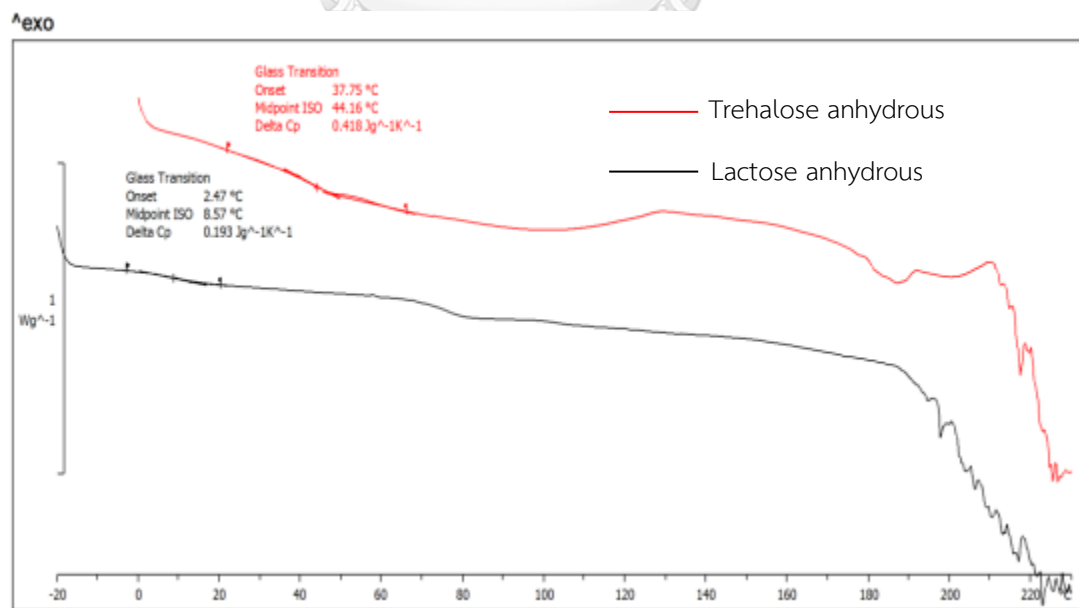


Figure 39 DSC thermogram of sucrose fiber containing the higher T_g saccharide groups at weight ratio of 1:1

Appendix 2

Calculated and experimental T_g (mix) of sucrose fiber containing trehalose dihydrate at different weight ratiosTable 13 Calculated and experimental T_g (mix) of sucrose fiber containing trehalose dihydrate at different weight ratios

Weight ratios of sucrose: trehalose dihydrate	T_g^* (calculated) (°C)	T_g (experiment) (°C)				average±sd
		#1	#2	#3		
100 : 0	55.20	57.39	53.00	-		55.20±3.10
87.5 : 12.5	55.84	42.13	42.52	42.29		42.31±0.20
75.0 : 25.0	56.48	21.39	30.77	25.05		25.74±4.70
62.5 : 37.5	57.12	24.57	24.46	24.00		24.34±0.30
50.0 : 50.0	57.76	25.39	24.60	-		25.0±0.56
37.5 : 62.5	58.39	28.23	19.42	-		23.83±6.23
25.0 : 75.0	59.03	30.33	30.81	34.14		31.76±2.08
12.5 : 87.5	59.67	44.96	45.09	40.48		43.51±2.62
0 : 100.0	60.31	61.64	58.13	61.67		60.31±1.90

* Simple Gordon-Taylor equation T_g (mix) = $\frac{[(w_1 T_{g1}) + (w_2 T_{g2})]}{[w_1 + w_2]}$

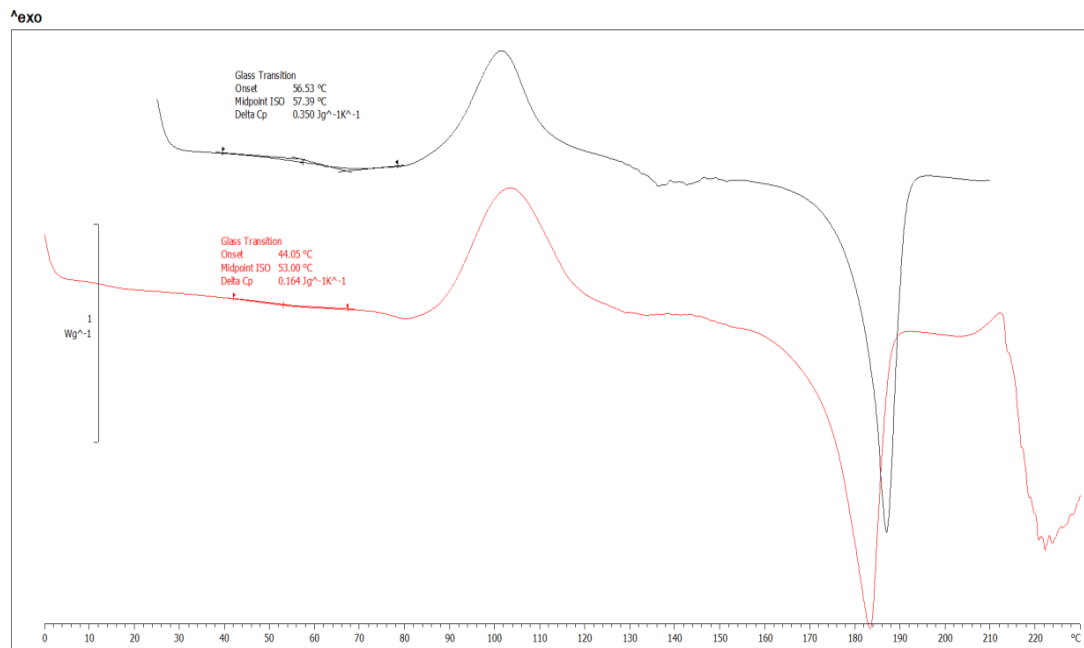


Figure 40 DSC thermograms of sucrose fiber containing trehalose dihydrate at weight ratio of 100.0 : 0

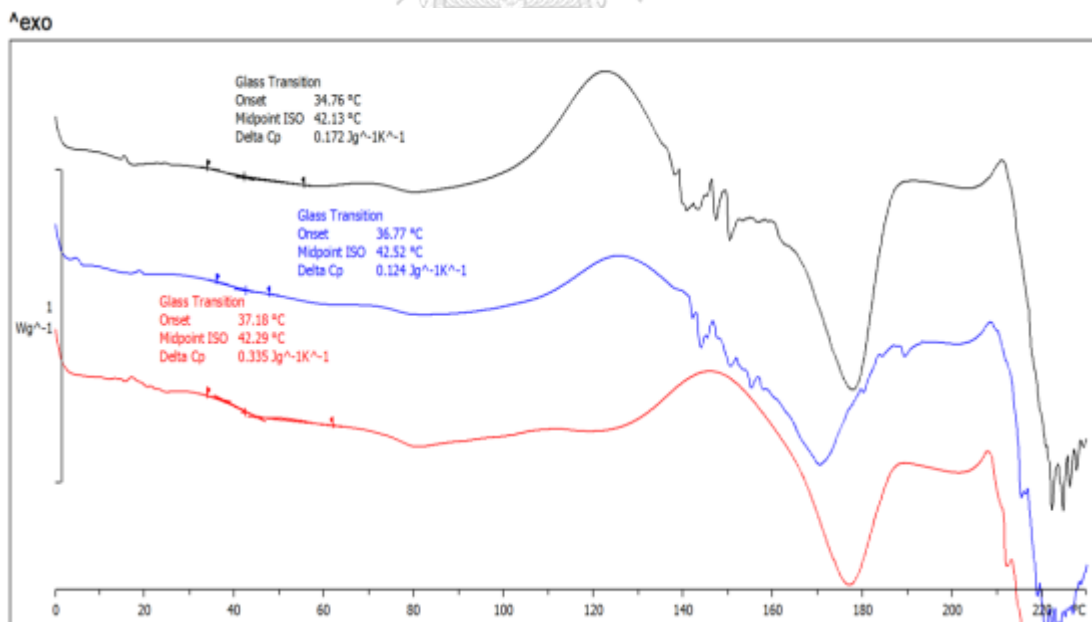


Figure 41 DSC thermograms of sucrose fiber containing trehalose dihydrate at weight ratio of 87.5 : 12.5

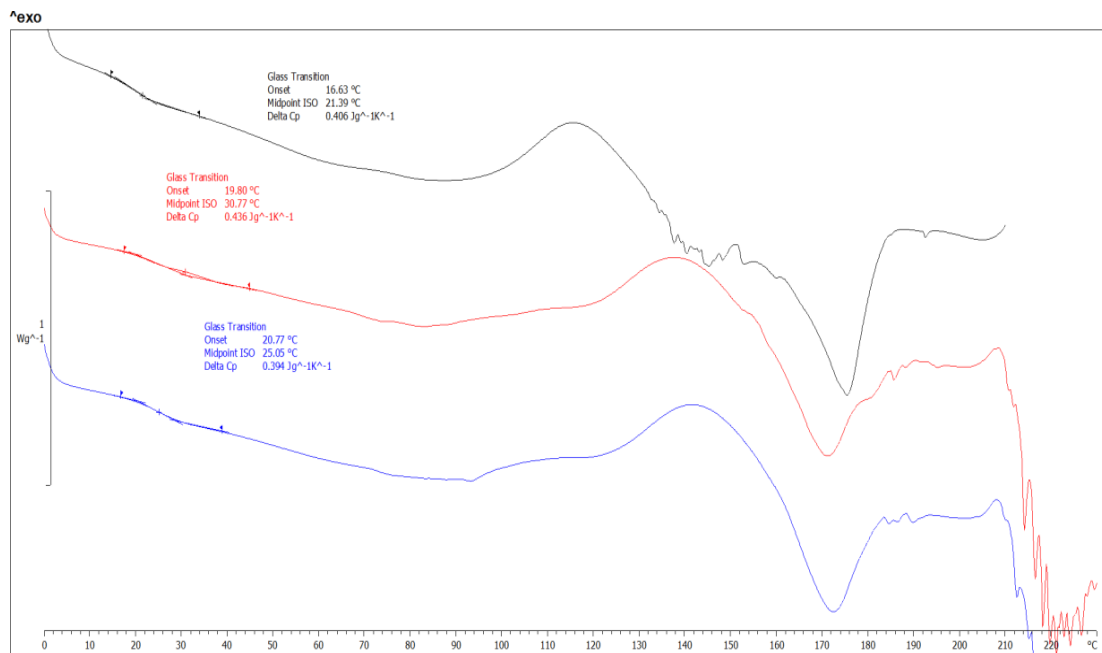


Figure 42 DSC thermograms of sucrose fiber containing trehalose dihydrate at weight ratio of 75.0 : 25.0

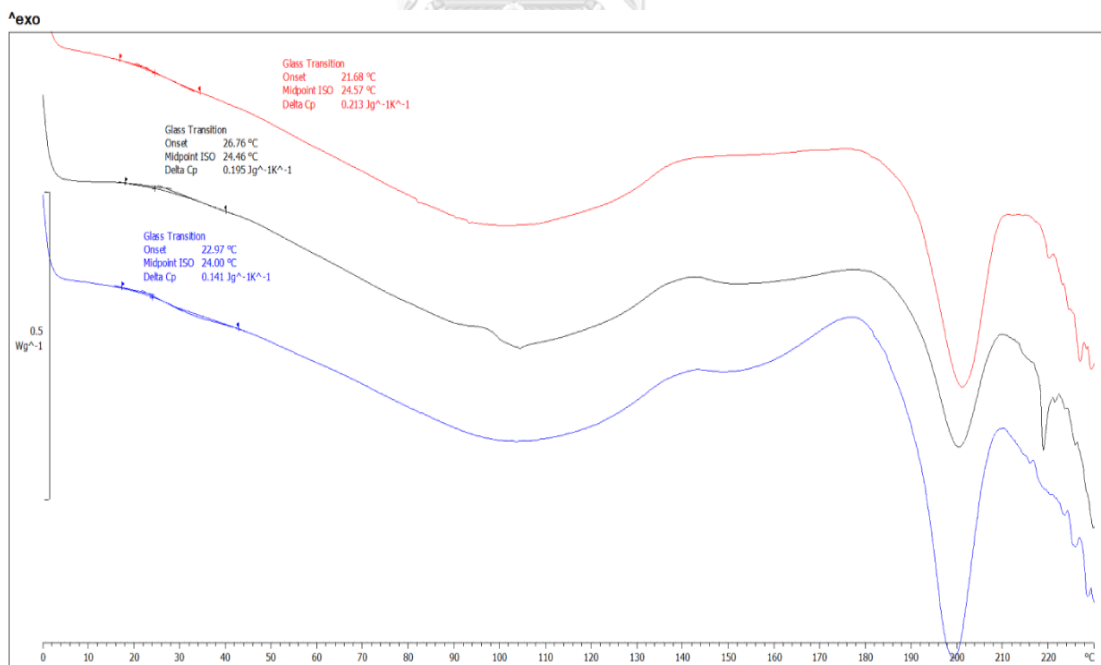


Figure 43 DSC thermograms of sucrose fiber containing trehalose dihydrate at weight ratio of 62.5 : 37.5

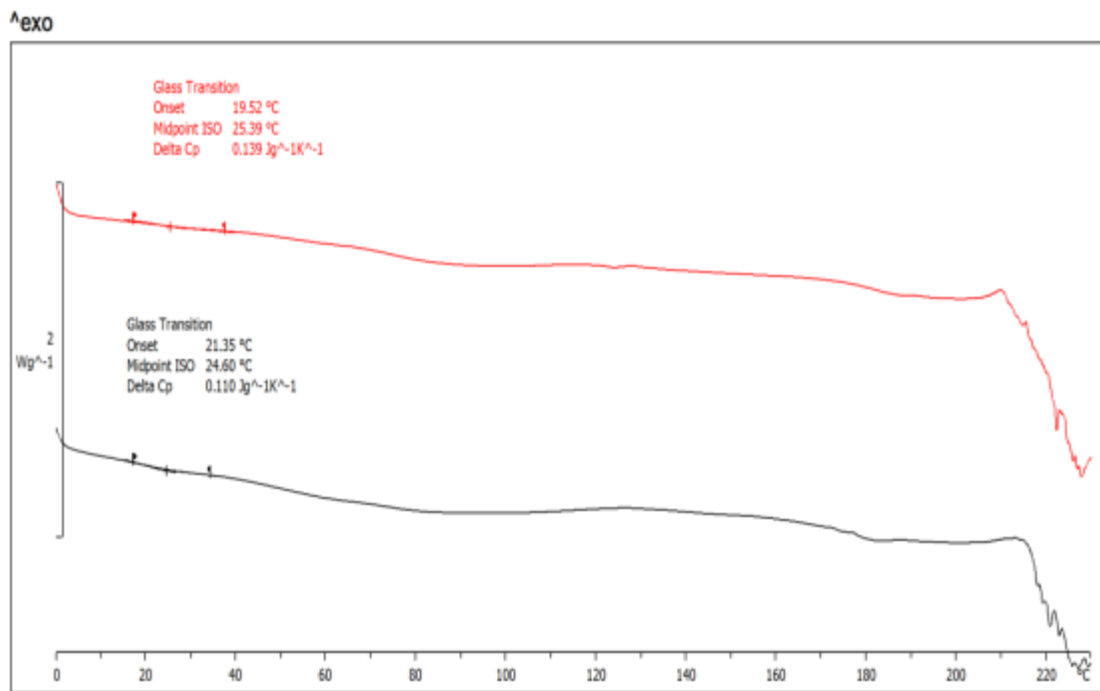


Figure 44 DSC thermograms of sucrose fiber containing trehalose dihydrate at weight ratio of 50.0 : 50.0

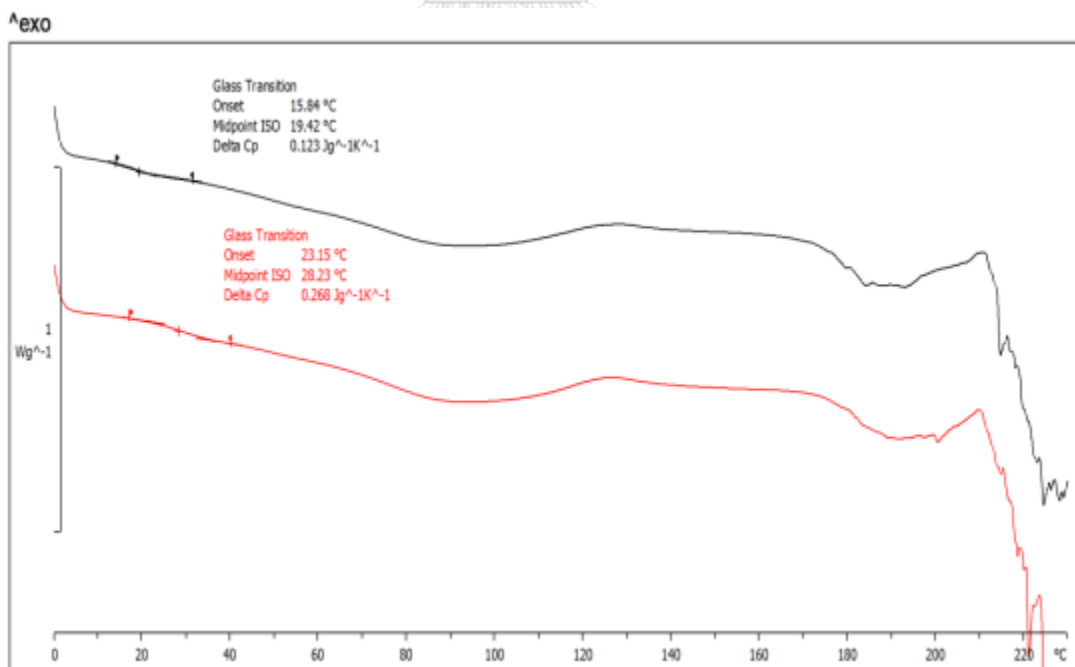


Figure 45 DSC thermograms of sucrose fiber containing trehalose dihydrate at weight ratio of 37.5 : 62.5

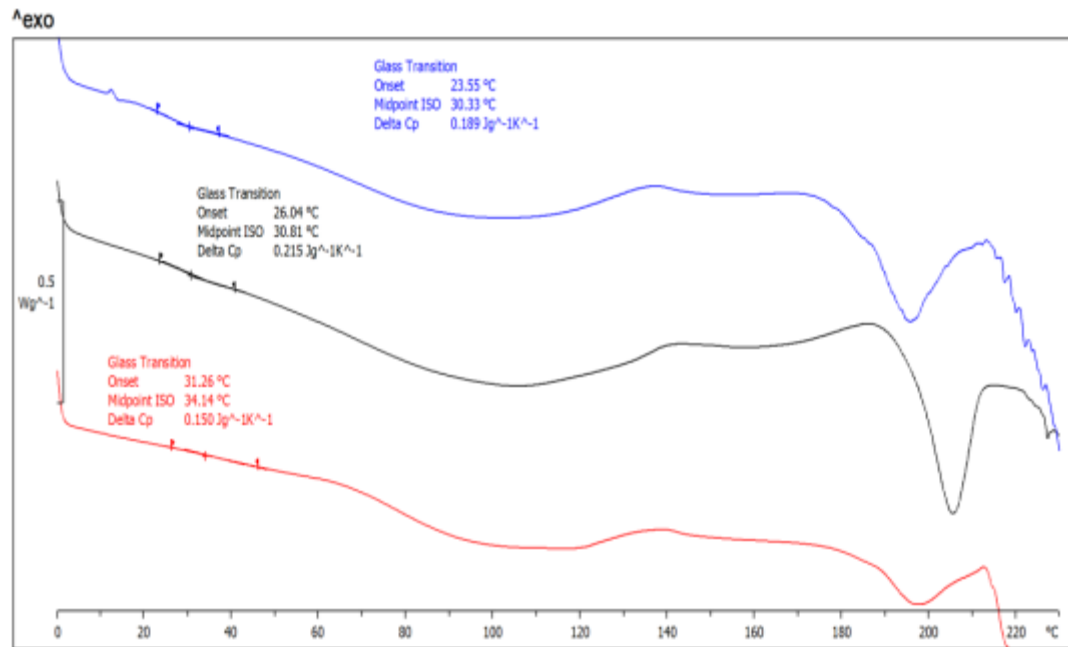


Figure 46 DSC thermograms of sucrose fiber containing trehalose dihydrate at weight ratio of 25.0 : 75.0

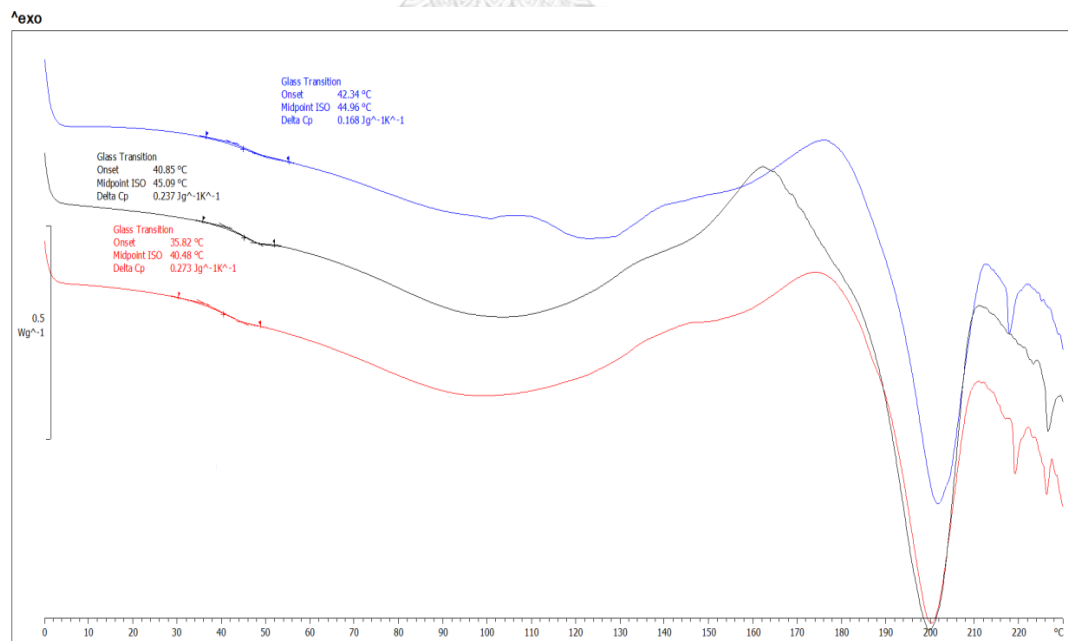


Figure 47 DSC thermograms of sucrose fiber containing trehalose dihydrate at weight ratio of 12.5 : 87.5

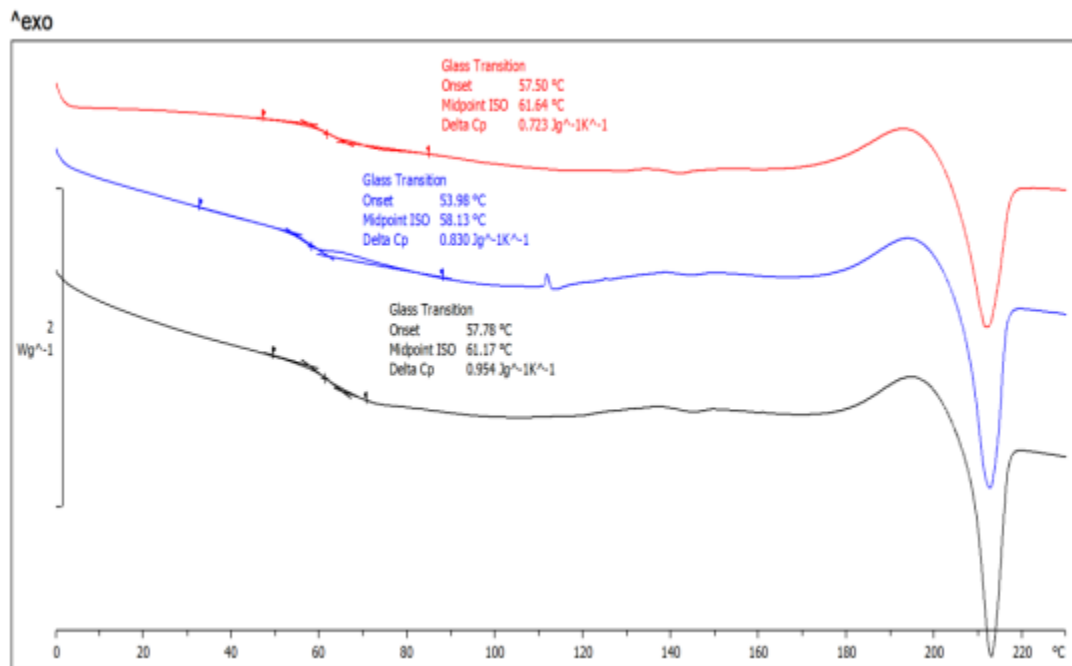


Figure 48 DSC thermograms of sucrose fiber containing trehalose dihydrate at weight ratio of 0 : 100.0

Appendix 3

Moisture sorption profile of amorphous sucrose fiber containing trehalose dihydrate at different weight ratios under storage condition of 30 ± 2 °C and $75\pm 5\%$ RH.

Denote : A - the transition time of amorphous glassy to rubbery state

B - the recrystallization time

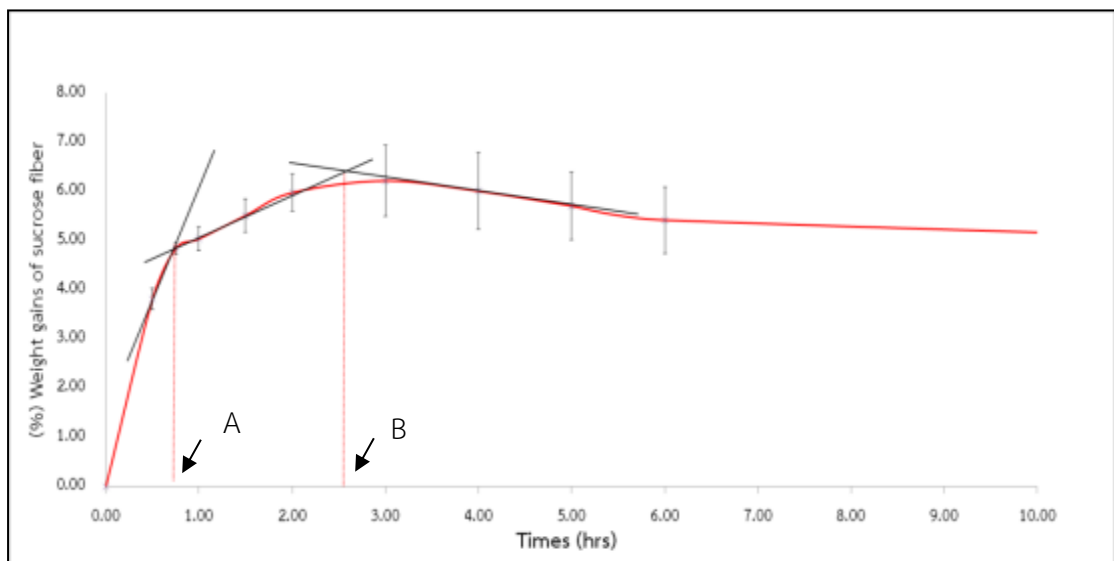


Figure 49 Moisture sorption profile of amorphous saccharide sucrose fiber

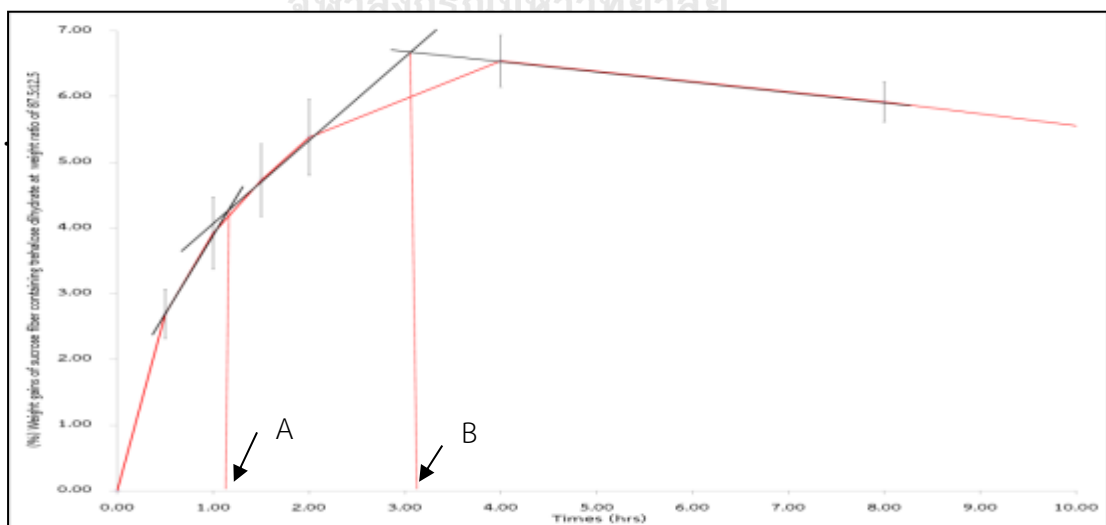


Figure 50 Moisture sorption profile of amorphous saccharide sucrose fiber containing trehalose dihydrate at weight ratio of 87.5 : 12.5

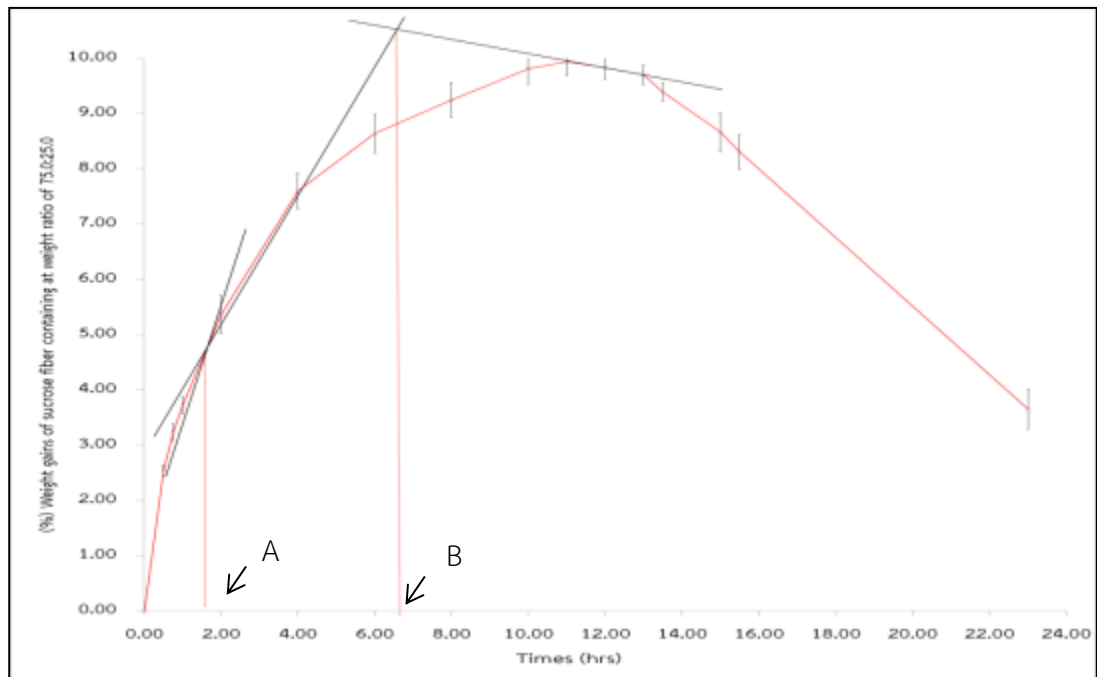


Figure 51 Moisture sorption profile of amorphous saccharide sucrose fiber containing trehalose dihydrate at weight ratio of 75.0 : 25.0

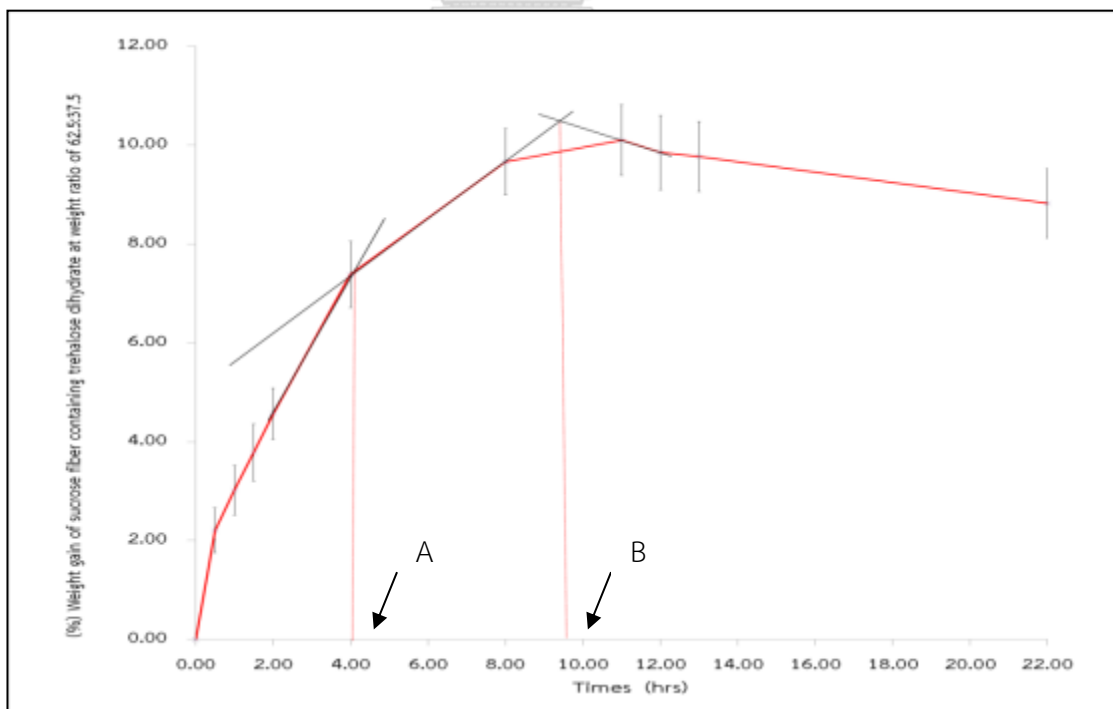


Figure 52 Moisture sorption profile of amorphous saccharide sucrose fiber containing trehalose dihydrate at weight ratio of 62.5 : 37.5

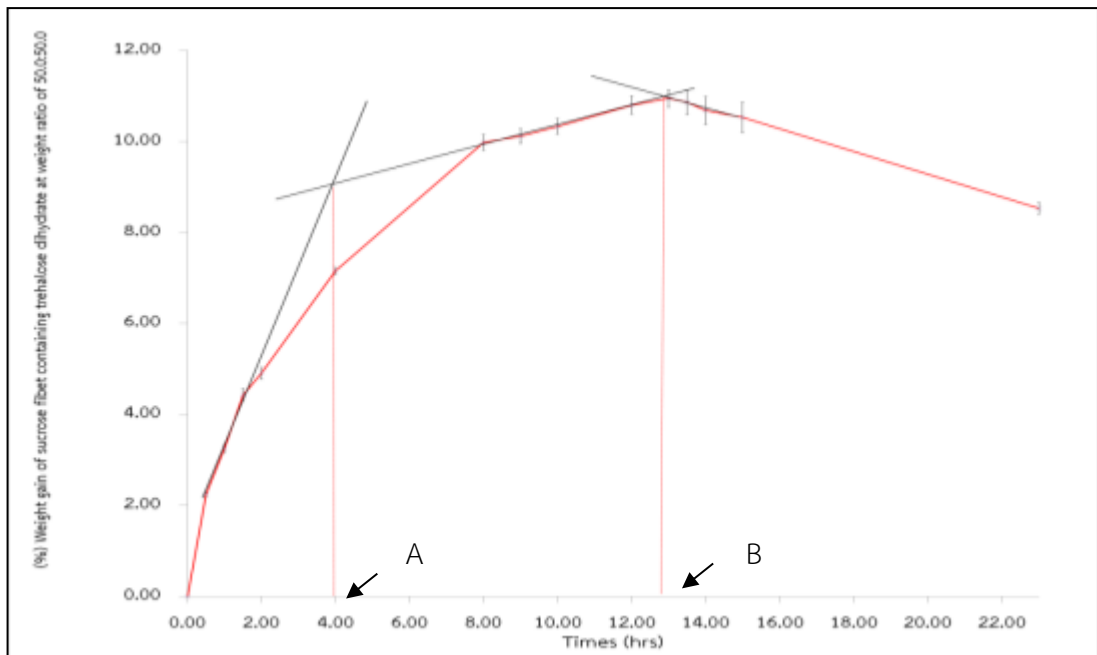


Figure 53 Moisture sorption profile of amorphous saccharide sucrose fiber containing trehalose dihydrate at weight ratio of 50.0 : 50.0

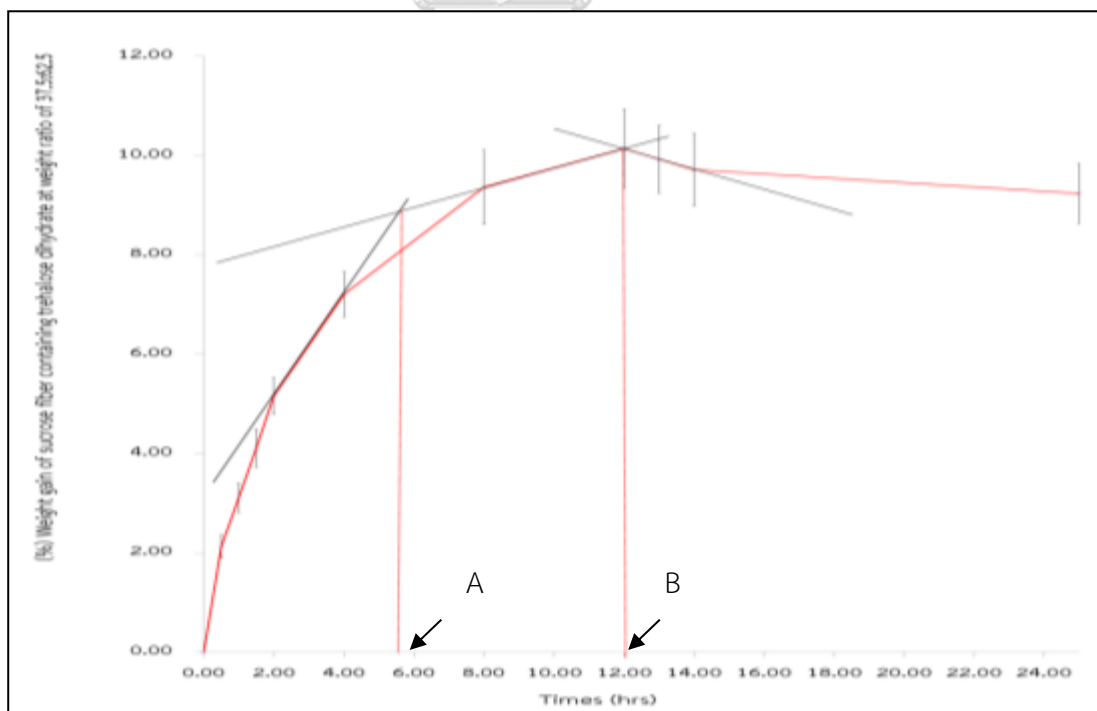


Figure 54 Moisture sorption profile of amorphous saccharide sucrose fiber containing trehalose dihydrate at weight ratio of 37.5 : 62.5

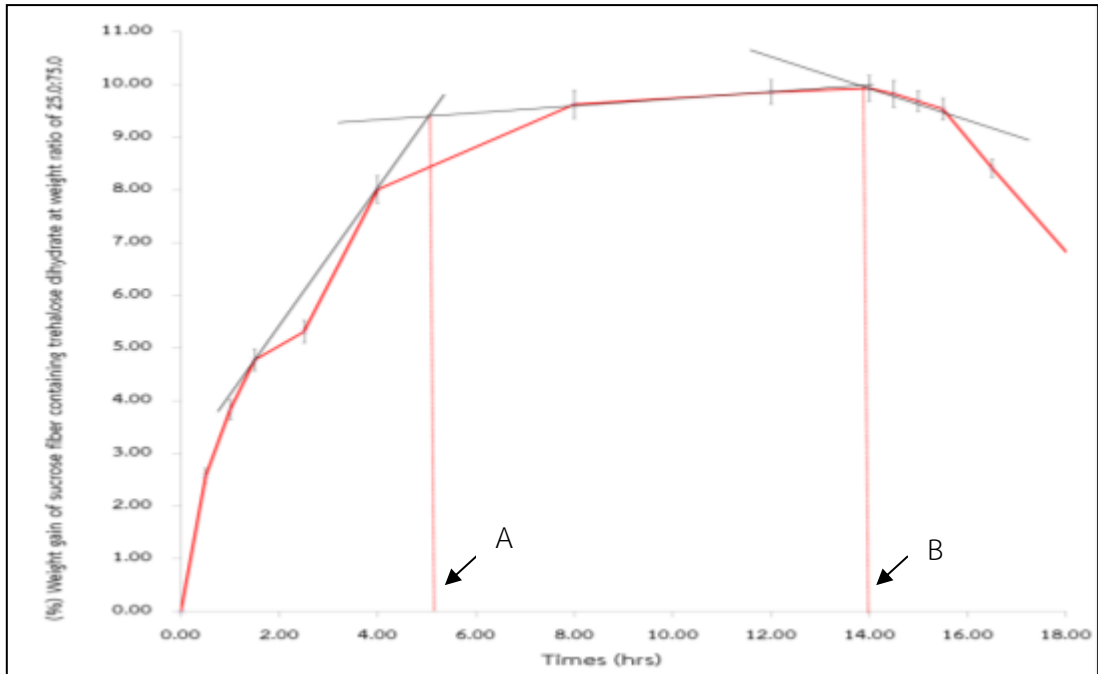


Figure 55 Moisture sorption profile of amorphous saccharide sucrose fiber containing trehalose dihydrate at weight ratio of 25.0 : 75.0

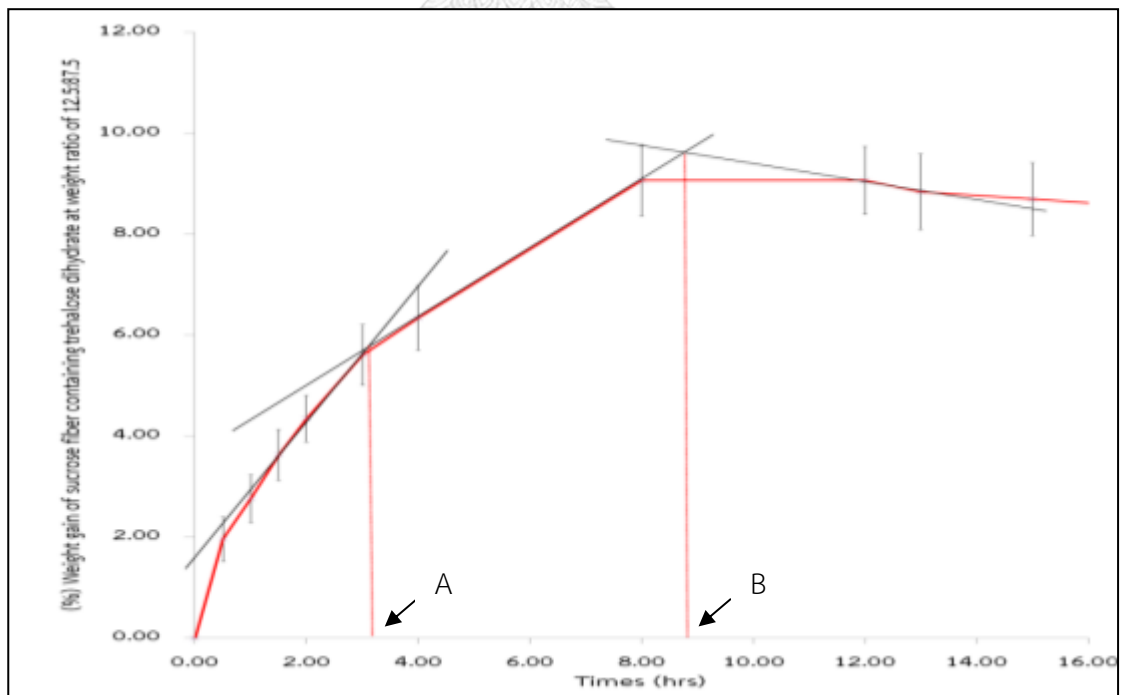


Figure 56 Moisture sorption profile of amorphous saccharide sucrose fiber containing trehalose dihydrate at weight ratio of 12.5 : 87.5

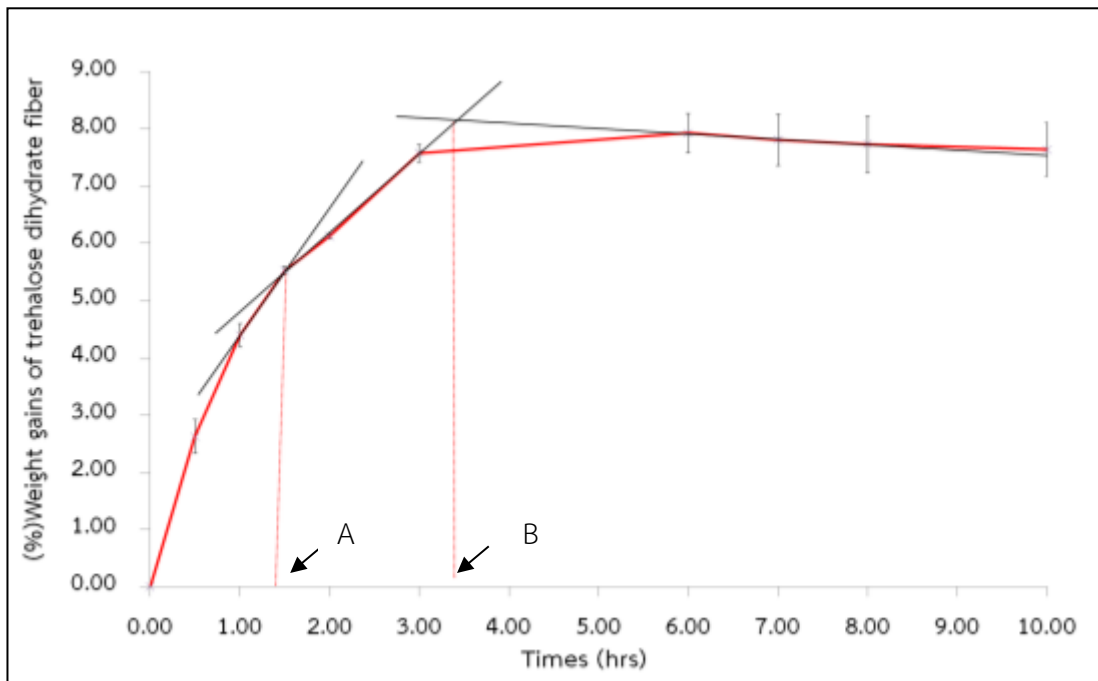


Figure 57 Moisture sorption profile of amorphous saccharide trehalose dihydrate fiber

Appendix 4

Moisture sorption profile of amorphous sucrose fiber containing trehalose dihydrate at different weight ratios under storage condition of 40 ± 2 °C and $75 \pm 5\%$ RH.

Table 14 The transition time and the recrystallization time of sucrose/trehalose dihydrate fiber with various weight ratios under exposing temperature of 40 ± 2 °C and $75 \pm 5\%$ RH

Weight ratios of sucrose : trehalose dihydrate	Transition time (hrs)				Recrystallization time (hrs)			
	#1	#2	#3	average±sd	#1	#2	#3	average±sd
100.0 : 0	0.50	0.50	0.61	0.54±0.06	2.19	2.51	1.83	2.18±0.34
87.5 : 12.5	0.50	0.59	0.50	0.53±0.05	1.25	1.50	1.07	1.27±0.22
75.0 : 25.0	1.00	1.00	1.00	1.00±0.00	5.10	5.01	4.39	4.80±0.44
62.5 : 37.5	1.05	0.66	1.27	0.99±0.31	7.99	7.72	5.56	7.09±1.33
50.0 : 50.0	1.01	1.08	1.00	1.03±0.04	7.86	6.66	7.96	7.49±0.72
37.5 : 62.5	1.96	2.60	1.57	2.25±0.32	8.56	8.65	9.16	8.79±0.32
25.0 : 75.0	2.52	2.52	2.42	2.49±0.06	9.87	10.92	13.50	11.43±1.87
12.5 : 87.5	3.43	3.94	3.11	3.49±0.42	12.06	12.10	12.15	12.10±0.05
0 : 100.0	1.74	1.68	1.69	1.70±0.03	5.69	4.98	5.00	5.22±0.4

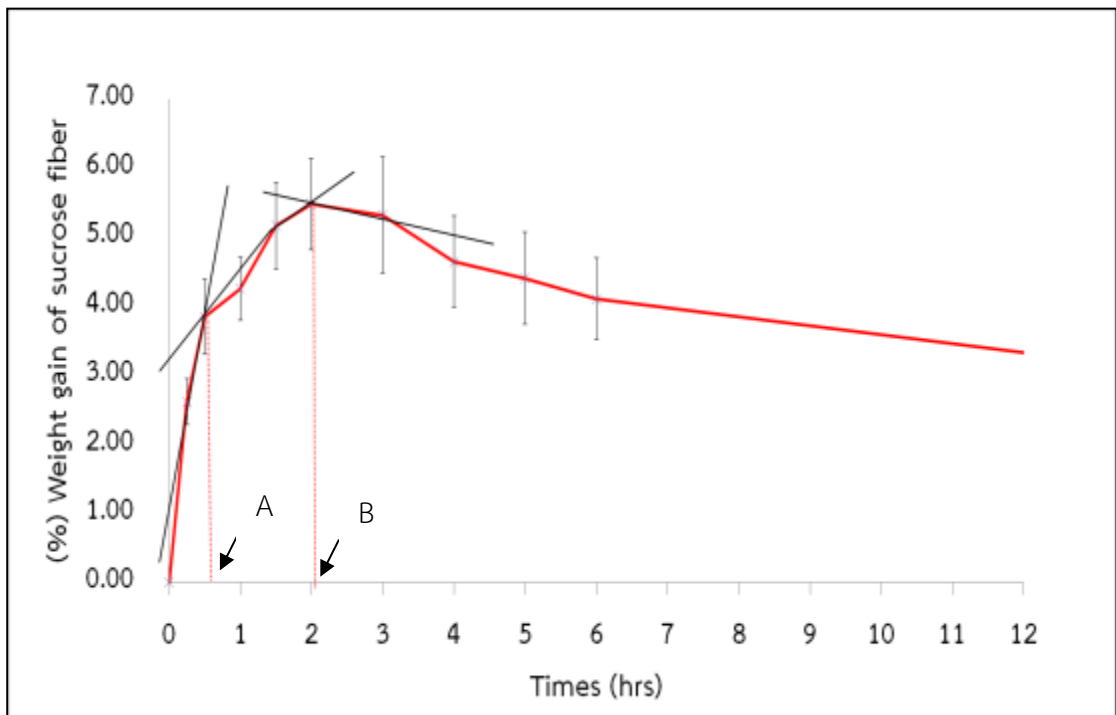


Figure 58 Moisture sorption profile of amorphous saccharide sucrose fiber

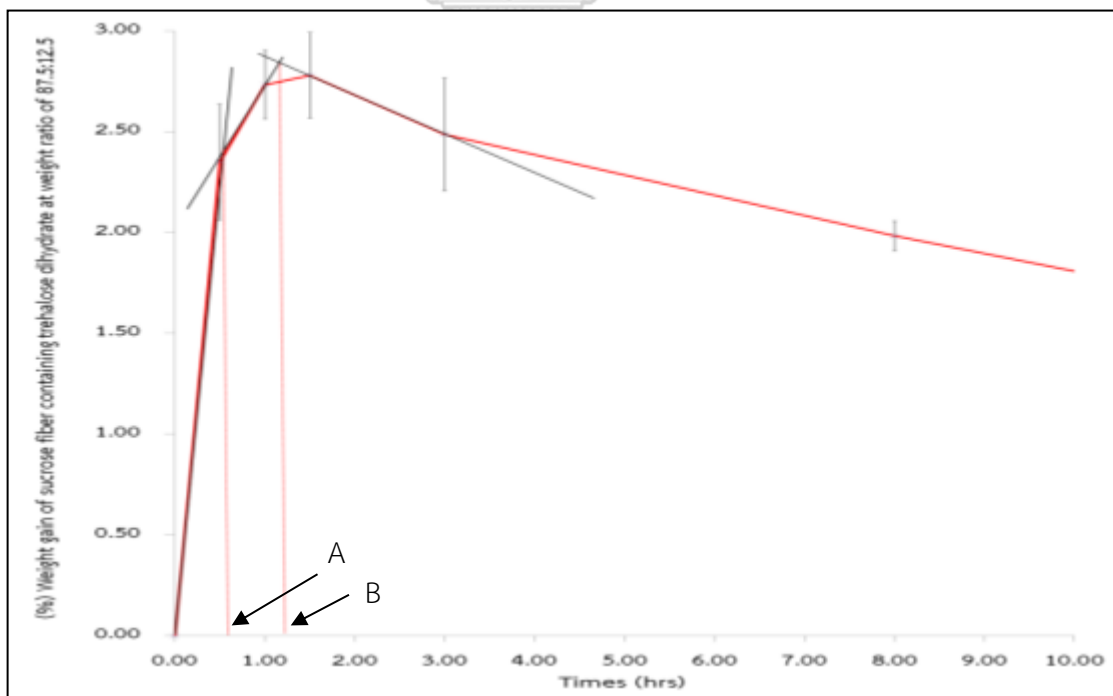


Figure 59 Moisture sorption profile of amorphous saccharide sucrose fiber containing trehalose dihydrate at weight ratio of 87.5 : 12.5

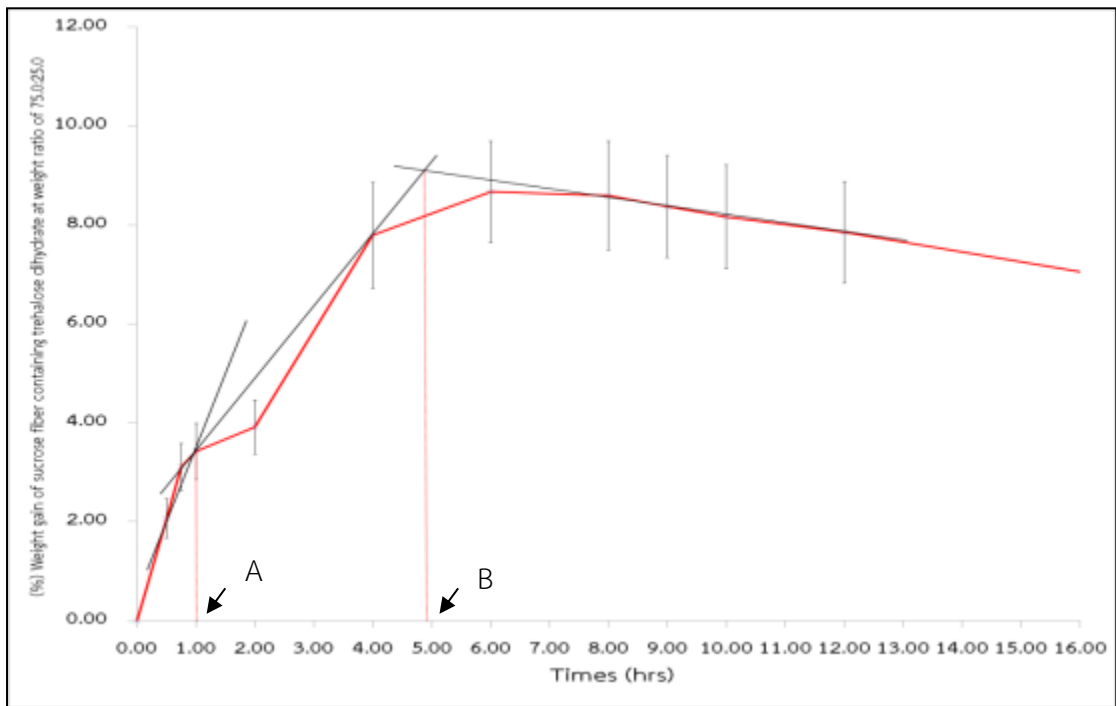


Figure 60 Moisture sorption profile of amorphous saccharide sucrose fiber containing trehalose dihydrate at weight ratio of 75.0 : 25.0

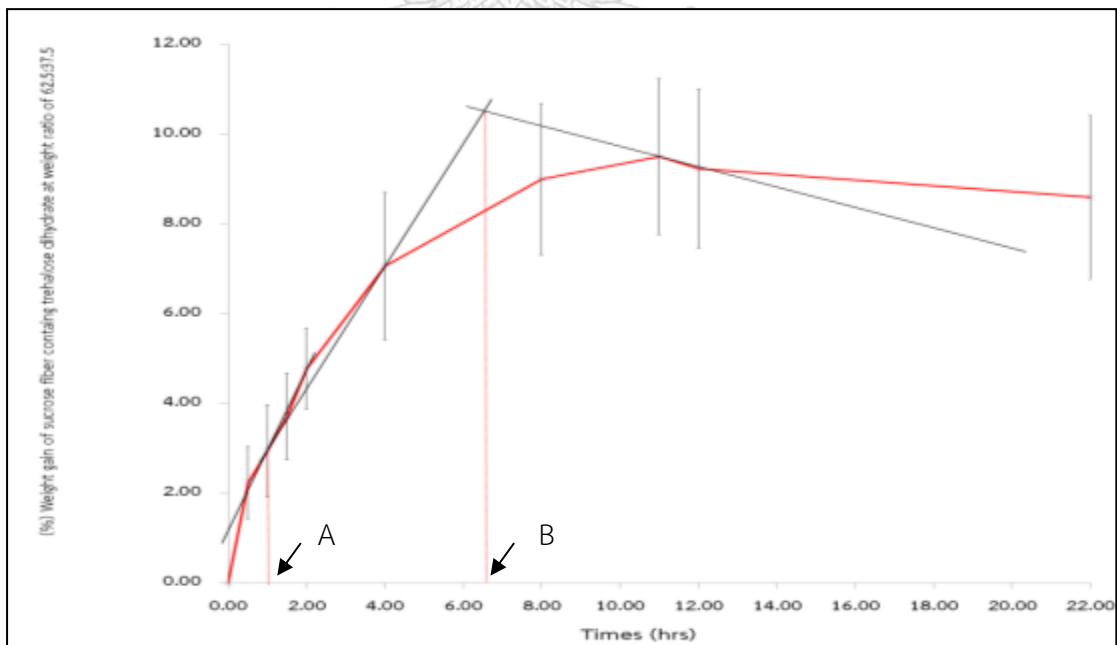


Figure 61 Moisture sorption profile of amorphous saccharide sucrose fiber containing trehalose dihydrate at weight ratio of 62.5 : 37.5

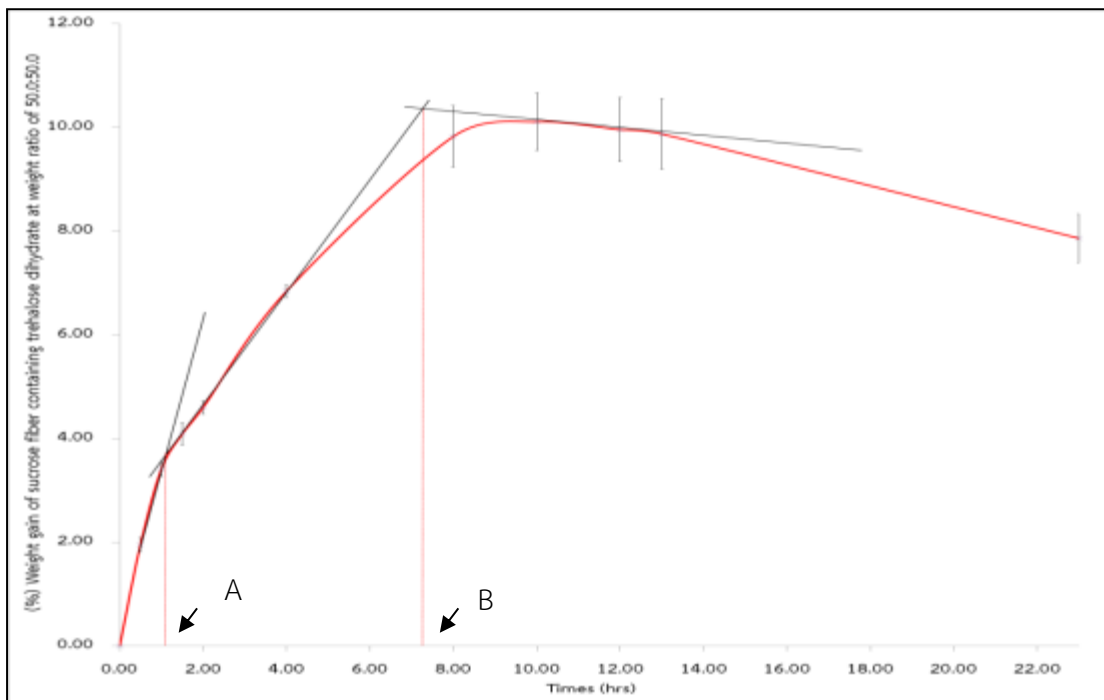


Figure 62 Moisture sorption profile of amorphous saccharide sucrose fiber containing trehalose dihydrate at weight ratio of 50.0 : 50.0

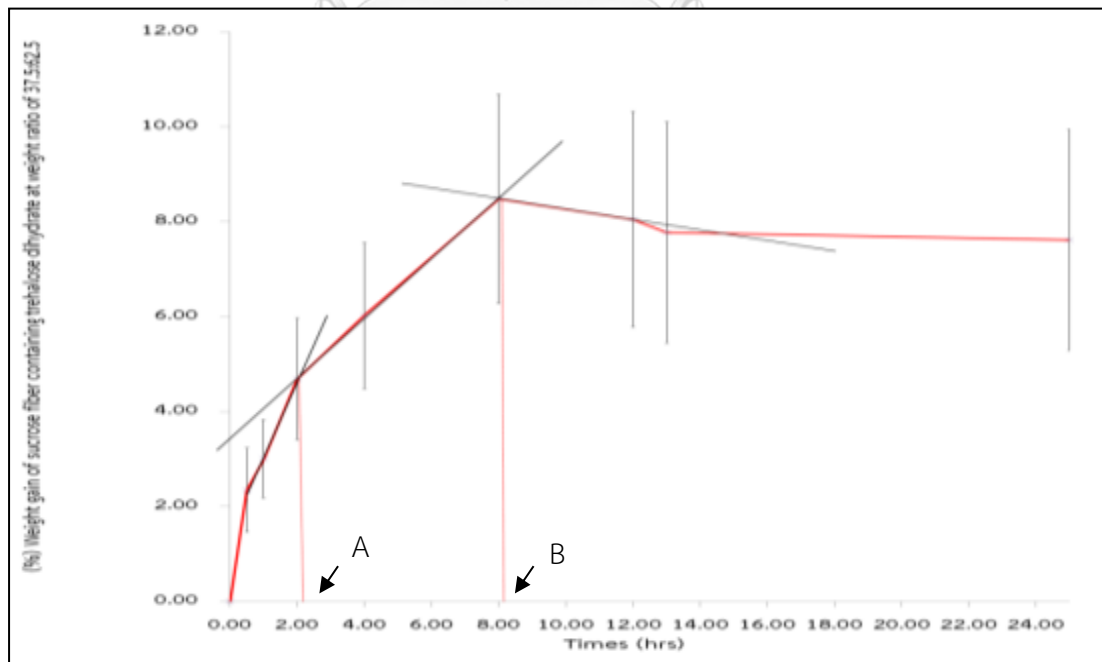


Figure 63 Moisture sorption profile of amorphous saccharide sucrose fiber containing trehalose dihydrate at weight ratio of 37.5 : 62.5

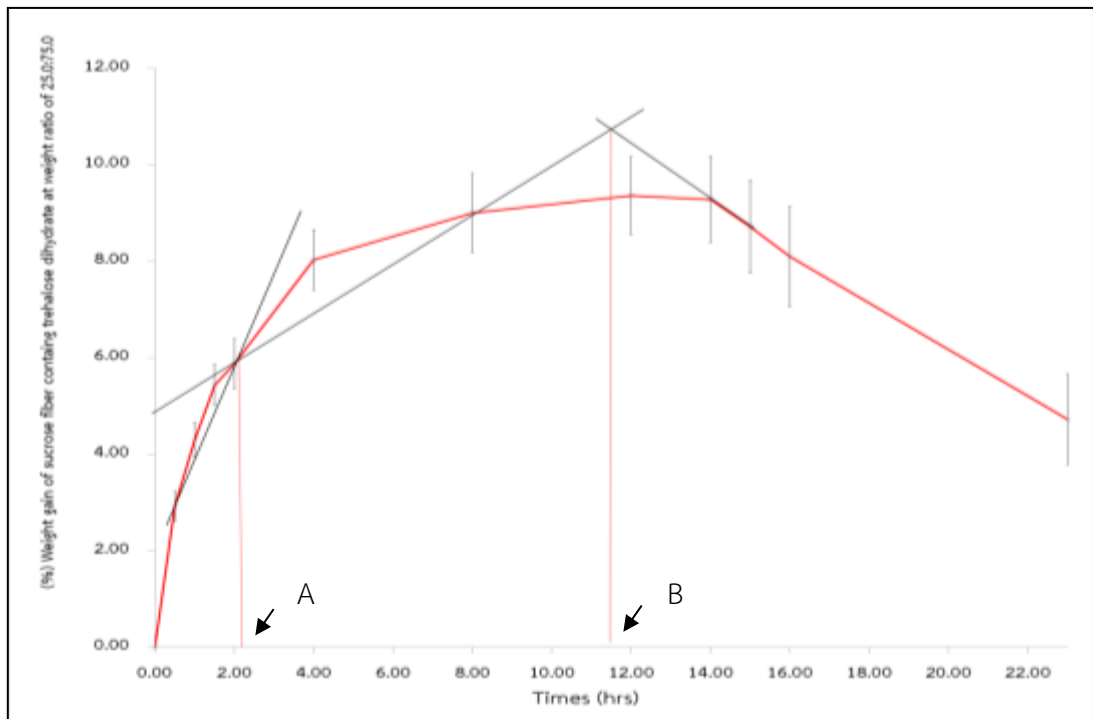


Figure 64 Moisture sorption profile of amorphous saccharide sucrose fiber containing trehalose dihydrate at weight ratio of 25.0 : 75.0

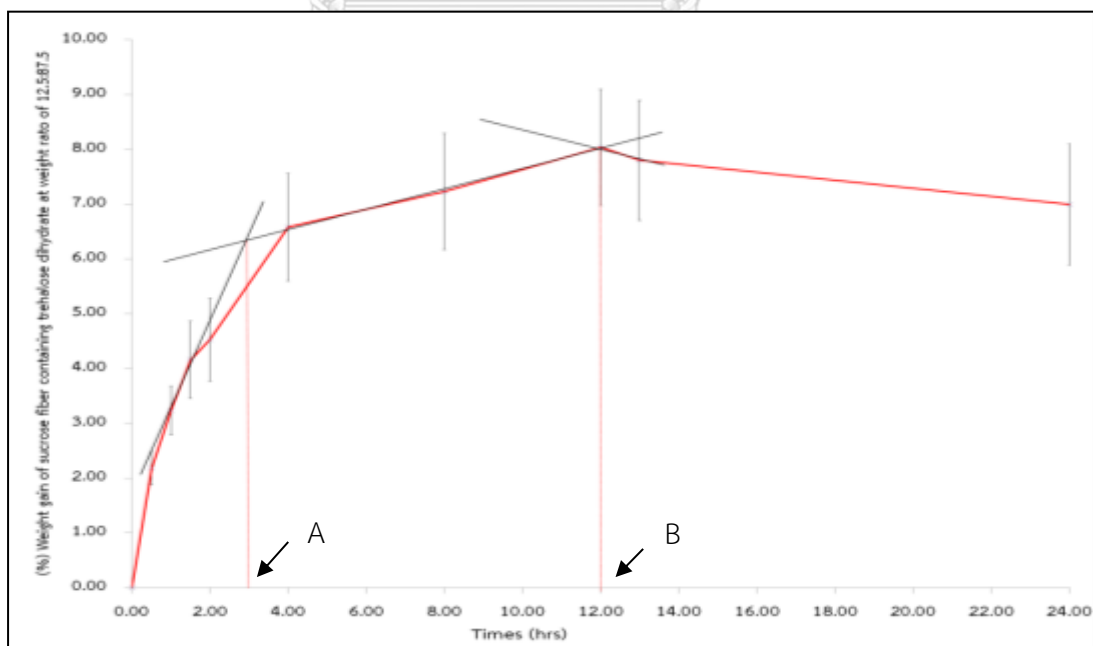


Figure 65 Moisture sorption profile of amorphous saccharide sucrose fiber containing trehalose dihydrate at weight ratio of 12.5 : 87.5

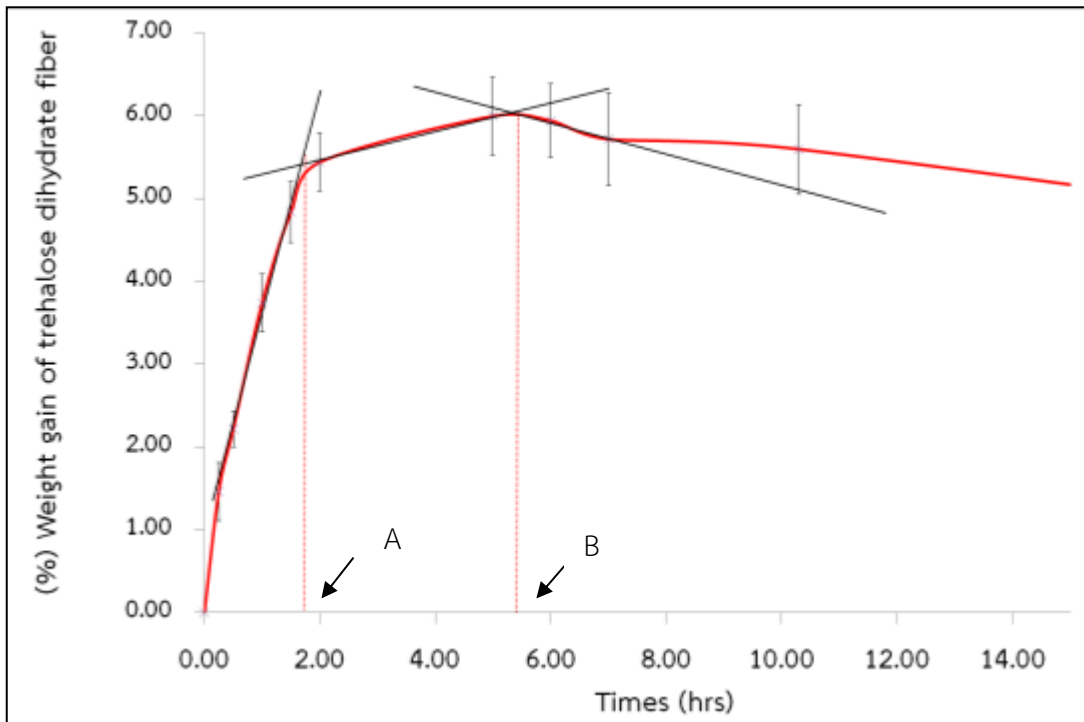


Figure 66 Moisture sorption profile of amorphous saccharide trehalose dihydrate fiber

Appendix 5

Polarized light photomicrograph of amorphous sucrose fiber containing trehalose dihydrate at different weight ratios before and after recrystallization

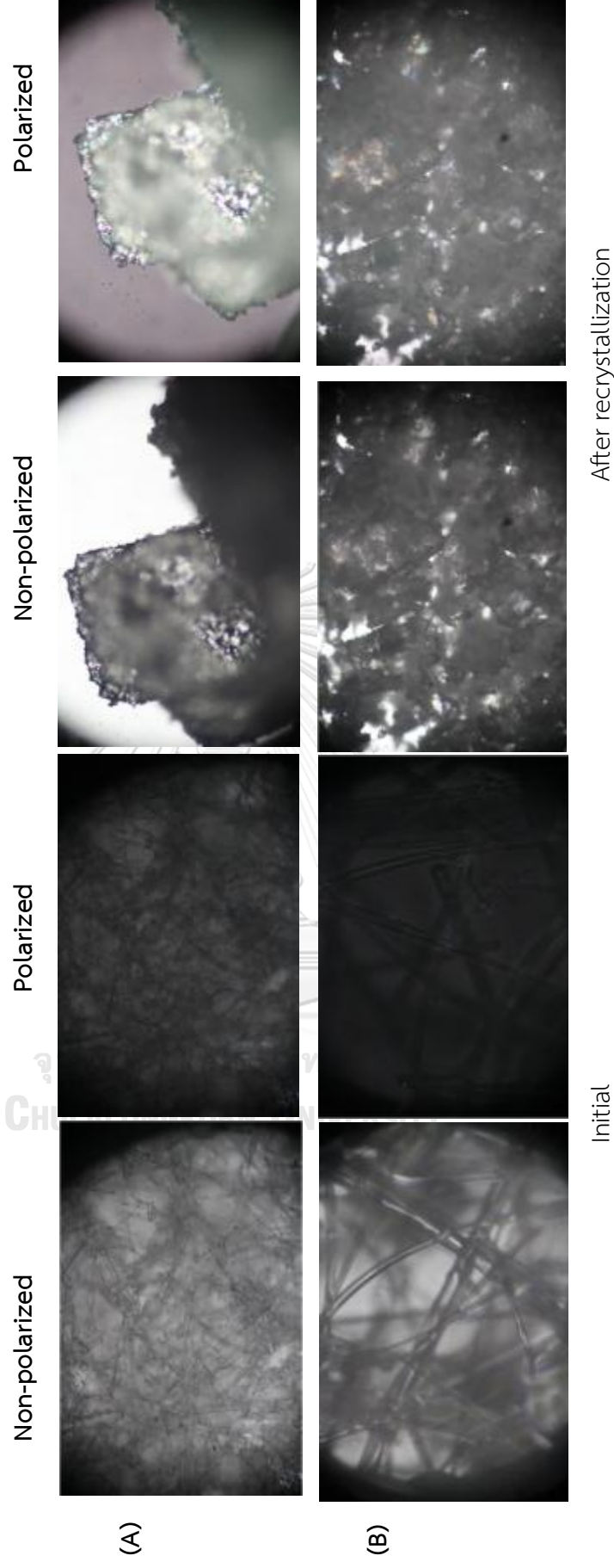


Figure 67 Photomicrographs of sucrose fiber containing trehalose dihydrate at different weight ratios (A)-(100.0:0), (B)-(87.5:12.5) (40*10 X)

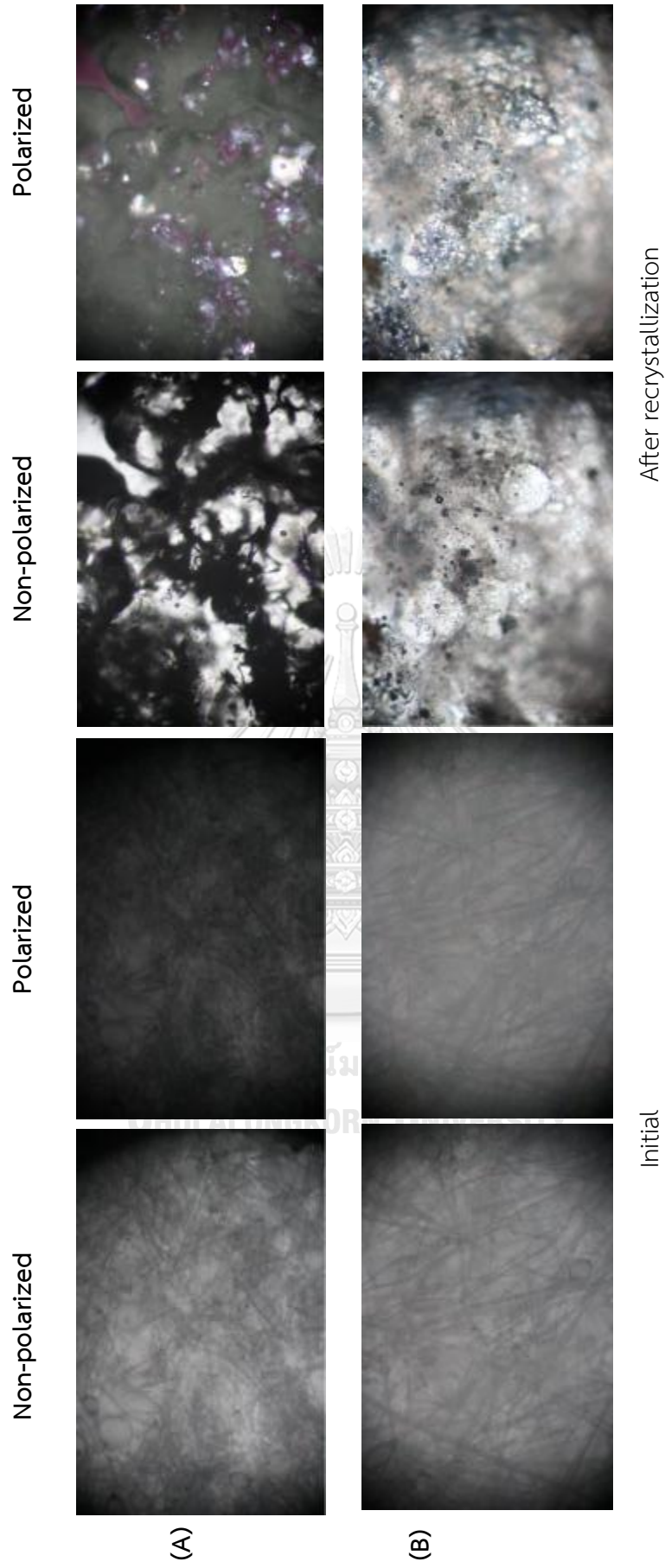


Figure 68 Photomicrographs of sucrose fiber containing trehalose dihydrate at different weight ratios (A)-(75.0:25.0), (B)-(62.5:37.5) (40*10 X)

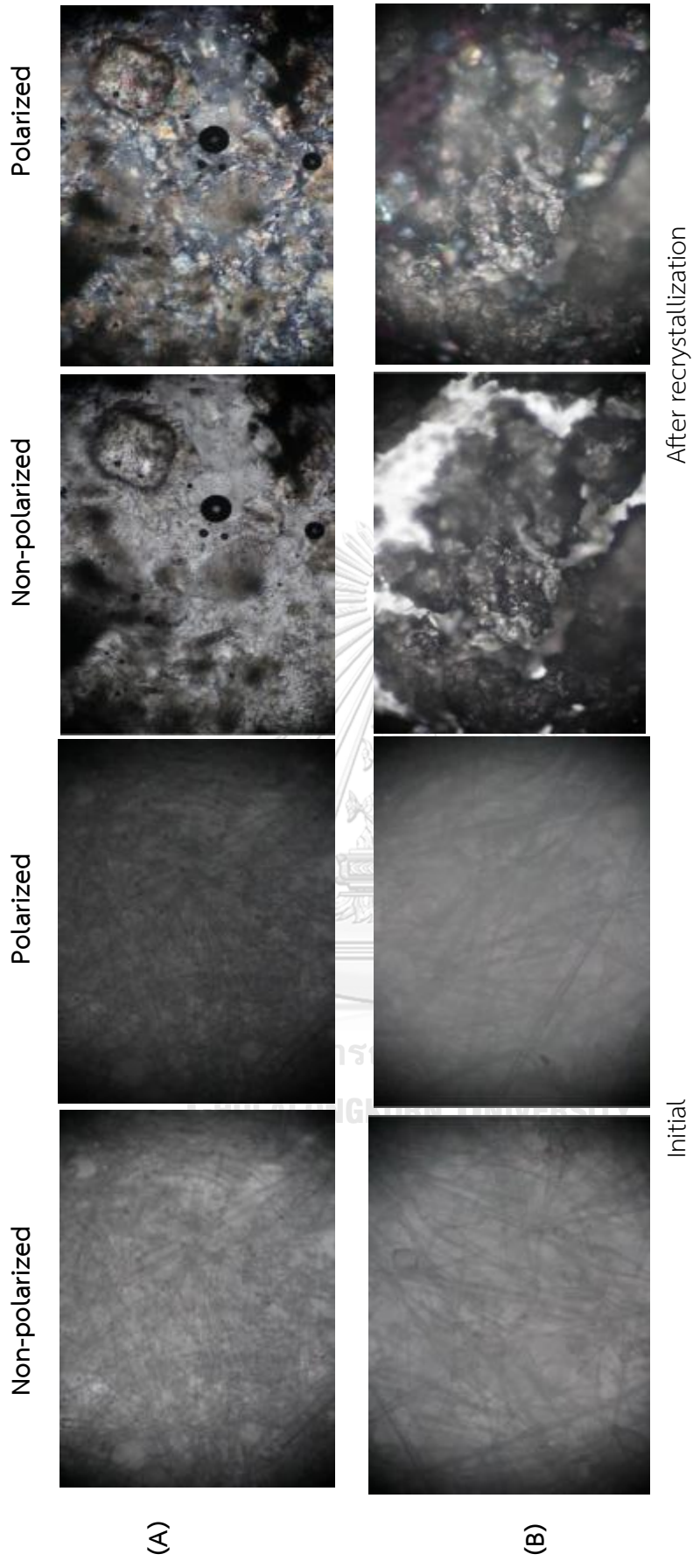


Figure 69 Photomicrographs of sucrose fiber containing trehalose dihydrate at different weight ratios (A)-(50.0:50.0), (B)-(37.5:62.5) (40*10 X)

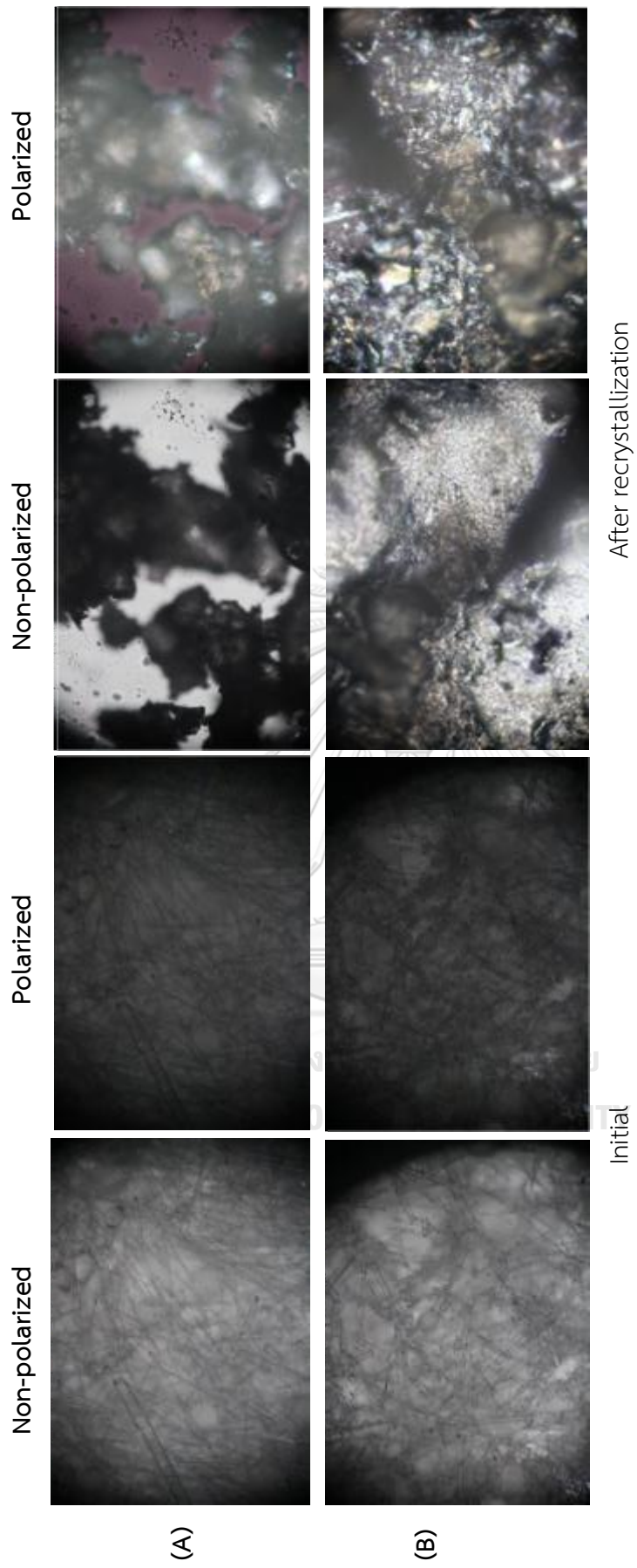


Figure 70 Photomicrographs of sucrose fiber containing trehalose dihydrate at different weight ratios (A)-(25.0:75.0), (B)-(12.5:87.5) (40*10 X)

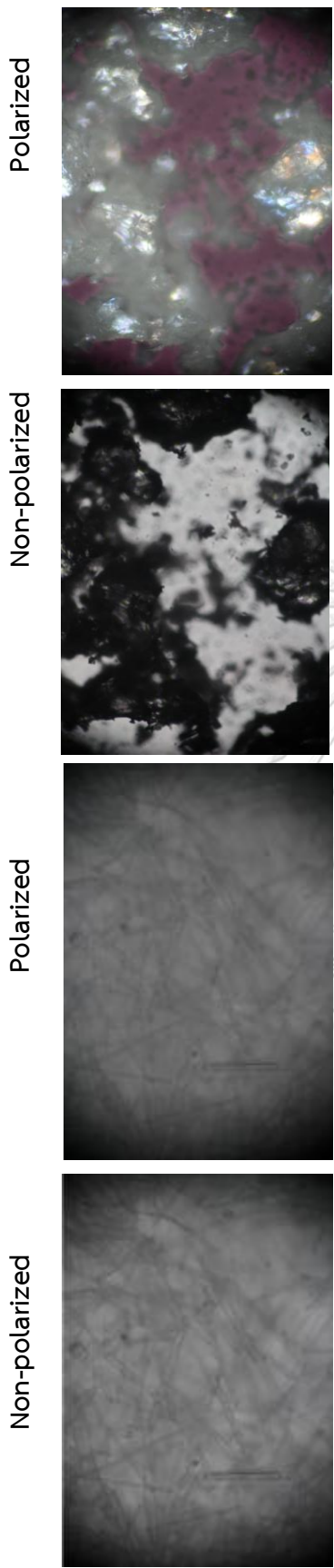


Figure 71 Photomicrographs of sucrose fiber containing trehalose dihydrate at different weight ratios (0:100.0) (trehalose dihydrate fiber) (40*10 X)



VITA

NAME Pattama Donghuntong

DATE OF BIRTH 20 April 1985

PLACE OF BIRTH Ratchaburi

INSTITUTIONS ATTENDED Bachelor of Pharmacy degree in 2008 from the Faculty of Pharmacy, Silpakorn University, Thailand

HOME ADDRESS The Key Prachachuen 169/92 Prachachuen Road
Bangkhen Mueang Nonthaburi 11000

PUBLICATION Proceeding poster of title "The effect of saccharides on the structural integrity of centrifugal spinning sucrose fiber" in the Thai Journal of Pharmaceutical Sciences (TJPS) 34TH International Annual Meeting in Pharmaceutical Sciences and 2ND CU FPhS -RIKEN CDB Symposium (IAMPS34 and 2ND CU FPhS -RIKEN CDB) "Advances in cellular and molecular biology" on March 8-9, 2018 at Arnoma Grand Hotel, Bangkok, Thailand